

Dissertation zur Erlangung des Doktorgrades
der Fakultät für Chemie und Pharmazie
der Ludwig-Maximilians-Universität München

Synthesis of Superelectrophiles from Small Oxocarbon Compounds

Manuel Tobias Schickinger

aus

Gräfelfing

2018

Erklärung

Diese Dissertation wurde im Sinne von § 7 der Promotionsordnung vom 28. November 2011 von Herrn Prof. Dr. Andreas J. Kornath betreut.

Eidesstattliche Versicherung

Diese Dissertation wurde selbständig, ohne unerlaubte Hilfe erarbeitet.

München, den 3. Januar 2019

.....
Manuel Schickinger

Dissertation eingereicht am 15. November 2018

1. Gutachter: *Prof. Dr. Andreas Kornath*

2. Gutachter: *Prof. Dr. Thomas Klapötke*

Mündliche Prüfung am 13. Dezember 2018

„Mir kommen die Wege, auf denen die Menschen zur Erkenntnis gelangen, fast ebenso
bewunderungswürdig vor wie die Natur der Dinge selbst.“

Johannes Kepler

Danksagung

Zuerst möchte ich mich besonders bei Herrn Prof. Dr. Andreas J. Kornath für die freundliche Aufnahme in seinem Arbeitskreis, für das sehr interessante und herausfordernde Thema dieser Dissertation, sein Vertrauen und seine Unterstützung sowie die Freiheit, in wissenschaftlicher Hinsicht meine Ideen zu verwirklichen, bedanken. Auch für die Möglichkeit, an zahlreichen Konferenzen teilnehmen zu dürfen, möchte ich mich ganz herzlich bedanken.

Des Weiteren möchte ich Herrn Prof. Dr. Thomas M. Klapötke für die Übernahme der Zweitkorrektur danken.

Als nächstes gilt mein Dank Joe und Can, die mich so freundlich in diesem Arbeitskreis aufgenommen haben und mir als Mentoren die nicht ganz alltäglichen Arbeitstechniken beigebracht haben. Darüber hinaus sind sie auch noch auf privater Ebene zu guten Freunden geworden.

Domi, Ines, Flo, Yvonne, Michi, Chris, Steffi, Alan, Lukas, Julia, Nedz und Marie möchte ich für die einzigartige Arbeitsatmosphäre danken. Es war jeden Tag eine Freude, mit euch zusammenzuarbeiten und in zahlreichen konstruktiven Gesprächen chemische Probleme zu diskutieren.

Besonders hervorheben möchte ich noch Karin und Yvonne, die in zahlreichen Arbeitsstunden auch die schwierigsten Kristalle gepickt und deren Kristallstrukturen gelöst haben und damit einen erheblichen Anteil am Erfolg dieser Dissertation haben.

Auch unserer „Rechenfee“ Flo möchte ich für seine Hilfe mit den quantenchemischen Rechnungen meinen ganz besonderen Dank aussprechen. Die zahlreichen Gespräche über diese Problematik werde ich sehr vermissen.

Natürlich danke ich auch meinen Praktikanten Thomas, Denise und Markus für ihren großen praktischen Anteil an dieser Arbeit.

Ohne die Hilfe von Herrn Ober und der kompletten Feinmechanik 1 und 2, Herrn Obst und Herrn Wolf in der Elektrotechnik, Herrn Hartmann, dem Hausmeisterteam, Fuchsi und dem kompletten HLS Team, sowie Michi, Ronald und Heidi in der zentralen Ver- und Entsorgung wäre ein reibungsloser Ablauf dieser Arbeit nicht möglich gewesen.

Wolfgang und Markus möchte ich für ihr offenes Ohr und die zahlreichen nachbarschaftlichen Gespräche auf dem Flur danken.

Mein ganz besonderer Dank gilt Gaby, deren Tür immer offen steht für die täglichen großen und kleinen Probleme, für die unermüdliche Unterstützung bei allen Anliegen. Als Zuhörerin und Ratgeberin warst du einfach unersetzbar.

Meiner Familie und meinen Freunden möchte ich für ihre Unterstützung, Geduld und ihr Verständnis danken.

Zum Schluss möchte ich noch meiner Freundin Kathi für ihr Verständnis, ihre Geduld und ihre Motivationsfähigkeit danken. Du bist einfach in jeder Lebenslage für mich da. Auch waren deine linguistischen Hilfestellungen immer Gold wert.

Table of Contents

Introduction	1
Objectives	7
Summary	8
1. Synthesis of gitonic superelectrophiles	8
1.1. Malononitrile	8
1.2. Malonic Acid	9
1.3. Oxalic Acid	12
1.4. Conclusion	14
2. Examination of Oxocarbon Species in Superacidic Media	15
2.1. <i>p</i> -Benzoquinone	15
2.2. Croconic Acid	16
2.3. Squaric Acid	18
2.4. Conclusion	20
Appendix	21
1 Protonation of Malononitrile in Superacidic Solutions	23
2 Investigation of Malonic Acid in Superacidic Solutions	29
2.1 Supporting Information	37
3 The Tetrahydroxydicarbenium Cation [(HO) ₂ CC(OH) ₂] ²⁺ : Synthesis and Structure	43
3.1 Supporting Information	52
4 Protonation of <i>p</i> -Benzoquinone in Superacidic Solutions	57
5 Investigations on Croconic Acid in Superacidic Media	63
5.1 Supporting Information	70
6 Investigations on Squaric Acid in Superacidic Media	75
6.1 Supporting Information	82

Introduction

Origin of the Term Electrophile

The term nucleophile, that still is in use today, and its antagonist, the electrophile, were introduced by *Ingold* in 1933.^[1,2] Here, the term nucleophile is composed of the word *nucleus* and the Greek word *φίλος* (*philos*), which translates as *to love*. *Ingold's* concept is based on works by *Lewis*, *Lapworth* and *Robinson* from the early 1920s.^[3-6] A basis for the term electrophile was *Lewis'* development of the first proton-independent acid-base concept by defining bases as electron pair donors and acids as electron pair acceptors. In 1925 *Robinson* classified conjugated systems into nine different classes using the terms *crotonoid* (later electrophilic) and *crotenoid* (later nucleophilic).^[5] Simultaneously with *Robinson*, *Lapworth* introduced his classification of reagents into *anionoid* and *cationoid* as they behave the same way like positive and negative ions.^[3] Both *Robinson's* and *Lapworth's* classifications were replaced in 1934 by the current terminology *nucleophile* and *electrophile*.

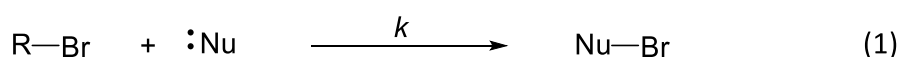
The History of Superelectrophiles

As early as 1901, *Norris*^[7] and *Kehrmann* and *Wentzel*^[8] independently succeeded in the first synthesis of a carbocation and thus the generation of an electrophile. Initially, they investigated the reactions of triphenylmethanol with concentrated sulfuric acid resulting in a strongly colored solution. One year later, *Baeyer* discovered the salt-like character of the orange product of the reaction of triphenylmethyl chloride with aluminum and tin.^[9,10] Decades later the strong coloring of both compounds was attributed to the delocalized electron system of the triphenylmethyl cation. Throughout his studies of *Wagner's* rearrangements of camphene hydrochloride to isobornyl chloride, *Meerwein* discovered in cooperation with *van Emster*, that the isomerization was not achieved by migration of the halogen atom, but by a rearrangement of the cationic intermediate.^[11] With their detailed kinetic and stereochemical investigations of unimolecular nucleophilic substitution (S_N1) and elimination ($E1$) reactions in the late 1920s, *Ingold* and *Hughes* laid the foundation for the role of cationic electron-deficient intermediates in organic chemistry.^[12] In the 1930s *Whitmore*

generalized *Ingold* and *Hughes*' concept describing that the addition of a halogen atom results in a positively charged transition state.^[13] However, at that time, carbocations were generally considered unstable and short-lived because they could not be observed directly. *Olah* made a breakthrough in the early 1960s, by creating carbenium ions in superacidic solutions and kinetically stabilizing them for the first time.^[14-16] Consequently in 1994 he was awarded the Nobel Prize for his work in the field of carbocation research.^[17] One year before *Olah*'s Nobel Prize, *Laube* and *Hollenstein* succeeded in obtaining the first crystal structure of the tertbutyl cation.^[18] Subsequently, it was *Christe* who succeeded in isolating and characterizing various cations as hexafluoride arsenates or hexafluoride antimonates, such as the H₃O⁺ and the H₃S⁺ cation.^[19,20]

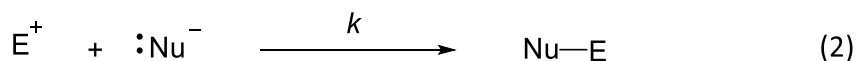
Experimental Quantification of Nucleophilicity and Electrophilicity

In 1953 *Swain* and *Scott* invented the first method to quantify nucleophilicity (Equation 1). Their free-energy relationship relates the pseudo first order reaction rate constant k of a reaction (in water at 25°C), normalized to the reaction rate k_w for a standard reaction with water as the nucleophile, to a nucleophilic constant n for a given nucleophile and to a substrate constant s that represents the sensitivity of a substrate for a nucleophilic attack (defined as 1 for methyl bromide).^[21]



$$\log\left(\frac{k}{k_w}\right) = s \cdot n$$

Later, in 1972, *Ritchie* replaced the substrate dependent constant s and the nucleophilic constant n by the nucleophilicity parameter N_+ (defined as 0 for water) to facilitate the comparison of nucleophiles (Equation 2). This equation assumes that two nucleophiles, irrespective of the properties of the electrophile, react with the same relative reactivity. It thus contradicts the principle of reactivity selectivity. That is why the Ritchie equation is also called the *constant selectivity relationship*.^[22]



$$\log\left(\frac{k}{k_w}\right) = N_+$$

Kane-Maguire and *Sweigart* successfully applied *Ritchie's* relationship to organometallic electrophiles in 1984. In doing so, they created a scale for the electrophilicity of complexes between transition metals and π -hydrocarbons.^[23]

Only in 1994 *Mayr* and *Patz* developed the first equation to quantify electrophilicity, depicted in Equation 3. Instead of n-nucleophiles like *Ritchie* and *Kane-Maguire*, *Mayr* and *Patz* used less reactive π -nucleophiles. This enabled them to even characterize strong electrophiles. Furthermore, they added a third parameter to *Ritchie's* two-parameter equation, the nucleophile-dependent slope parameter s , which is defined as 1 when using 2-methyl-1-pentene as the nucleophile. This slope parameter s , together with the nucleophilicity parameter N and the electrophilicity parameter E (0 for An_2CH^+) exhibit a dependence on the second order reaction rate constant k for a reaction temperature of 20°C.

$$\log k_{20^\circ C} = s(N + E) \quad (3)$$

The electrophilicity E therefore is not an absolute value, as it still is dependent on the choice of the nucleophile N , the solvent and the reaction temperature. Furthermore, the electrophilicity of dications cannot yet be determined from the *Mayr-Patz* equation.^[24]

Preparation of Superelectrophiles

For the generation of a superelectrophile, an electrophile is needed that is able to interact with strong *Brønsted* or *Lewis* acids. Here, the interaction represents an activation which greatly increases the reactivity of the electrophile.^[25] This becomes apparent in the reaction of hydrogen peroxide with ethane, wherein the reactants do not react with each other under standard conditions.^[26] Only the activation of the electrophile by protonation leads to the formation of a superelectrophile that initiates the reaction. Here, the protonation reduces the

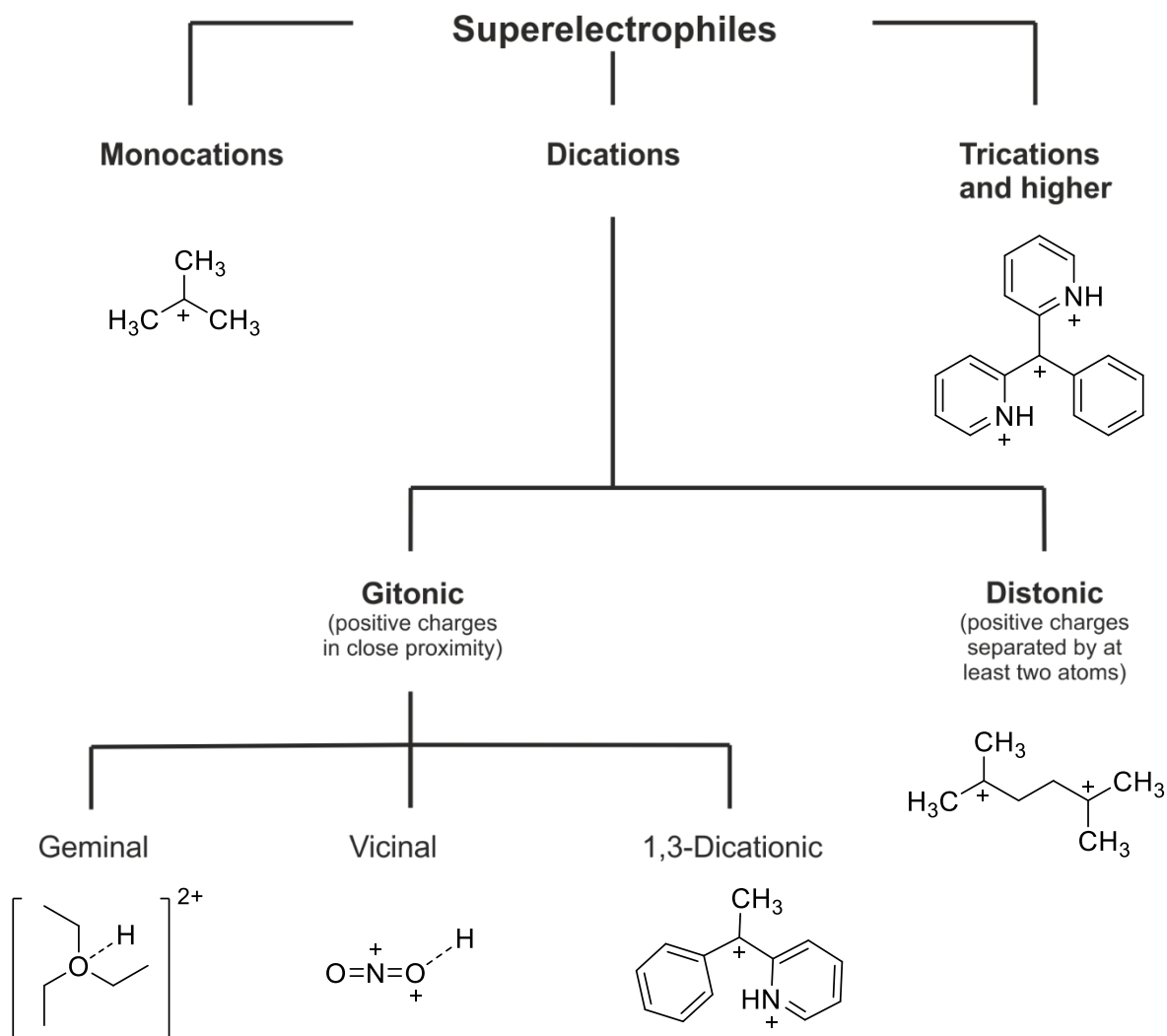
$\text{H}_3\text{C}-\text{CH}_3$ + $\text{H}-\text{O}-\text{O}-\text{H}$ \longrightarrow $\text{H}_3\text{C}-\text{CH}_2\text{OH}$
 HOMO = -9.40 eV LUMO = 0.21 eV

$\text{H}_3\text{C}-\text{CH}_3$ + $\text{H}-\text{O}-\text{O}^+-\text{H}$ $\xrightarrow{-40^\circ\text{C}}$ $\left[\text{H}_3\text{C}-\text{CH}_2\cdots\text{H}\cdots\text{O}-\text{O}-\text{H} \right]^+ \xrightarrow{-\text{H}_3\text{O}^+} \text{H}_3\text{C}-\text{CH}_2\text{OH}$
 HOMO = -9.40 eV LUMO = -9.18 eV
 Superelectrophile

Classification of Superelectrophiles

Only the group of dications can be further divided into gitonic and distonic superelectrophiles. In gitonic superelectrophiles the two charges are in close proximity, whereas in distonic superelectrophiles the charges are separated by at least two carbon or other heavy atoms. The subgroup of gitonic superelectrophiles can in turn be further divided into geminal gitonic, vicinal gitonic and 1,3-dicationic superelectrophiles. In geminal gitonic superelectrophiles both positive charges are located at or around an atom. Vicinal gitonic superelectrophiles

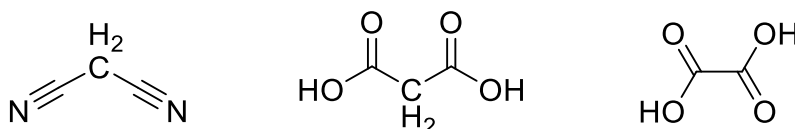
describe a cation in which the two positive charges are adjacent, but located on different atoms. In the case of a 1,3-dicationic superelectrophiles, as the name suggests, the two positive charges are separated by an atom.



- [1] C. Ingold, *J. Chem. Soc.* **1933**, 0, 1120-1127.
- [2] C. Ingold, *Chem. Rev.* **1934**, 15, 225-274.
- [3] A. Lapworth, *Nature* **1925**, 115, 625.
- [4] J. Allan, A. Oxford, J. Smith, R. Robinson. *J. Chem. Soc.* **1926**, 129, 401-411.
- [5] R. Robinson, *J. Soc. Chem. Ind.*, **1925**, 44, 456.
- [6] G. Lewis, *Valence and Structure of Molecules*, The chemical catalogue Co., Inc., New York, **1923**.
- [7] J. Norris, *Am. Chem. J.* **1901**, 25, 117-122.
- [8] F. Kehrman, F. Wentzel, *Ber. Dtsch. Chem. Ges.* **1901**, 34, 3815-3819.
- [9] A. Baeyer, V. Villiger *Ber. Dtsch. Chem. Ges.* **1902**, 35, 1189-1201.
- [10] A. Baeyer, *Ber. Dtsch. Chem. Ges.* **1905**, 38, 569-590.
- [11] H. Meerwein, K. van Emster, *Ber. Dtsch. Chem. Ges.* **1922**, 55, 2500-2528.
- [12] C. Ingold, *Structure and Mechanism in Organic Chemistry*, Cornell Univ. Press, Ithaca, NY, **1953**.
- [13] F. Whitmore, *J. Am. Chem. Soc.* **1932**, 54, 3274-3283.
- [14] G. Olah, S. Kuhn. W. Tolgbesi. E. Baker. *J. Am. Chem. Soc.* **1962**, 84, 2733-2740.
- [15] G. Olah, E. Baker, J. Evans, W. Tolgyesi, J. McIntyre, I. Bastien, *J. Am. Chem. Soc.* **1963**, 86, 1360-1373.
- [16] G. Olah, G. Prakash, A. Molnar, J. Sommer, *Superacid Chemistry*, John Wiley& Sons, Inc, New Jersey, 2. Ed., **2009**.
- [17] G. Olah, *Angew. Chem. Int. Ed. Engl.* **1995**, 34, 1393-1405.
- [18] S. Hollenstein, T. Laube, *J. Am. Chem. Soc.* **1993**, 115, 7240-7245.
- [19] K. Christe, C. Shack, R. Wilson, *Inorg. Chem.* **1975**, 14, 2224-2230.
- [20] K. Christe, P. Charpin, E. Soulie, R. Bougon, J. Fawcett, D. Russel, *Inorg. Chem.* **1984**, 23, 3756-3766.
- [21] C. Swain, C. Scott, *J. Am. Chem. Soc.* **1953**, 75, 141-147.
- [22] C. Ritchie, *Acc. Chem. Res.* **1972**, 5(10), 348-354.
- [23] L. Kane-Maguire, E. Honig, D. Sweigart, *Chem. Rev.* **1984**, 84, 525-543.
- [24] H. Mayr, M. Patz, *Angew. Chem. Int. Ed. Engl.* **1994**, 33, 938-957.
- [25] G. Olah, *Angew. Chem.* **1993**, 105, 805-827.
- [26] H. Shi, Y. Wang, Z. Zhang, *J. Mol. Catal. A-Chem.*, **2006**, 258, 35-45.
- [27] G. Olah, *Angew. Chem. Int. Ed. Engl.* **1993**, 32, 767-788.
- [28] G. Olah, D. Klumpp, *Superelectrophiles and their Chemistry*, John Wiley& Sons, Inc, New Jersey, 1. Ed., **2008**.
- [29] J. Lehmann, University of Illinois at Urbana-Champaign, *Reactions of Superelectrophiles* **2015**. (http://faculty.scs.illinois.edu/burke/files/group_meetings/JWL_535ppt.pdf) (last downloaded on 10/22/2018)

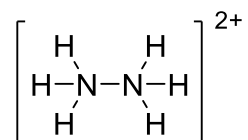
Objectives

This thesis aims to address two issues. Firstly, the behavior of malononitrile, malonic acid and subsequently oxalic acid was examined as to what extent it is possible to prepare, isolate and structurally characterize a vicinal, gitonic superelectrophile based on a carbon framework.



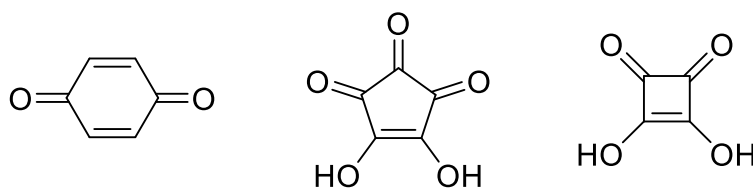
Scheme 3. Lewis structures of malononitrile (left), malonic acid (middle) and oxalic acid (right).

Examining malononitrile and malonic acid in binary superacids, it was initially tested whether it was possible to isolate and characterize 1,3-dicationic gitonic superelectrophiles, which are more stable than vicinal gitonic superelectrophiles. Subsequently, the behavior of oxalic acid in superacidic media was investigated with the aim to isolate and characterize a vicinal, gitonic superelectrophile with a carbon skeleton. At this point it should be noted, that diprotonated hydrazine is the only known vicinal gitonic cation.^[1]



Scheme 4. Cation of the diprotonated hydrazine molecule.

The second issue addresses the behavior of three oxocarbon and oxocarbon-like compounds, namely *p*-benzoquinone, croconic acid and squaric acid, in binary superacidic media. Here, the question whether it was possible to generate polycations from small ring systems in superacidic media, is sought to be answered. Subsequently, it was examined whether a trend regarding ring size and degree of protonation could be deduced.



Scheme 5. Examined oxocarbon and oxocarbon-like compounds.

[1] T. Klapötke, P. White; I. Tornieporth-Oetting, *Polyhedron* **1996**, *15*, 2579-2582.

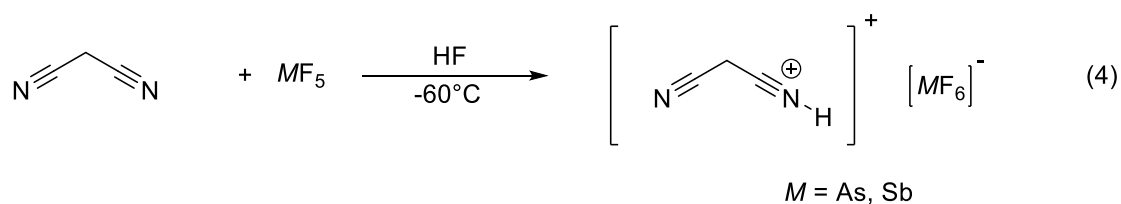
Summary

1. Generating Gtonic Superelectrophiles

This thesis deals with the behavior of small dinitriles and dicarbonic acids in superacidic media regarding the generation of monocations as well as 1,3-dicationic and vicinal superelectrophiles. For this, malononitrile, malonic acid and oxalic acid were reacted in the superacidic media with HF/SbF₅ and HF/AsF₅. The resulting substances were structurally characterized using low-temperature Raman and IR spectroscopy. For an improved structural understanding, the structures and vibrational frequencies of all resultant cations were quantum chemically calculated. In the following, the results are summarized and the crystal structures of the most important compounds are depicted. All compounds were also synthesized as deuterated isotopomers and characterized by vibrational spectroscopy.

1.1. Malononitrile

The monoprotonated salts of malononitrile are synthesized by reacting malononitrile with an equivalent of Lewis acid, as illustrated in Equation 4.



Due to the low thermal stability the salts of the monoprotonated malononitrile could not be further examined by vibrational spectroscopy. Our experimental results were confirmed by the quantum chemical calculations of the monoprotonated cation of malononitrile (Fig. 1), which was conducted using the PBE1PBE/6-311G(3df,3pd) level of theory. It was shown that the [H₂C(CNH)₂]²⁺ cation is by 390 kJ/mol more stable than the [(CN)H₂C(CNH)]⁺ cation.

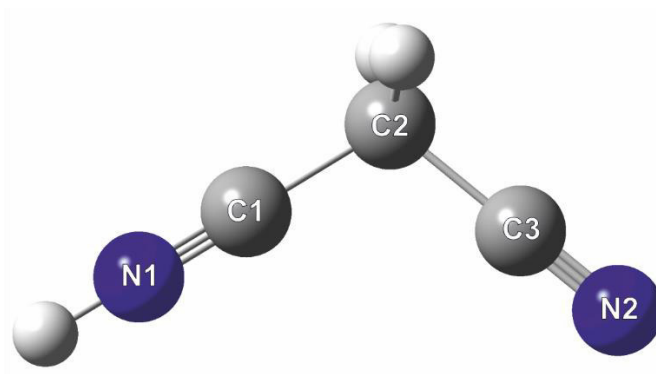
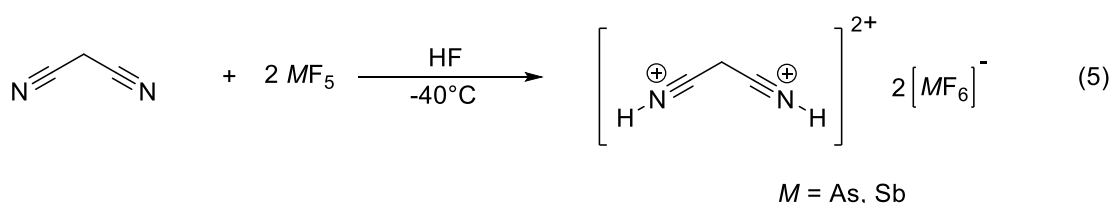


Figure 1. Calculated structure of the $[(\text{CN})\text{H}_2\text{C}(\text{CNH})]^+$ cation.

By increasing the ratio of malononitrile to Lewis acid to 2:1, as depicted in Equation 5, salts of diprotonated malononitrile were synthesized.



In contrast to the monoprotonated salts, the diprotonated salts of malononitrile could be entirely characterized by vibrational spectroscopy despite their thermal instability. Moreover, we succeeded in conducting a single-crystal X-ray structure analysis of the hexafluoroarsenate of the diprotonated malononitrile. Here, the co-crystallized HF molecule, which is highly relevant for the stability of $\text{H}_2\text{C}(\text{CNH})_2[\text{AsF}_6]_2 \cdot \text{HF}$, represents an intriguing characteristic of the structure. Figure 2 depicts the associated short C...F distances ($\text{C2}\cdots\text{F13}$: 2.666(5) Å and $\text{C3}\cdots\text{F13}$: 2.645(4) Å). These short distances suggest a positive charge at the two terminal carbon atoms and thus the successful synthesis of a 1,3-dicationic gitonic superelectrophile. Apart from the synthesis of the 1,3-dicationic gitonic superelectrophile, $[\text{H}_2\text{C}(\text{CNH})_2][\text{AsF}_6]_2 \cdot \text{HF}$ exhibits the shortest C-N distance (N1-C2 : 1.108(4) Å and N2-C3 : 1.109(4) Å) amongst protonated cyano groups.

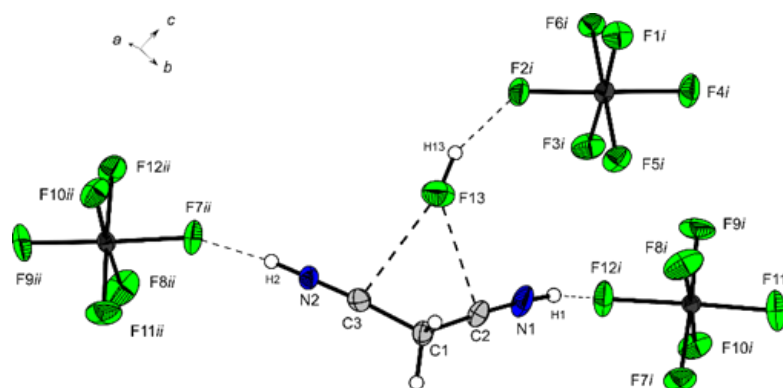
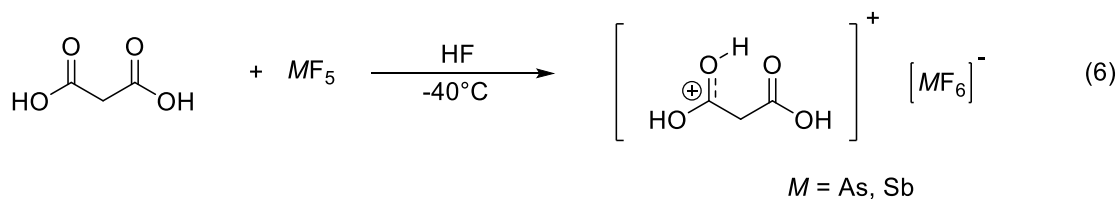


Figure 2. Projection of the interionic contacts between anion and cation of $[H_2C(CNH)_2][AsF_6]_2 \cdot HF$ (50% probability displacement ellipsoids). Symmetry codes: $i = x, 0.5-y, 0.5+z$ and $ii = 1-x, -y, -z$.

1.2. Malonic acid

As a consequence of the successful diprotonation of malononitrile, malonic acid was examined under the same reaction conditions (Equation 6 and 7).



Here, the monoprotection of malonic acid leads to an intriguing six-membered ring-like structure of the $[H_2C(CNH)_2][AsF_6]_2 \cdot HF$ cation. Throughout the protonation process, an intramolecular hydrogen bond ($O_3-H_3 \cdots O_1$) is built between the two carbonyl oxygens. The structure was characterized using vibrational spectroscopy. The almost planar cation structure of the crystal structure of $[H_2C(CNH)_2][AsF_6]$ (Fig. 3) was confirmed as a global minimum by quantum chemical calculations using the MP2/aug-cc-pVTZ level of theory. Further possible structural isomers turned out to be energetically less stable.

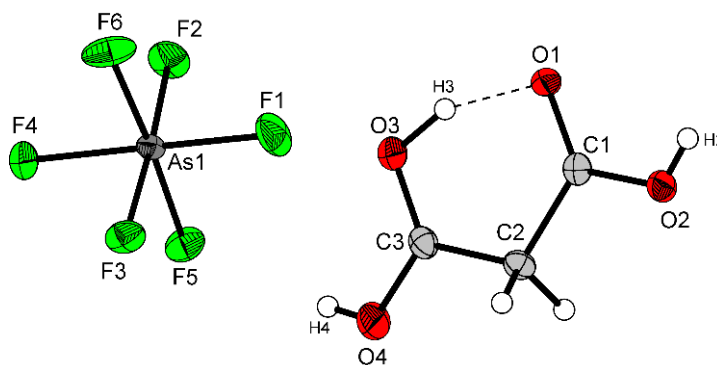
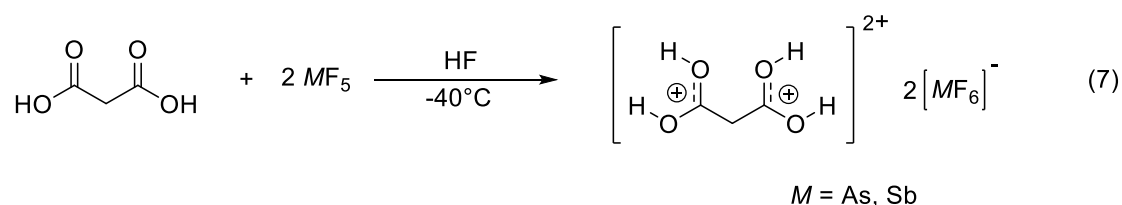


Figure 3. Asymmetric unit of $[\text{HOOCH}_2\text{C}(\text{OH})_2][\text{AsF}_6]$.

The salts of diprotonated malonic acid were synthesized by increasing the molar ratio of Lewis acid to malonic acid to 2:1, shown in Equation 7.



Here, we succeeded in the synthesis of a 1,3-dicationic gitionic superelectrophile. The resulting superelectrophiles were examined and entirely characterized by vibrational spectroscopy. Moreover, we succeeded in recording a single-crystal X-ray structure of $[(\text{HO})_2\text{CCH}_2\text{C}(\text{OH})_2][\text{AsF}_6]_2$, which is depicted in Figure 4. For a complete characterization, quantum chemical calculations of the $[(\text{HO})_2\text{CCH}_2\text{C}(\text{OH})_2]^{2+}$ cation were conducted on the MP2/aug-cc-pVTZ level of theory and the resulting geometric parameters were compared with the experimental ones.

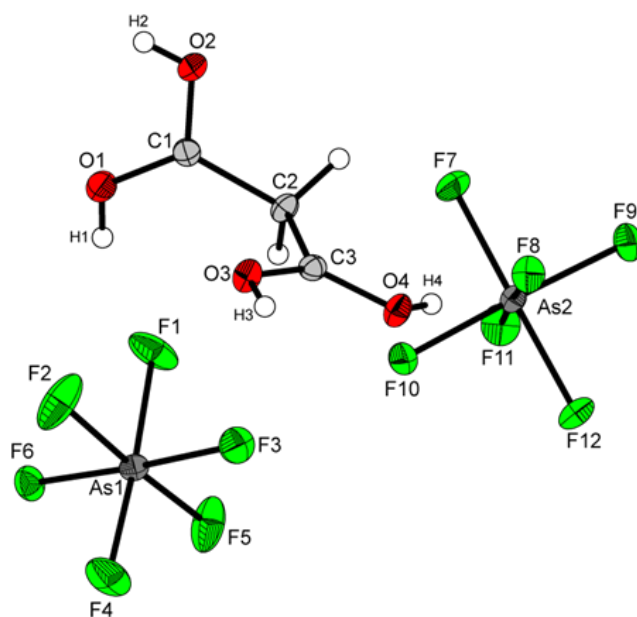
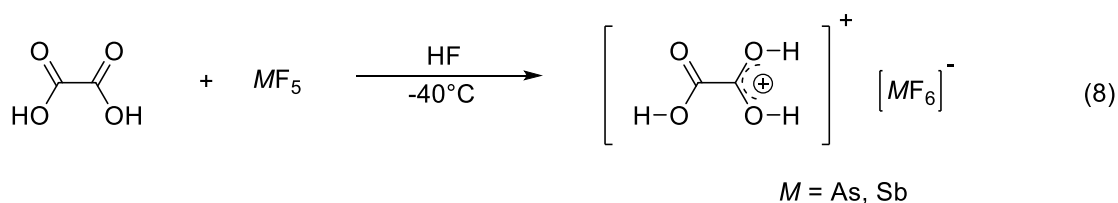


Figure 4. Asymmetric unit of $[(HO)_2CCH_2C(OH)_2][AsF_6]_2$.

1.3. Oxalic Acid

Analogously to the two aforementioned compounds, oxalic acid was reacted with an equimolar ratio of Lewis acid in the two binary superacidic systems HF/SbF₅ and HF/AsF₅, which is illustrated in Equation 8.



The resultant salts of monoprotonated oxalic acid were entirely characterized by vibrational spectroscopy. Furthermore, in the case of $[\text{HOCC}(\text{OH})_2][\text{AsF}_6]$ it was possible to conduct a single-crystal X-ray structure analysis (Fig. 5). Surprisingly, in the elementary cell of the structure, two symmetrically independent formula units of $[\text{HOCC}(\text{OH})_2][\text{AsF}_6]$ were found. In addition, a quantum chemical calculation was performed for the $[\text{HOCC}(\text{OH})_2]^+$ cation using the B3LYP/aug-cc-pVTZ level of theory.

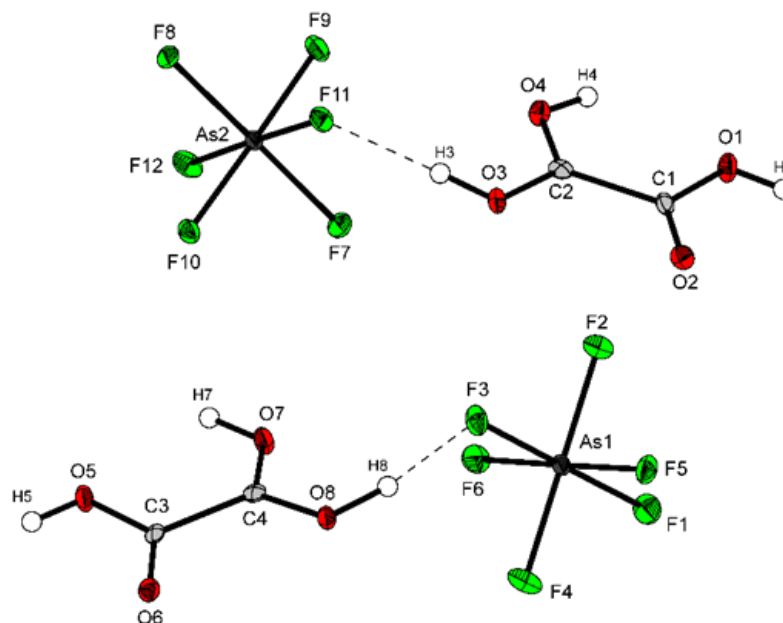
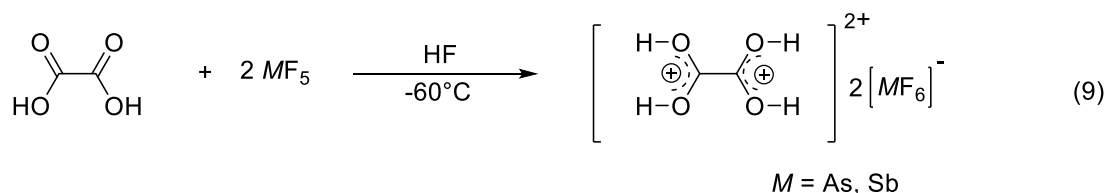


Figure 5. Projection of the asymmetric unit of $[\text{HOOCC}(\text{OH})_2][\text{AsF}_6]$ (50% probability displacement ellipsoids). Hydrogen bonds are drawn as dashed lines.

With the synthesis of the 1,3-dicationic gitonic superelectrophiles of the salts of diprotonated malonic acid being successful, the salts of the diprotonated oxalic acid were generated analogously. Solely the reaction temperature was reduced to -60°C , due to the expected increase in reactivity of the vicinal gitonic superelectrophile.



The resultant diprotonated salts of oxalic acid could be isolated and characterized by vibrational spectroscopy. In case of $[(\text{HO})_2\text{CC}(\text{OH})_2][\text{SbF}_6]_2$, it was possible to conduct a single-crystal X-ray structure analysis, as depicted in Figure 6. Here, as already found for $[\text{H}_2\text{C}(\text{CNH})_2][\text{AsF}_6]_2 \cdot \text{HF}$, a very short $\text{C} \cdots \text{F}$ distance was measured.

In addition to this, an MEP analysis together with the NPA charges of $[(\text{OH})_2\text{CC}(\text{OH})_2]^{2+}$, $[(\text{OH})_2\text{CC}(\text{OH})_2]^{2+} \cdot 6\text{HF}$ and oxalic acid were calculated, on the B3LYP/aug-cc-pVTZ-level of theory to locate the positive charge. Surprisingly, the protonation of oxalic acid does not lead to a remarkable change of the C-C bond length, which is discussed for the entire series of the oxalic skeleton, starting with the dianion and ending with the

tetrahydroxy dication. A former crystal structure of diprotonated oxalic acid published by *Minkwitz et al.* is thus more correctly described as $[\text{H}_5\text{O}_2]_2[\text{SbF}_6]_2 \cdot \text{C}_2\text{O}_4\text{H}_2$.

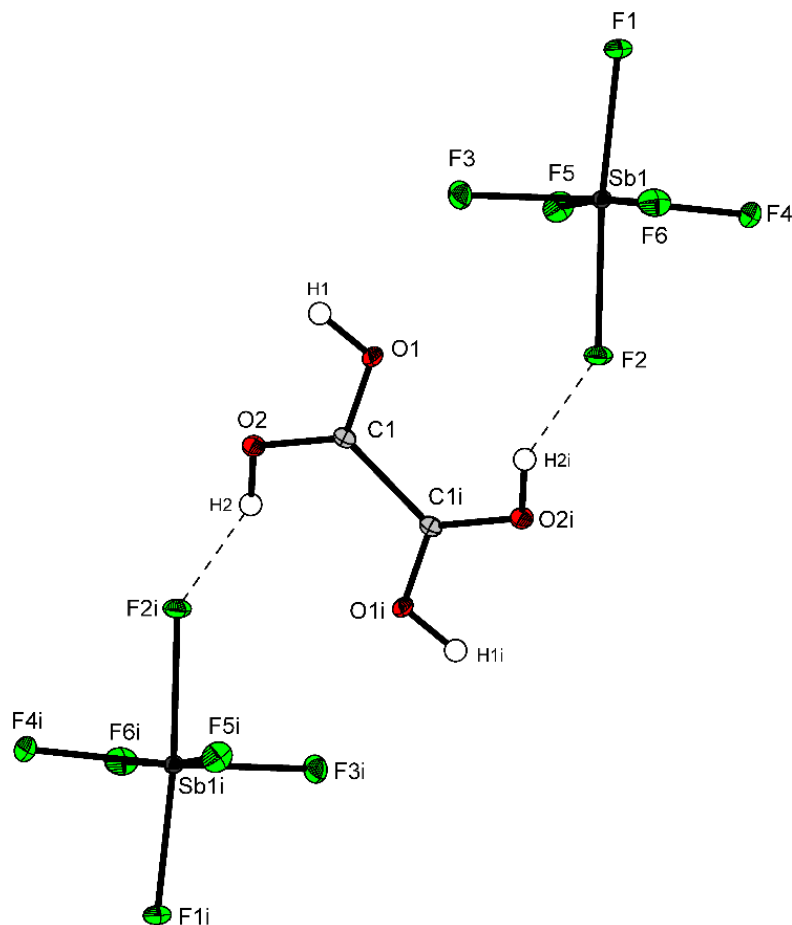


Figure 6. Projection of the formula unit of $[(\text{HO})_2\text{CC}(\text{OH})_2][\text{SbF}_6]_2$ (50% probability displacement ellipsoids). Hydrogen bonds are drawn as dashed lines. Symmetry code: $i = 1-x, -y, 1-z$.

1.4. Conclusion

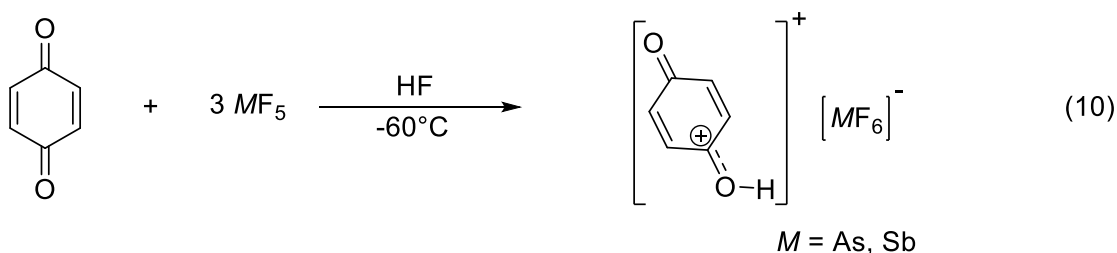
We succeeded in synthesizing and structurally characterizing a 1,3-dicationic superelectrophile starting from the simplest, under standard conditions solid, dinitrile, namely malononitrile. Subsequently it was possible to repeat the synthesis of the salts of diprotonated malonic acid. Hence, the simplest 1,3-dicationic superelectrophile with an oxocarbon framework could be isolated and characterized. Based on these results, we succeeded in isolating and structurally characterizing the simplest superelectrophile with an oxocarbon framework – the tetrahydroxy dicarbenium salts.

2. Examination of Oxocarbon and Oxocarbon-like Species in Superacidic Media

The second issue of this thesis addresses the behavior of ring-shaped oxocarbon and oxocarbon-like compounds in the binary superacidic systems HF/SbF₅ and HF/AsF₅. For this, *p*-benzoquinone, croconic acid and squaric acid were examined regarding their degree of protonation. For an enhanced structural understanding, the structures and vibrational frequencies of all resulting cations were quantum chemically calculated. In the following, the results are summarized, and the crystal structures of the most significant compounds are depicted. All compounds were synthesized as deuterated isotopomers and examined by vibrational spectroscopy.

2.1. *p*-Benzoquinone

p-Benzoquinone was reacted in the superacidic media HF/SbF₅ and HF/AsF₅, according to the following Equation 10.



As a consequence of the dark green color of the product, the salts of the protonated *p*-benzoquinone, [OC₆H₄(OH)][MF₆] (*M* = As, Sb), could only be examined spectroscopically by infrared spectroscopy. The conducted single-crystal X-ray structure analysis of monoprotonated *p*-benzoquinone [OC₆H₄(OH)][SbF₆] (Fig. 7) shows that the structure can better be described as double hemi-protonated. In spite of a significant increase of the acid strength, no higher protonated species of *p*-benzoquinone could be isolated.

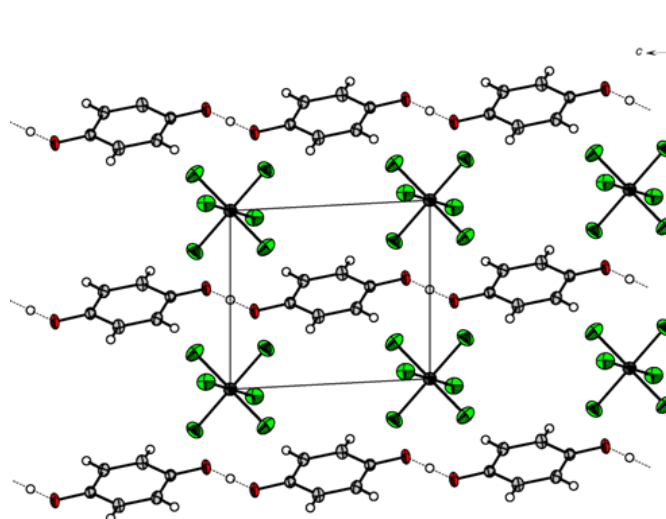
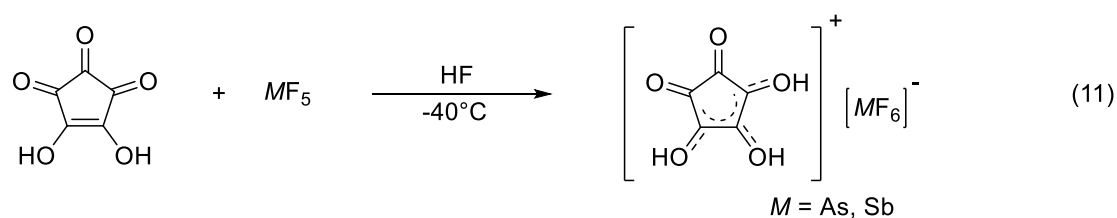


Figure 7. Crystal packing of $[\text{OC}_6\text{H}_4(\text{OH})][\text{SbF}_6]$. Hydrogen bonds are drawn as dashed lines. (50% probability displacement ellipsoids).

Symmetry codes: $i = 1-x, 1-y, 1-z$; $ii = -x, -y, -z$.

2.2. Croconic Acid

Based on the results of chapter 2.1, the behavior of croconic acid in binary superacidic media was examined, as shown in Equation 11.



The resultant salts of monoprotonated croconic acid were structurally characterized by IR- as well as Raman spectroscopy. Furthermore, we succeeded in recording a single-crystal X-ray structure of $[\text{H}_3\text{O}_5\text{C}_5][\text{AsF}_6]$, which is depicted in Figure 8. Moreover, quantum chemical calculations were conducted on the PBE1PBE/6-311G++(3df,3pd) level of theory.

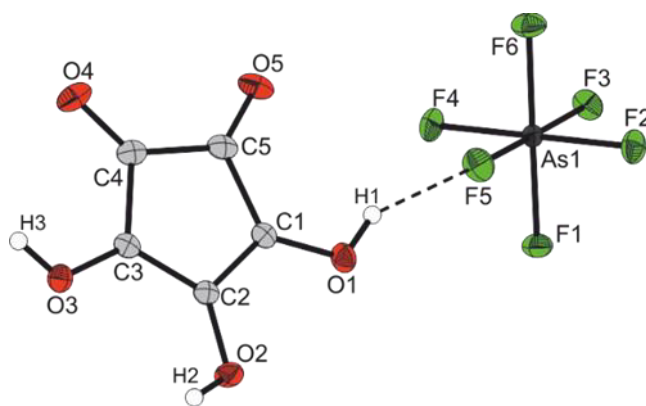
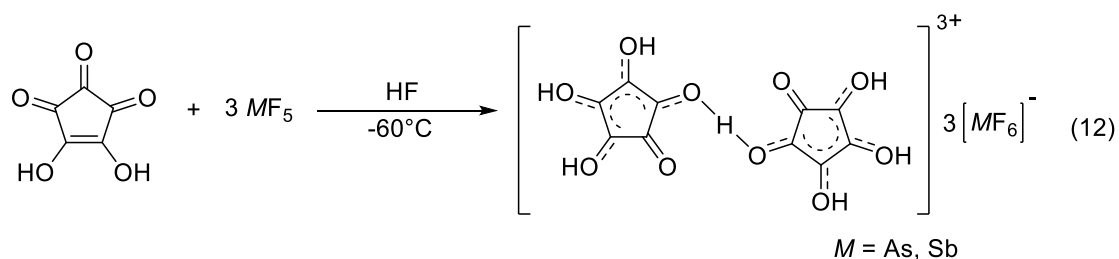
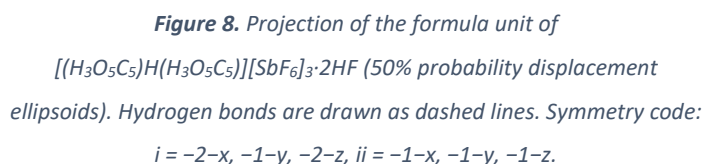


Figure 8. Projection of the formula unit of $[H_3O_5C_5][AsF_6]$ (50% probability displacement ellipsoids). Hydrogen bonds are drawn as dashed lines.

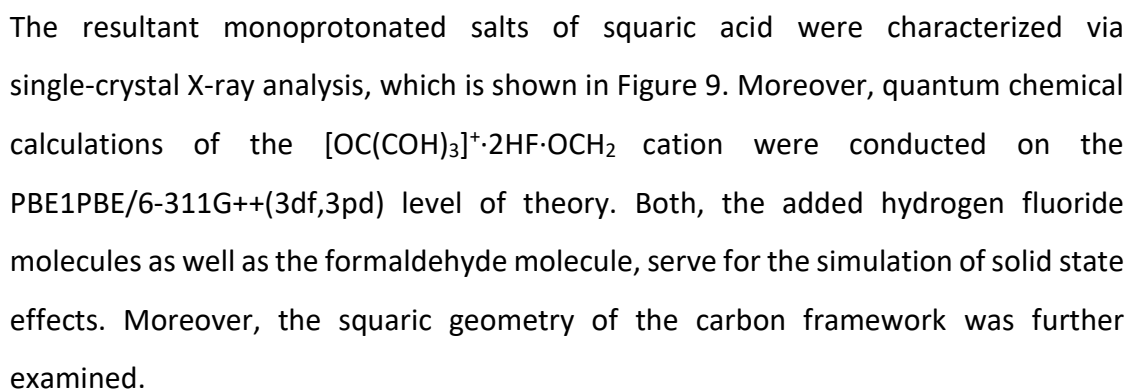
Surprisingly the increase of the ratio of Lewis acid to croconic acid to 3:1 did not lead to the diprotonated salts of croconic acid, but instead to sesquiprotonated salts of croconic acid, as illustrated in Equation 12.



Here, a single-crystal X-ray structure of $[(H_3O_5C_5)H(H_3O_5C_5)][SbF_6]_3 \cdot 2HF$ could be recorded. A higher degree of protonation could not be achieved despite an increased acid strength.



Apart from croconic acid, another oxocarbon compound, squaric acid, was examined regarding its behavior in binary superacidic media. For this, squaric acid was reacted according to the following Equation 13.



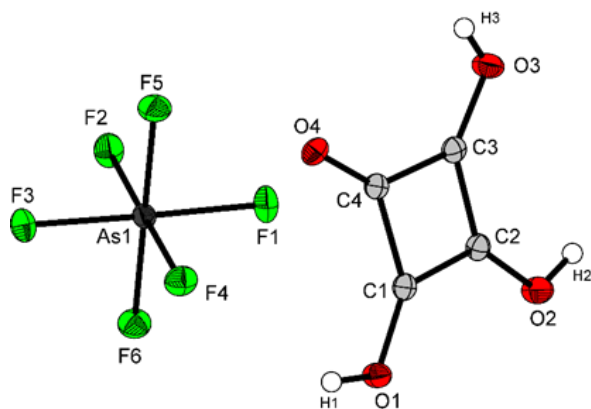
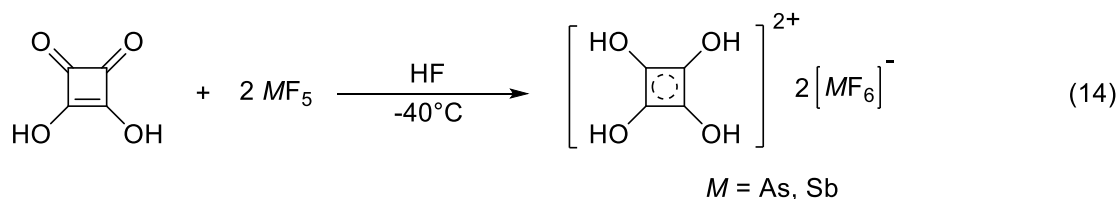


Figure 9. Projection of the interionic contacts between anions and cations of $[\text{OC}(\text{COH})_3][\text{AsF}_6]$ (50% probability displacement ellipsoids).

By further increasing the acid strength, salts of diprotonated squaric acid were synthesized according to Equation 14.



The resulting hexafluoroarsenate and hexafluoroantimonate of the protonated species were entirely characterized by vibrational spectroscopy. In addition, a single-crystal X-ray structure was recorded for $[(\text{COH})_4][\text{AsF}_6]_2 \cdot 2\text{HF}$, which is depicted in Figure 10. With the help of this analysis and the quantum chemical calculations of the $[(\text{COH})_4]^{2+} \cdot 4\text{HF}$ cation on the PBE1PBE/6-311G++(3df,3pd) level of theory, 2π -aromaticity was proven. To the best of our knowledge, this is the first example of a prepared and isolated 2π -aromatic four-membered ring structure.

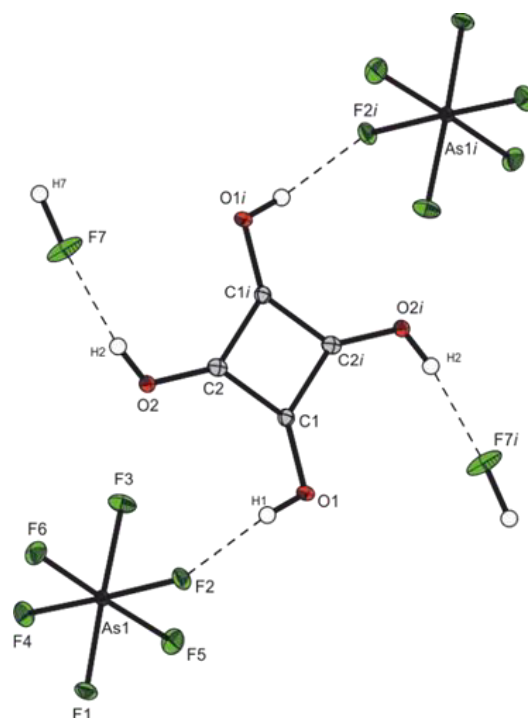


Figure 10. Projection of the interionic contacts between anions and cations of $[(\text{COH})_4][\text{AsF}_6]_2 \cdot 2\text{HF}$ (50% probability displacement ellipsoids).

Symmetry code: $i = 2-x, 1-y, 1-z$.

2.4. Conclusion

In consequence of the above-described examinations, a relationship between ring size and degree of protonation could be found for our reaction conditions. Here, the degree of protonation of the compound decreases with an increasing ring size. Higher degrees of protonations, such as tri- or higher-protonated compounds, could not be observed with our experimental techniques.

Appendix

The following appendix contains the list of publications, which are already published, in press or submitted during this dissertation. The publications are thematically listed. In the first part publications dealing with the generation of superelectrophiles from small dinitriles and dicarboxylic acids and their structural investigation are listed. The second part contains publications dealing with the investigation of oxocarbon species in superacidic media.

Publications

1. Protonation of Malononitrile in Superacidic Solutions, M. Schickinger, Y. Morgenstern, K. Stierstorfer, A. Kornath, *Z. anorg. allg. Chem.*, **2017**, 643 (21), 1431-1435.
(DOI: 10.1002/zaac.201700220)
2. Investigation of Malonic Acid in Superacidic Solutions, M. Schickinger, F. Zischka, K. Stierstorfer, A. Kornath, *Euro. J. Org. Chem.* **2018**, in press.
(DOI: 10.1002/ejoc.201801382)
3. The Tetrahydroxydicarbenium Cation $[(\text{HO})_2\text{CC}(\text{OH})_2]^{2+}$: Synthesis and Structure, M. Schickinger, T. Saal, F. Zischka, J. Axhausen, Y. Morgenstern, K. Stierstorfer, A. Kornath, *ChemistrySelect* **2018**, 3 (43), 12396-12404.
(DOI: 10.1002/slct.201802456)
4. Protonation of *p*-Benzoquinone in Superacidic Solutions, M. Schickinger, M. Siegert, Y. Morgenstern, F. Zischka, K. Stierstorfer, A. Kornath, *Z. anorg. allg. Chem.*, **2018**, 644 (23), 1564-1569.
(DOI: 10.1002/zaac.201800394)

5. Investigations on Croconic Acid in Superacidic Media, M. Schickinger, C. Jessen, Y. Morgenstern, K. Muggli, F. Zischka, A. Kornath, *Euro. J. Org. Chem.* **2018**, 45, 6223-6229.

(DOI: 10.1002/ejoc.201801035)

6. Investigations on Squaric Acid in Superacidic media, M. Schickinger, D. Cibu, F. Zischka, K. Stierstorfer, C. Jessen, A. Kornath, *Chem. Eur. J.* **2018**, 24, 13355-13361.

(DOI: 10.1002/chem.201802516)

Poster contributions

1. Squaric Acid in Super Acids, M. Schickinger, A. Kornath, **2015**, *International Chemical Congress of Pacific Basin Societies*, Honolulu, Hawaii.
2. *p*-Benzoquinone in Super Acids, M. Schickinger, A. Kornath, **2015**, *21th International Symposium on Fluorine Chemistry*, Como, Italy.
3. Protonation of Malonic Acid: Preparation and Characterization of the Mono- and Diprotonated Malonic Acid, M. Schickinger, A. Kornath, **2013**, *17th European Symposium on Fluorine Chemistry*, Paris, France.

Protonation of Malononitrile in Superacidic Solutions

Manuel Schickinger,^[a] Yvonne Morgenstern,^[a] Karin Stierstorfer,^[a] and Andreas Kornath*^[a]

Dedicated to Professor Wolfgang Schnick on the Occasion of his 60th Birthday

Abstract. Malononitrile reacts in superacidic solutions HF/MF₅ (*M* = As, Sb) with formation of the corresponding salts [H₂C(CNX)₂][MF₆]₂ (*M* = As, Sb; *X* = H, D). The occurrence of double protonation is strongly dependent on the stoichiometric ratio of the Lewis acid with regard to malononitrile. Deuterated species were obtained by replacing hydrogen fluoride with deuterium fluoride. The double protonated salts

were characterized by vibrational spectroscopy and in the case of [H₂C(CNH)₂][AsF₆]₂·HF (**3**) by a single-crystal X-ray structure analysis. The salt crystallizes in the monoclinic space group *P*2₁/*c* with four formula units per unit cell. The vibrational spectra were compared to quantum chemical calculations of the free cation [(CN)₂H₂C(CNH)]⁺.

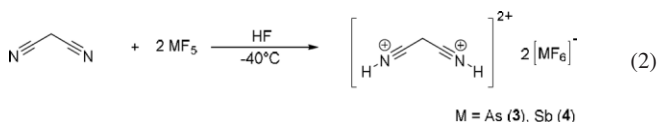
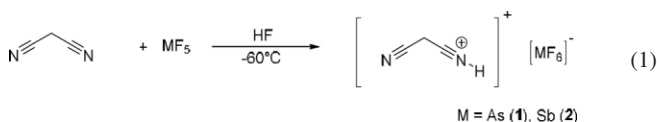
Introduction

Cyanomethane, better known as acetonitrile, is known to be a suitable aprotic solvent in organic and inorganic chemistry. Olah et al. already reported the existence of protonated acetonitrile by nuclear magnetic resonance spectroscopy in 1968, which was confirmed by Haiges et al. in 2016.^[1,2] As a consequence, the question concerning the behavior of dicyanomethane in superacidic media was raised. The previous experiments on acetonitrile suggest the existence of the [(CN)₂H₂C(CNH)]⁺ cation or at least the [H₂C(CNH)₂]²⁺ cation. In the course of our studies, we examined malononitrile in binary superacidic solutions with the aim of isolating and characterizing the mono- and diprotonated species.

Results and Discussion

Synthesis and Properties of [(CN)₂H₂C(CNH)][MF₆] and [H₂C(CNH)₂][MF₆]₂ (*M* = As, Sb)

The syntheses were carried out according to Equation (1) and Equation (2) as two-step reactions:



* Prof. Dr. A. Kornath
Fax: +49-89-2180-77867
E-Mail: andreas.kornath@cup.uni-muenchen.de

[a] Department Chemie
Ludwig-Maximilians-Universität München
Butenandtstr. 5–13(D)
81377 München, Germany

Initially the superacidic systems HF/AsF₅ and HF/SbF₅ were prepared using an excess of hydrogen fluoride. In order to achieve a complete solvation of the Lewis acid, the mixture was homogenized at –20 °C. Following this, malononitrile was added to the frozen superacidic system in an inert gas atmosphere. The reaction mixture was slowly warmed up to –40 °C, resulting in an immediate formation of the protonated species. After the removal of the excess of aHF at –78 °C in vacuo, the air- and temperature-sensitive salts remained as colorless solids with quantitative yield. The single protonated salts of malononitrile [(CN)₂H₂C(CNH)][AsF₆] (**1**) and [(CN)₂H₂C(CNH)][SbF₆] (**2**) are stable up to –60 °C and the double protonated salts [H₂C(CNH)₂][AsF₆]₂ (**3**) as well as [H₂C(CNH)₂][SbF₆]₂ (**4**) are stable up to –20 °C. Due to the low thermal stability, single protonated malononitrile could not be further characterized by vibrational spectroscopy.

Choosing the superacidic system DF/AsF₅ instead of HF/AsF₅ leads to the corresponding salts, [(CN)₂H₂C(CND)][AsF₆] (**5**) and [H₂C(CND)₂][AsF₆]₂ (**6**), respectively.

Vibrational Spectra of 3, 4, 6 and 9

The infrared and Raman spectra of [H₂C(CNH)₂][AsF₆]₂ (**3**), [H₂C(CNH)₂][SbF₆]₂ (**4**), and [H₂C(CND)₂][AsF₆]₂ (**6**) are illustrated in Figure 1 and the observed frequencies are summarized in Table 1 together with the quantum chemically calculated frequencies. According to the calculated structure of the [H₂C(CNH)₂]²⁺ cation of C_s symmetry, 21 fundamental vibrations are expected, of which 15 are Raman and 17 are infrared active. The assignment of the vibrations was performed by analyzing the Cartesian displacement coordinates of the calculated vibrational modes.^[3]

The IR spectrum of [H₂C(CNH)₂][AsF₆]₂ exhibits a ν(NH) vibration at 3603 cm^{–1}, which implies a successful protonation of the nitrogen of the cyanide group. This assumption is supported by a ν(ND) vibration of the deuterated species (**6**). The ν(ND) vibration is detected at 2534 cm^{–1} (Raman) and 2402 cm^{–1} (IR), respectively, and is in good agreement with

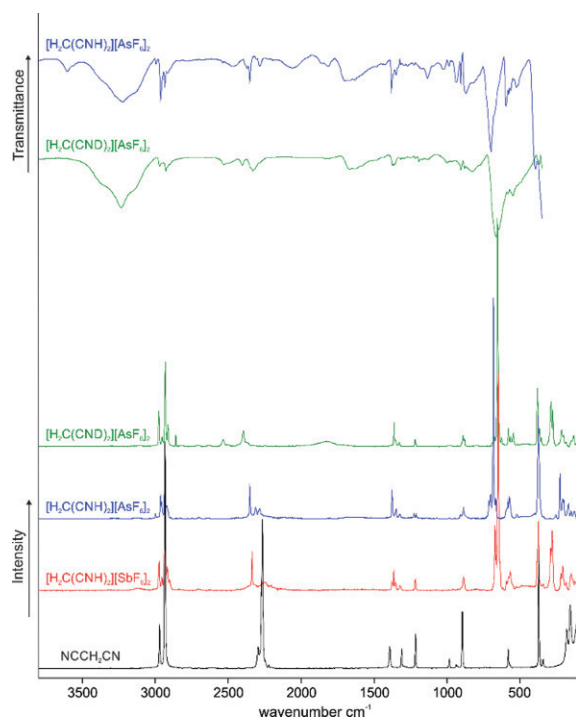


Figure 1. Low temperature Raman spectra of $\text{CH}_2(\text{CN})_2$, $[\text{H}_2\text{C}(\text{CNH})_2][\text{SbF}_6]$, $[\text{H}_2\text{C}(\text{CNH})_2][\text{AsF}_6]$, and $[\text{H}_2\text{C}(\text{CND})_2][\text{AsF}_6]$, and IR spectra of $[\text{H}_2\text{C}(\text{CND})_2][\text{AsF}_6]$ and $[\text{H}_2\text{C}(\text{CNH})_2][\text{AsF}_6]$.

Table 1. Experimental vibrational frequencies $/\text{cm}^{-1}$ of $[\text{CH}_2(\text{CNH})_2][\text{SbF}_6]$, $[\text{CH}_2(\text{CNH})_2][\text{AsF}_6]$, and $[\text{CH}_2(\text{CND})_2][\text{AsF}_6]$, and calculated vibrational frequencies $/\text{cm}^{-1}$ of $[\text{CH}_2(\text{CNH})_2]^{2+}$ and $[\text{CH}_2(\text{CND})_2]^{2+}$.

$[\text{CH}_2(\text{CNH})_2][\text{SbF}_6]$ Raman	$[\text{CH}_2(\text{CNH})_2][\text{AsF}_6]$ IR	$[\text{CH}_2(\text{CNH})_2][\text{AsF}_6]$ Raman	$[\text{CH}_2(\text{CND})_2][\text{AsF}_6]$ IR	$[\text{CH}_2(\text{CND})_2][\text{AsF}_6]$ Raman	$[\text{CH}_2(\text{CNH})_2]^{2+}$ calcd. ^{a)} (IR/Raman)	$[\text{CH}_2(\text{CND})_2]^{2+}$ calcd. ^{a)} (IR/Raman)	Assignment
	3603(w)				3551(338/32) 3537(1463/4)		$\nu(\text{NH})$ $\nu(\text{NH})$
2973(13) 2932(33)	2962(m) 2934(w)	2964(10) 2933(21)	2958(m) 2917(m)	2959(26) 2932(22), 2919(72) 2534(2)	3016(119/39) 2975(153/120)	3016(120/39) 2978(96/117)	$\nu_{\text{as}}(\text{CH}_2)$ $\nu_{\text{s}}(\text{CH}_2)$
2337(18) 2246(4)	2351(m) 2285(w)	2351(15) 2312(5), 2285(4)	2402(w) 2331(m)	2396(6)	2443(12/139) 2437(5/35)	2828(224/18) 2816(740/4) 2217(19/113) 2216(84/28)	$\nu(\text{ND})$ $\nu(\text{ND})$ $\nu(\text{CN})$ $\nu(\text{CN})$
1379(4), 1366(10) 1353(4) 1219(5)	1382(m) 1351(w)	1378(13) 1351(4) 1227(3)	1374(m) 1317(vw) 1218(vw)	1364(10) 1328(2) 1220(3)	1366(48/6) 1354(1/1) 1238(0/1)	1366(47/6) 1353(1/1) 1238(0/1)	$\delta(\text{CH}_2)$ $\omega(\text{CH}_2)$ $\tau(\text{CH}_2)$?
890(6)	1135(m) 987(vw) 907(m) 1199(s)	889(5)	906(m) 881(w)	892(5)	985(1/0) 904(5/0) 881(0/3) 720(188/0) 715(53/0) 677(265/0) 675(0/1) 583(17/2)	976(2/0) 904(9/0) 876(0,3/3)	$\nu_{\text{as}}(\text{CC})$ $\rho(\text{CH}_2)$ $\nu_{\text{s}}(\text{CC})$ $\delta(\text{CNH})$ $\delta(\text{CNH})$ $\delta(\text{CNH})$ $\delta(\text{CNH})$ $\delta(\text{CCC})$ $\delta(\text{CND})$ $\delta(\text{CND})$ $\delta(\text{CND})$ $\delta(\text{CND})$ $\delta(\text{CCN})$ $\delta(\text{CCN})$ $\delta(\text{CCN})$ $\delta(\text{CCN})$ Lattice $\delta(\text{CCN})$
665(17) 595(5)	597(s)	668(9) 583(9)	585(vw) 550(w)	581(7) 567(4) 547(5)	399(0/3) 368(7) 355(3) 217(7) 133(5)	610(24/2) 566(20/1) 534(0/1) 529(108/0) 519(72/1) 374(0/2) 369(8/1) 330(27/0,4)	$\nu_{\text{as}}(\text{CC})$ $\rho(\text{CH}_2)$ $\nu_{\text{s}}(\text{CC})$ $\delta(\text{CNH})$ $\delta(\text{CNH})$ $\delta(\text{CNH})$ $\delta(\text{CNH})$ $\delta(\text{CCC})$ $\delta(\text{CND})$ $\delta(\text{CND})$ $\delta(\text{CND})$ $\delta(\text{CCN})$ $\delta(\text{CCN})$ $\delta(\text{CCN})$ $\delta(\text{CCN})$ Lattice $\delta(\text{CCN})$
375(32) 221(8) 152(8)	701 (vs, br) 579 (vw) 396 (w)	337(46) 228(20) 152(3) 704 (11) 683 (100) 575 (10) 370 (34)	373(m)	382(25) 368(7) 355(3) 217(7) 133(5)	150(3/5)	140(2/4)	$[\text{AsF}_6]^-$ $[\text{AsF}_6]^-$ $[\text{AsF}_6]^-$ $[\text{AsF}_6]^-$ $[\text{SbF}_6]^-$ $[\text{SbF}_6]^-$ $[\text{SbF}_6]^-$ $[\text{SbF}_6]^-$
673 (30) 650 (100) 571 (9) 282 (28)			664(s)	677(4) 654(100) 288(19) 571(28)			$[\text{AsF}_6]^-$ $[\text{SbF}_6]^-$ $[\text{SbF}_6]^-$ $[\text{SbF}_6]^-$

a) Calculated at the PBE1PBE/6-311G(3df,3pd) level of theory. IR intensity in $\text{km}\cdot\text{mol}^{-1}$ and Raman intensity in $\text{\AA}^4\cdot\mu^{-1}$. Abbreviations for IR intensities: v = very, s = strong, m = medium, w = weak. Raman activity is stated to a scale of 1 to 100.

the Teller-Redlich rule for an H/D isotopic effect.^[4] The $\nu(\text{CN})$ vibrations of **3** and **4** are blue-shifted by 56 cm^{-1} and 42 cm^{-1} compared to the unprotonated malononitrile (**9**). A shift to higher wavenumbers indicates a stronger $\text{C}\equiv\text{N}$ bond. This result is in good agreement with the data obtained from the crystal structure and the results of Haiges et al.^[2]

For the anions $[\text{MF}_6]^-$ ($M = \text{As}, \text{Sb}$) with an ideal octahedral symmetry two bands in the IR spectrum and three lines in the Raman spectrum are expected. In both cases, more than five vibrations are observed. This indicates a lower symmetry, which is in accordance with the crystal structure analysis.

Crystal Structure of $[\text{H}_2\text{C}(\text{CNH})_2][\text{AsF}_6]$

The diprotonated malononitrile salt $[\text{H}_2\text{C}(\text{CNH})_2][\text{AsF}_6]\cdot\text{HF}$ (**3**) crystallizes in the monoclinic space group $P2_1/c$ with four formula units per unit cell. An illustration of the molecular structure is shown in Figure 2. Table 2 contains selected geometric parameters. The C–C bond lengths in **3** [1.450(4) Å and 1.457(4) Å] are all between a formal single and double bond.^[5] In contrast to the average $\text{C}\equiv\text{N}$ bond length of alkyl-nitrile derivatives of 1.136 Å, the $\text{C}\equiv\text{N}$ bond lengths in $[\text{H}_2\text{C}(\text{CNH})_2][\text{AsF}_6]\cdot\text{HF}$ are with 1.108(4) Å and 1.109(4) Å significantly shorter.^[6] Compared to other protonated nitriles the $\text{C}\equiv\text{N}$ bond length is slightly smaller (Table 3).^[2] The CCC angle of protonated malononitrile [113.7(3)°] is slightly

widened compared to malononitrile.^[7] Both CCN units differ with 175.8(3)° and 177.1(4)° slightly from the expected linear arrangement.

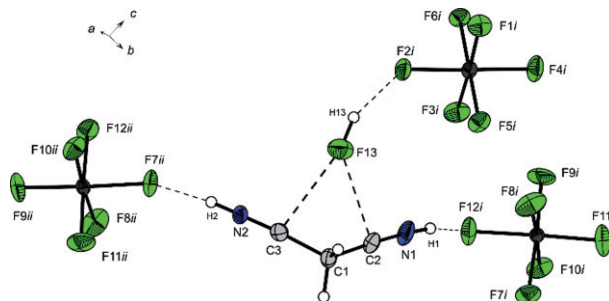


Figure 2. Projection of the interionic contacts between anion and cation of $[\text{H}_2\text{C}(\text{CNH})_2][\text{AsF}_6]_2\cdot\text{HF}$ (50% probability displacement ellipsoids). Symmetry codes: $i = x, 0.5-y, 0.5+z$ und $ii = 1-x, -y, -z$.

Table 2. Selected bond lengths and angles of **3** with estimated standard deviations in parentheses. Symmetry codes: $i = x, 0.5-y, 0.5+z$ and $ii = 1-x, -y, -z$.

Bond length / Å			
C1–C2	1.450(4)	N1–C2	1.108(4)
C1–C3	1.457(4)	N2–C3	1.109(4)
Bond angles / °			
C2–C1–C3	113.7(3)	N2–C3–C1	175.8(3)
N1–C2–C1	177.1(4)		
Dihedral angles / °			
C3–C1–C2–N1	–163(8)	C2–C1–C3–N2	160(5)
Interatomic distances D...A / Å			
N2–(H2)...F7	2.606(3)	N1–(H1)...F12	2.582(3)
F13–(H13)...F2	2.660(3)	C3...F13	2.645(4)
C2...F13	2.666(5)		
Interatomic angles D–H...A / °			
N2–(H2)...F7	172(5)	N1–(H1)...F12	163(5)
F13–(H13)...F2	154(6)		

Table 3. Summary of $\text{C}\equiv\text{N}$ distances of some selected protonated nitriles.^[7]

Compound	$\text{C}\equiv\text{N}$ distance / Å
$[\text{CH}_2(\text{CNH})_2][\text{AsF}_6]_2$	1.108(4) and 1.109(4)
$[\text{CH}_3\text{CNH}][\text{AsF}_6]$	1.118(3)
$[\text{CH}_3\text{CNH}][\text{Sb}_2\text{F}_{11}]$	1.117(3)
$[\text{CH}_3\text{CH}_2\text{CNH}][\text{AsF}_6]$	1.115(3)
$[\text{CH}_3\text{CH}_2\text{CH}_2\text{CNH}][\text{AsF}_6]$	1.116(9)
$[\text{C}_6\text{H}_5\text{CNH}][\text{AsF}_6]$	1.132(6)
$[p\text{-C}_6\text{H}_5(\text{CNH})_2][\text{AsF}_6]_2$	1.125(2)

The As–F bond lengths of the $[\text{AsF}_6]^-$ anion are in the range between 1.688(2) Å and 1.745(2) Å. These values are typical for an $[\text{AsF}_6]^-$ anion.^[8] The anions form slightly distorted octahedrons. The As–F bonds, which are involved in hydrogen bonds (As1–F6, As1–F2, and As2–F7, As2–F8, and As2–F12) are slightly longer than the other As–F bonds.

In the crystal structure of **3** the ions are connected by a network of moderate $\text{N}\cdots\text{H}\cdots\text{F}$ hydrogen bonds (Figure 3), with the bond lengths and angles summarized in Table 2. The cations and anions form chains along the b axis via moderate hydrogen bonds $\text{N2}\cdots\text{H2}\cdots\text{F7ii}$ and $\text{N1}\cdots\text{H1}\cdots\text{F12i}$. The co-crystallized HF solvent molecule forms along the c axis the hydrogen bond $\text{F13}\cdots\text{H13}\cdots\text{F2}$ towards another hexafluoride arsenate.^[9] Moreover, contacts between F13 and C2, as well as F13 and C3, are observed. Both contacts are with 2.666(5) Å and 2.645(4) Å below the sum of the van der Waals radii (3.17 Å).^[10]

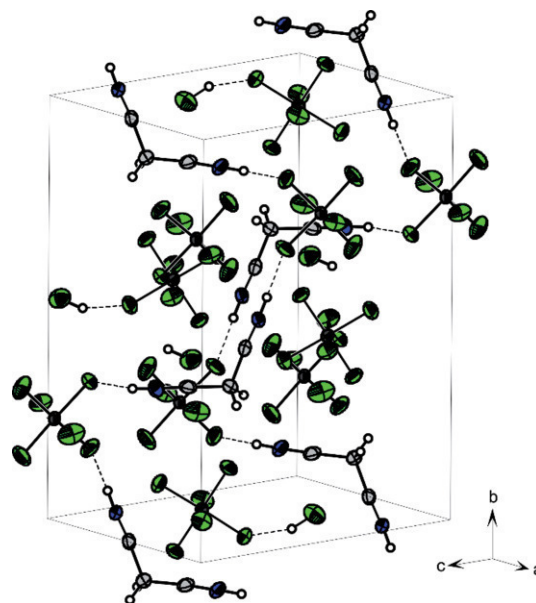


Figure 3. Crystal packing of $[\text{H}_2\text{C}(\text{CNH})_2][\text{AsF}_6]_2\cdot\text{HF}$. Hydrogen bonds are drawn as dashed lines (50% probability displacement ellipsoids). Symmetry codes: $i = x, 0.5-y, 0.5+z$ and $ii = 1-x, -y, -z$.

Theoretical Calculations

All calculations were performed at the PBE1PBE/6-311G(3df,3pd) level of theory with the Gaussian program package.^[11] Bond lengths and angles of $[\text{H}_2\text{C}(\text{CNH})_2]^{2+}$ are shown in Figure 4.

Compared to the experimental data of the $[\text{H}_2\text{C}(\text{CNH})_2]^{2+}$ cation from the crystal structure, all bond lengths and angles are in good agreement with the calculated structure, except for the $\text{C}\equiv\text{N}$ bond, which is slightly longer. Due to the hydrogen bonds in the solid state, the experimental vibrational frequencies are red-shifted compared to the calculated ones. In former studies hydrogen bonds were simulated by adding hydrogen fluoride molecules to the cation in the gas phase.^[12] Applying this method to the $[\text{H}_2\text{C}(\text{CNH})_2]^{2+}$ cation did not lead to meaningful results. The calculations confirmed our observation, that the diprotonated cation is more stable than the monoprotonated cation $[(\text{CN})\text{H}_2\text{C}(\text{CNH})]^+$ (390 kJ·mol^{–1}).

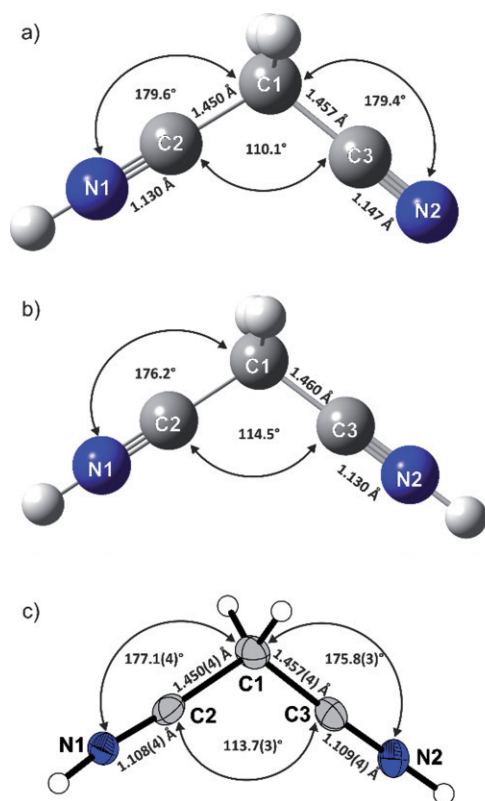


Figure 4. (a) Calculated structure of $[(\text{CN})\text{H}_2\text{C}(\text{CNH})]^+$. (b) Calculated structure of $[\text{H}_2\text{C}(\text{CNH})_2]^{2+}$. (c) $[\text{H}_2\text{C}(\text{CNH})_2]^{2+}$ cation of the single-crystal X-ray structure.

Conclusions

By using a ratio of two to one or higher of Lewis acid to malononitrile, the diprotonated species is formed. The existence of $[\text{H}_2\text{C}(\text{CNH})_2][\text{AsF}_6]_2 \cdot \text{HF}$ is confirmed by vibrational spectroscopy and a single crystal structure analysis. Supporting theoretical calculations show that the additional crystal HF molecule plays an important role concerning the stability of **3**. Interestingly, the bond strength of the cyanide group increases due to protonation. The C≡N bond length is shortened compared to malononitrile and it is the shortest C≡N bond among protonated cyano groups known in literature.

Monoprotonated malononitrile was synthesized using an equimolar ratio of Lewis acid and malononitrile in *a*HF. $[(\text{CN})\text{H}_2\text{C}(\text{CNH})][\text{AsF}_6]$ was stable under inert gas atmosphere and temperatures below -60°C . The change of color from colorless to red, irrespective of the chosen anion, indicates polymerization at the point of decomposition. According to the quantum chemical calculation, the existence of mono-protonated malononitrile has been predicted. However, due to its low thermal stability, it could not be well characterized.

Experimental Section

CAUTION! Avoid contact with any of these compounds. Note that hydrolysis of these salts might form HF, which burns skin and causes

irreparable damage. Safety precautions should be taken when using and handling these materials.

Apparatus and Materials: All reactions were performed by employing standard Schlenk techniques using a stainless-steel vacuum line. Syntheses were carried out in FEP/PFA reactors, closed with a stainless-steel valve. In advance of usage, all reaction vessels and the stainless-steel line were dried with fluorine. IR spectra were recorded with a Bruker Vertex 80V FTIR spectrometer. Raman measurements were carried out with a Bruker MultiRAM FT-Raman spectrometer with Nd:YAG laser excitation ($\lambda = 1064\text{ nm}$). The low-temperature X-ray diffraction of **3** was performed with an Oxford XCalibur3 diffractometer equipped with a Spellman generator (voltage 50 kV, current 40 mA) and a KappaCCD detector, operating with Mo- K_α radiation ($\lambda = 0.7107\text{ \AA}$). Data collection at 123 K was performed using the CrysAlis CCD software,^[13] the data reductions were carried out using the CrysAlis RED software.^[14] The solution and refinement of the structure was performed with the programs SHELXS^[15] and SHELXL-97^[16] implemented in the WinGX software package^[17] and finally checked with the PLATON software.^[18] The absorption correction was performed with the SCALE3 ABSPACK multi-scan method.^[19] Selected data and parameters of the X-ray analysis are given in Table 4. All quantum chemical calculations were performed on the PBE1PBE/6311G++(3df, 3pd)-level of theory by Gaussian 09.^[11]

Table 4. X-ray data and parameters of $[\text{H}_2\text{C}(\text{CNH})_2][\text{AsF}_6]_2 \cdot \text{HF}$ (**3**).

	$[\text{H}_2\text{C}(\text{CNH})_2][\text{AsF}_6]_2 \cdot \text{HF}$ (3)
Formula	$\text{C}_3\text{H}_4\text{N}_2\text{AsF}_6$
M_r /g·mol ⁻¹	465.93
Crystal size /mm ³	$0.17 \times 0.23 \times 0.24$
Crystal system	monoclinic
Space group	$P2_1/c$
a /Å	7.6797(4)
b /Å	14.9467(7)
c /Å	10.2543(5)
α /°	90.00
β /°	98.950(4)
γ /°	90.00
V /Å ³	1162.72(10)
Z	4
ρ_{calcd} /g·cm ⁻³	2.662
$\mu(\text{Mo-}K_\alpha)$ /cm ⁻¹	0.71073
$F(000)$	880
T /K	173(2)
hkl range	$-11:9; -21:22; -15:11$
Refl. measured	4594
Refl. unique	4185
Parameters	192
$R(F)/wR(F^2)^a$ (all reflections)	0.0372 / 0.0748
Weighting scheme ^{b)}	0.0232 / 0.0
S (GooF) ^{c)}	1.046
Residual density /e·Å ⁻³	0.731/−1.139
Device type	Oxford XCalibur
Solution/refinement	SHELXS-97 ^[15] / SHELXL-97 ^[16]

a) $R_1 = \sum |F_o| - |F_c| / \sum |F_o|$. b) $wR_2 = [\sum (w(F_o^2 - F_c^2)^2) / \sum (w(F_o^2)^2)]^{1/2}$; $w = [\sigma_c^2(F_o^2) + (xP)^2 + yP]^{-1}$; $P = (F_o^2 + 2F_c^2)/3$. c) $\text{GooF} = \{\sum [w(F_o^2 - F_c^2)^2] / (n-p)\}^{1/2}$ (n = number of reflections; p = total number of parameters).

Crystallographic data (excluding structure factors) for the structure in this paper have been deposited with the Cambridge Crystallographic Data Centre, CCDC, 12 Union Road, Cambridge CB21EZ, UK. Copies

of the data can be obtained free of charge on quoting the depository number CCDC-1557857 (for compound **3**) (Fax: +44-1223-336-033; E-Mail: deposit@ccdc.cam.ac.uk, <http://www.ccdc.cam.ac.uk>).

Synthesis of [(CN)H₂C(CNH)][AsF₆] (1), [(CN)H₂C(CND)][AsF₆] (5), and [H₂C(CNH)₂][AsF₆]₂ (3), [H₂C(CND)₂][AsF₆]₂ (7): Initially, anhydrous hydrogen fluoride, *α*HF, (150 mmol, 3 mL) and arsenic pentafluoride (1.00 mmol or 3.00 mmol, 170 mg or 510 mg) were condensed into a 7 mL FEP-tube-reactor and cooled to −196 °C. In order to form the superacidic system, the mixture was warmed up to −30 °C. The reaction vessel was cooled to −196 °C again and malononitrile (1 mmol, 66 mg) was added in an inert gas atmosphere. The reaction vessel was warmed up to −30 °C for 5 min and cooled to −78 °C again afterwards. The excess of *α*HF was removed in a dynamic vacuum at −78 °C. [(CN)H₂C(CNH)][AsF₆] and [H₂C(CNH)₂][AsF₆]₂ were obtained as a colorless crystalline solid in quantitative yield. [(CN)H₂C(CND)][AsF₆] and [H₂C(CND)₂][AsF₆]₂ were prepared analogously, by using deuterium fluoride, DF, instead of *α*HF.

Synthesis of [(CN)H₂C(CNH)][SbF₆] (2), [(CN)H₂C(CND)][SbF₆] (6), and [H₂C(CNH)₂][SbF₆]₂ (4) and [H₂C(CND)₂][SbF₆]₂ (8): Anhydrous hydrogen fluoride, *α*HF, (150 mmol, 3 mL) was added to a 7 mL FEP-tube-reactor with antimony pentafluoride, SbF₅, (1.00 mmol or 2.00 mmol, 217 mg or 434 mg) condensed in before at −196 °C. To form the superacidic system, the mixture was warmed up to 0 °C. The reaction vessel was cooled to −196 °C again and malononitrile (1 mmol, 66 mg) was added in an inert gas atmosphere. The reaction vessel was warmed up to −30 °C for five minutes and cooled to −78 °C afterwards. The excess of *α*HF was removed in a dynamic vacuum at −78 °C. [(CN)H₂C(CNH)][SbF₆] and [H₂C(CNH)₂][SbF₆]₂ were obtained as a colorless crystalline solid in quantitative yield. [(CN)H₂C(CND)][SbF₆] and [H₂C(CND)₂][SbF₆]₂ were prepared analogously, by using deuterium fluoride, DF, instead of *α*HF.

Acknowledgements

We are grateful to the Department of Chemistry of the Ludwig-Maximilian University, Munich and the Deutsche Forschungsgemeinschaft (DFG) for the support of this work.

Keywords: Superacidic systems; Vibrational spectroscopy; X-ray diffraction; Protonated malononitrile; Ab initio calculations

References

- [1] G. Olah, T. Kiovsky, *J. Am. Chem. Soc.* **1968**, *90*, 4666–4672.

- [2] R. Haiges, A. Baxter, N. Goetz, J. Axhausen, T. Soltner, A. Kornath, K. Christe, *Dalton Trans.* **2016**, *45*, 8494–8499.
 [3] R. Savoie, R. Brousseau, C. Nolin, *Can. J. Chem.* **1976**, *54*, 3293–3302.
 [4] J. Weidlein, U. Müller, K. Dehnicke, in: *Schwingungsspektroskopie*, Georg Thieme Verlag, Stuttgart, **1988**, pp 29–30.
 [5] A. F. Holleman, E. Wiberg, *Lehrbuch der anorganischen Chemie* (Ed.: N. Wiberg), 102. ed., de Gruyter, Berlin, **2007**, p. 2006.
 [6] F. Allen, O. Kennard, D. Watson, L. Brammer, A. Orpen, R. Taylor, *J. Chem. Soc. Perkin Trans. 2* **1987**, 1–19.
 [7] M. Dove, A. Rae, *Faraday Discuss. Chem. Soc.* **1980**, *69*, 98–106.
 [8] R. Minkwitz, F. Neikes, U. Lohmann, *Eur. J. Inorg. Chem.* **2002**, 27–30.
 [9] G. Jeffrey, *An Introduction to Hydrogen Bonding*, Oxford University Press, Oxford, **1997**.
 [10] A. Bondi, *J. Phys. Chem.* **1964**, *68*, 441–451.
 [11] M. J. Frisch, G. W. Trucks, H. B. Schlegel, G. E. Scuseria, M. A. Robb, J. R. Cheeseman, G. Scalmani, V. Barone, G. A. Petersson, H. Nakatsuji, X. Li, M. Caricato, A. Marenich, J. Bloino, B. G. Janesko, R. Gomperts, B. Mennucci, H. P. Hratchian, J. V. Ortiz, A. F. Izmaylov, J. L. Sonnenberg, D. Williams-Young, F. Ding, F. Lipparini, F. Egidi, J. Goings, B. Peng, A. Petrone, T. Henderson, D. Ranasinghe, V. G. Zakrzewski, J. Gao, N. Rega, G. Zheng, W. Liang, M. Hada, M. Ehara, K. Toyota, R. Fukuda, J. Hasegawa, M. Ishida, T. Nakajima, Y. Honda, O. Kitao, H. Nakai, T. Vreven, K. Throssell, J. A. Montgomery, Jr., J. E. Peralta, F. Ogliaro, M. Bearpark, J. J. Heyd, E. Brothers, K. N. Kudin, V. N. Staroverov, T. Keith, R. Kobayashi, J. Normand, K. Raghavachari, A. Rendell, J. C. Burant, S. S. Iyengar, J. Tomasi, M. Cossi, J. M. Millam, M. Klene, C. Adamo, R. Cammi, J. W. Ochterski, R. L. Martin, K. Morokuma, O. Farkas, J. B. Foresman, D. J. Fox, Gaussian 09, Revision a.02, Gaussian Inc., Pittsburgh, PA, USA, **2003**.
 [12] T. Soltner, N. Goetz, A. Kornath, *Eur. J. Inorg. Chem.* **2011**, 3076–3081.
 [13] *CrysAlisCCD*, Version 1.171.35.11 (release 16–05–2011 CrysAlis 171.NET), Oxford Diffraction Ltd., Oxford, UK, **2011**.
 [14] *CrysAlisRED*, Version 1.171.35.11 (release 16–05–2011 CrysAlis 171.NET), Oxford Diffraction Ltd., Oxford, UK, **2011**.
 [15] G. Sheldrick, *SHELXS-97*, Program for Crystal Structure Solution, University of Göttingen, Germany, **1997**.
 [16] G. Sheldrick, *SHELXL-97*, Programm for the Refinement of Crystal Structures, University of Göttingen, Germany, **1997**.
 [17] L. Farrugia, *J. Appl. Crystallogr.* **1999**, *32*, 837–838.
 [18] A. Spek, *PLATON*, A Multipurpose Crystallographic Tool, Utrecht University, Utrecht, The Netherlands, **1999**.
 [19] *SCALE3 ABSPACK*, An Oxford Diffraction Program, Oxford Diffraction Ltd., Oxford, UK, **2005**.

Received: July 12, 2017

Published Online: August 2, 2017

Superacid Chemistry | Very Important Paper |

VIP Investigation of Malonic Acid in Superacidic Solutions

Manuel Schickinger,^[a] Florian Zischka,^[a] Karin Stierstorfer,^[a] and Andreas Kornath*^[a]

Abstract: Malonic acid reacts with the superacidic solutions XF/MF_5 ($\text{X} = \text{H}, \text{D}$; $\text{M} = \text{As}, \text{Sb}$) to form their corresponding salts $[(\text{OH})_2\text{CCH}_2\text{C}(\text{O})\text{OH}][\text{MF}_6]$ and $[(\text{OH})_2\text{CCH}_2\text{C}(\text{OH})_2][\text{MF}_6]_2$. The hexafluorometalates of the mono- and diprotonated malonic acid have been characterized by vibrational spectroscopy and single-crystal X-ray structure analyses. Monoprotonated malonic acid, $[(\text{OH})_2\text{CCH}_2\text{C}(\text{O})\text{OH}][\text{AsF}_6]$, crystallizes in the orthorhombic space group $Pbca$ with eight formula units per unit cell: $a = 9.6739(4) \text{ \AA}$, $b = 11.8355(5) \text{ \AA}$, $c = 13.9826(6) \text{ \AA}$, and

diprotonated malonic acid, $[(\text{OH})_2\text{CCH}_2\text{C}(\text{OH})_2][\text{AsF}_6]_2$, crystallizes in the monoclinic space group $P2_1/n$ with four formula units per unit cell: $a = 7.3348(2) \text{ \AA}$, $b = 9.8437(3) \text{ \AA}$, $c = 16.6903(6) \text{ \AA}$, $\beta = 97.818(3)^\circ$. The experimental data are compared to quantum chemical calculations at the MP2/aug-cc-pVTZ-level of theory for the free cations $[(\text{OH})_2\text{CCH}_2\text{C}(\text{O})\text{OH}]^+$ and $[(\text{OH})_2\text{CCH}_2\text{C}(\text{OH})_2]^{2+}$. A six-membered ring-like structure containing an intramolecular hydrogen bond was found for the monoprotonated species of malonic acid.

Introduction

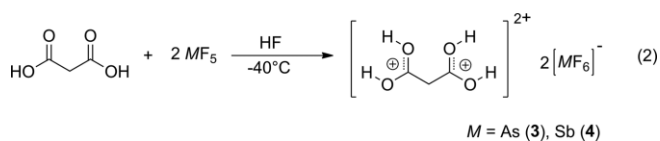
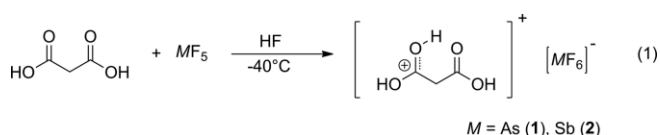
Malonic acid can be isolated from sugar beet molasses and is less frequently found in flora than its related derivative oxalic acid. Its name is derived from the Latin word *malum*, meaning apple, due to the fact that malonic acid is accessible via oxidation of malic acid.^[1,2] In a former study of our group, the existence of the mono- and diprotonated species of malononitrile was confirmed.^[3] In contrast to malononitrile ($\text{p}K_{\text{a}} = 11$) malonic acid is more acidic ($\text{p}K_{\text{a}1} = 2.83$, $\text{p}K_{\text{a}2} = 5.69$), which impedes a possible protonation.^[4,5] As yet, only Olah provided a first indication of the existence of diprotonated malonic acid in solution by ^{13}C -NMR spectroscopy in the late 1960s.^[6] This fact and the existence of diprotonated malononitrile, with two neighboring positive charges separated only by a methylene group, prompted us to isolate and structurally characterize mono- and diprotonated malonic acid.

Results and Discussion

Synthesis and Properties of $[\text{HOOCCH}_2\text{C}(\text{OH})_2][\text{MF}_6]$ and $[(\text{HO})_2\text{CCH}_2\text{C}(\text{OH})_2][\text{MF}_6]_2$ ($\text{M} = \text{As}, \text{Sb}$)

All salts were prepared in a two-step reaction in quantitative yield. The syntheses were conducted according to equations (1) and (2) as illustrated in Scheme 1.

Initially, the superacidic medium was prepared. For this, the Lewis acid, SbF_5 or AsF_5 , was mixed with an excess of hydrogen fluoride at a low temperature. Complete solvation was achieved by homogenizing the superacid solution at -20°C . Following



Scheme 1. Synthesis of the mono- and diprotonated salts of malonic acid.

this, malonic acid was added to the frozen superacidic system under inert gas atmosphere. After warming the reaction mixture slowly to -40°C , the protonated species were formed immediately. The excess of aHF was removed at -78°C in vacuo. All products were obtained as colorless salts in quantitative yield with the monoprotonated salts of malonic acid $[\text{HOOCCH}_2\text{C}(\text{OH})_2][\text{AsF}_6]$ (1) and $[\text{HOOCCH}_2\text{C}(\text{OH})_2][\text{SbF}_6]$ (2) being stable up to 15°C and the diprotonated salts $[(\text{HO})_2\text{CCH}_2\text{C}(\text{OH})_2][\text{AsF}_6]_2$ (3) as well as $[(\text{HO})_2\text{CCH}_2\text{C}(\text{OH})_2][\text{SbF}_6]_2$ (4) being stable up to 20°C . All protonated compounds are sensitive towards moisture.

The corresponding deuterated salts, $[\text{DOOCCH}_2\text{C}(\text{OD})_2][\text{AsF}_6]$ (5), $[\text{DOOCCH}_2\text{C}(\text{OD})_2][\text{SbF}_6]$ (6), $[(\text{DO})_2\text{CCH}_2\text{C}(\text{OD})_2][\text{AsF}_6]_2$ (7) and $[(\text{DO})_2\text{CCH}_2\text{C}(\text{OD})_2][\text{SbF}_6]_2$ (8), were obtained by changing the superacidic system from HF/MF_5 to DF/MF_5 ($\text{M} = \text{As}, \text{Sb}$). The hydroxyl hydrogen atoms are entirely replaced by deuterium, as deuterium fluoride is used in large excess. The degree of deuteration approximates 96 %. The CH_2 protons remain unaffected.

Quantum Chemical Calculations

All calculations were performed at the MP2/aug-cc-pVTZ-level of theory with the Gaussian program package.^[7]

[a] Department Chemie, Ludwig-Maximilians-Universität München, Butenandtstr. 5-13, 81377 München, Germany
E-mail: andreas.kornath@cup.uni-muenchen.de
<http://www.org.chemie.uni-muenchen.de/ac/kornath/>

Supporting information and ORCID(s) from the author(s) for this article are available on the WWW under <https://doi.org/10.1002/ejoc.201801382>.

The monoprotonated cation of malonic acid and its deuterated isotopologue were calculated for a better assignment of the vibrational modes and for a comparison of the calculated and experimentally determined geometric parameters. The same was conducted for the diprotonated cation of malonic acid and its deuterated isotopologue.

Interestingly, for the cation of monoprotonated malonic acid, three stationary points on the isosurface can be found. These are illustrated in Figure 1 together with their difference in energy. All geometries are true minima, as they show no negative frequencies.

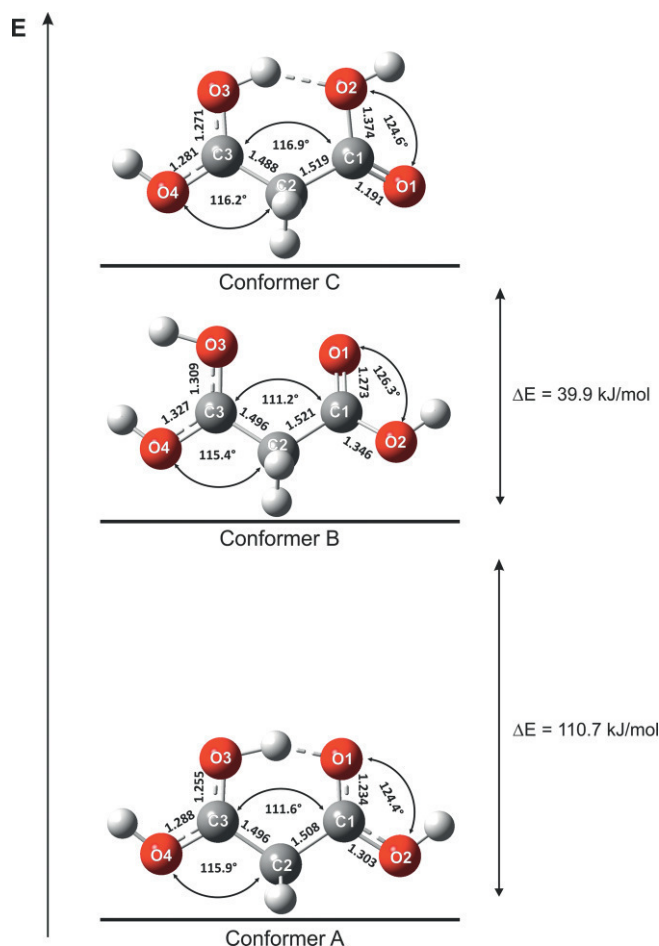


Figure 1. Three possible conformers of the $[XOOCCH_2C(OX)_2]^+$ cation ($X = H, D$) and their calculated energy. All bond lengths are given in Å.

The global energetic minimum is found for the structure calculations of the $[HOOCCH_2C(OH)_2]^+$ cation (Conformer A), locating the C3O3–H proton in the bridging position between the two carbonyl oxygen atoms O1 and O3.

Compared to Conformer A, with an energetic difference of 110.7 kJ/mol, Conformer B is less stable. Here, in contrast to Conformer A, the C3O3–H proton is not bridging to the O1 atom, but rotated by 180° around the C3–O3 axis. The absence of the intramolecular hydrogen bridge $[O3-(H3)\cdots O1]$ explains the high energy difference between Conformer A and B. The structure of Conformer C differs from Conformer A only in the orientation of the O1–C1–O2 group, which is rotated by 180° around the C1–C2 axis. As for Conformer A, an intramolecular

hydrogen bond is formed here, too. In contrast to the strong intramolecular hydrogen bond in Conformer A, the intramolecular hydrogen bond in Conformer C is only moderate, which explains the lower stability.^[8]

If solid state effects and intermolecular interactions were not considered, the structure of Conformer A should be preferred for the $[XOOCCH_2C(OX)_2]^+$ cation ($X = H, D$). Nevertheless, we considered all three geometries for the further discussion, since interionic interaction might have an influence on the stability of the conformers. In former studies such interionic solid-state interactions could be simulated by adding HF-molecules to the cation in the gas phase. In the present case this method did not lead to satisfying results.^[9]

Vibrational Spectroscopy

The Infrared and Raman spectra of $[HOOCCH_2C(OH)_2][AsF_6]$ (**1**), $[(HO)_2CCH_2C(OH)][AsF_6]_2$ (**3**), $[DOOCCH_2C(OD)_2][AsF_6]$ (**5**), $[(DO)_2CCH_2C(OD)_2][SbF_6]_2$ (**8**) and malonic acid are illustrated in Figure 2. Table 1 summarizes selected observed Infrared and Raman frequencies of **1** and **3** together with the quantum chemically calculated frequencies of the cations $[C_3H_5O_4]^+$ and $[C_3H_2D_3O_4]^+$. In Table 2 selected observed Infrared and Raman frequencies of **5** and **8** together with the quantum chemically calculated frequencies of the cations $[C_3H_6O_4]^{2+}$ and

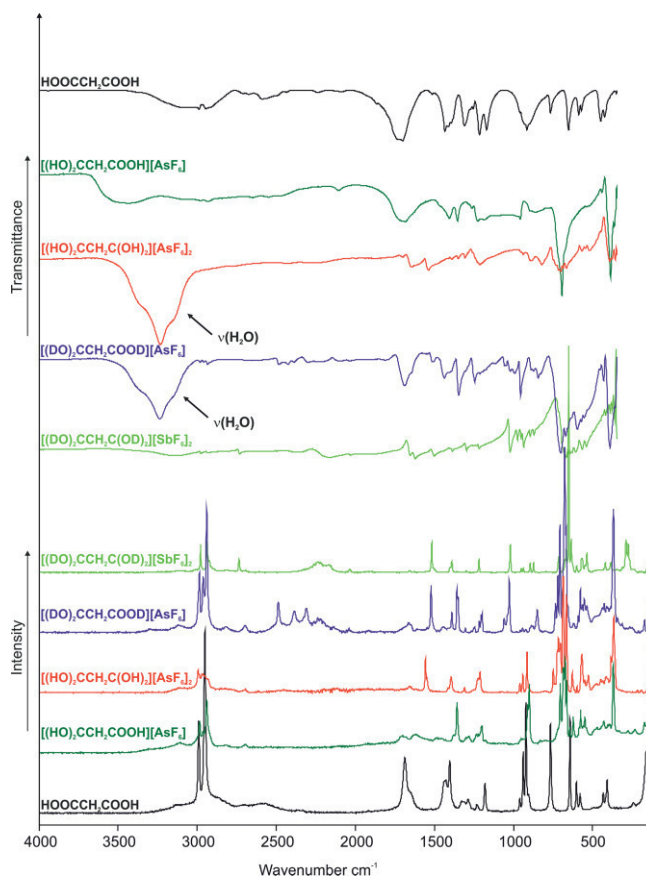


Figure 2. Low temperature Raman and IR spectra of $CH_2(COOH)_2$, $[HOOCCH_2C(OH)_2][AsF_6]$ (**1**), $[(HO)_2CCH_2C(OH)_2][AsF_6]_2$ (**3**) and $[DOOCCH_2C(OD)_2][AsF_6]$ (**5**) and $[(DO)_2CCH_2C(OD)_2][SbF_6]_2$.

Table 1. Selected experimental vibrational frequencies (in cm^{-1}) of $[\text{HOOCCH}_2\text{C}(\text{OH})_2][\text{AsF}_6]$ (**1**) and $[\text{DOOCCH}_2\text{C}(\text{OD})_2][\text{AsF}_6]$ (**5**) and calculated vibrational frequencies (in cm^{-1}) of $[\text{C}_3\text{H}_5\text{O}_4]^+$ and $[\text{C}_3\text{H}_2\text{D}_3\text{O}_4]^+$.

$[\text{HOOCCH}_2\text{C}(\text{OH})_2][\text{AsF}_6]$ (1)		$[\text{DOOCCH}_2\text{C}(\text{OD})_2][\text{AsF}_6]$ (5)		$[\text{C}_3\text{H}_5\text{O}_4]^+$	$[\text{C}_3\text{H}_2\text{D}_3\text{O}_4]^+$	Assignment ^[b]
IR	Raman	IR	Raman	calcd. ^[a] (IR/Raman)	calcd. ^[a] (IR/Raman)	
3450(m)		2486(vw)	2491(17)	3496(210/96)	2544(120/48)	$\nu(\text{OX})$
		2390(vw)	2389(6)	3475(277/81)	2530(168/37)	$\nu(\text{OX})$
		2294(vw)	2313(10)	1895(566/9)	1268(442/11)	$\nu(\text{OX})$
	2988(20)	2986(vw)	2990(22)	2984(27/37)	2984(27/37)	$\nu_{\text{as}}(\text{CH}_2)$
1705(s,br)	2967(5), 2943(61)	2963(vw), 2938(vw)	2967(5), 2943(61)	2939(32/99)	2939(31/101)	$\nu_{\text{s}}(\text{CH}_2)$
	1704(5)	1689(m)	1664(5)	1693(253/12)	1685(362/9)	$\nu_{\text{as}}(\text{CO}_2)$
	1622(9)	1519(w)	1525(25)	1610(248/1)	1627(97/2)	$\nu_{\text{as}}(\text{CO}_2)$
	1489(5)	1443(m)	1446(2)	1487(626/7)	1471(171/5)	$\nu_{\text{s}}(\text{CO}_2)$
1409(m)		1395(sh)	1393(9)	1420(5/8)	1421(330/1)	$\nu_{\text{s}}(\text{CO}_2)$
	709(48)		723(20)			$[\text{MF}_6]^-$
697(vs)	690(15)	705(vs)	710(49)			$[\text{MF}_6]^-$
	677(100)		680(100)			$[\text{MF}_6]^-$
545(w)	579(33)	573(vw)	581(19)			$[\text{MF}_6]^-$
	373(86)		372(64)			$[\text{MF}_6]^-$

[a] Calculated at the MP2/aug-cc-pVTZ-level of theory. IR intensity in km/mol and Raman intensity in $\text{\AA}^4/\text{u}$. Abbreviations for IR intensities: vs = very strong, s = strong, m = medium, w = weak. Experimental Raman activity is stated to a scale of 1 to 100. Frequencies are scaled with an empirical factor of 0.95. [b] M = As/Sb, X = O/D.

Table 2. Selected experimental vibrational frequencies (in cm^{-1}) of $[(\text{HO})_2\text{CCH}_2\text{C}(\text{OH})_2][\text{AsF}_6]_2$ (**5**) and $[(\text{DO})_2\text{CCH}_2\text{C}(\text{OD})_2][\text{SbF}_6]_2$ (**8**) and calculated vibrational frequencies (in cm^{-1}) of $[\text{C}_3\text{H}_6\text{O}_4]^{2+}$ and $[\text{C}_3\text{H}_2\text{D}_4\text{O}_4]^{2+}$.

$[(\text{HO})_2\text{CCH}_2\text{C}(\text{OH})_2][\text{AsF}_6]_2$		$[(\text{DO})_2\text{CCH}_2\text{C}(\text{OD})_2][\text{SbF}_6]_2$		$[\text{C}_3\text{H}_6\text{O}_4]^{2+}$	$[\text{C}_3\text{H}_2\text{D}_4\text{O}_4]^{2+}$	Assignment ^[b]
IR	Raman	IR	Raman	calcd. ^[a] (IR/Raman)	calcd. ^[a] (IR/Raman)	
			2350–2125(5)	3457(365/88)	2523(1951/38)	$\nu(\text{OX})$
			2350–2125(5)	3453(371/27)	2520(218/12)	$\nu(\text{OX})$
			2350–2125(5)	3366(500/79)	2452(303/35)	$\nu(\text{OX})$
		2159(s, br)	2350–2125(5)	3362(424/41)	2449(231/20)	$\nu(\text{OX})$
	2998(20)	2981(w)	2984(11)	2953(40/29)	2953(41/30)	$\nu_{\text{as}}(\text{CH}_2)$
	2971(4)	2938(w)	2943(13)	2901(40/29)	2902(45/87)	$\nu_{\text{s}}(\text{CH}_2)$
	1651(m)	1662(4)	1656(m)	1639(328/2)	1624(328/1)	$\nu_{\text{as}}(\text{CO}_2)$
	1541(m)	1561(30)	1625(s)	1601(273/1)	1588(346/1)	$\nu_{\text{as}}(\text{CO}_2)$
		1417(2)	1506(s)	1497(321/2)	1468(202/6)	$\nu_{\text{s}}(\text{CO}_2)$
	1395(w)	1398(14)		1496(4/16)	1465(5/18)	$\nu_{\text{s}}(\text{CO}_2)$
		719(31)				$[\text{MF}_6]^-$
	704(vs)	706(17)	653(vs)			$[\text{MF}_6]^-$
		687(100)				$[\text{MF}_6]^-$
	571(w)	571(32)	568(vs)	575(5)		$[\text{MF}_6]^-$
	396(s)	369(65)	294(14)			$[\text{MF}_6]^-$

[a] Calculated at the MP2/aug-cc-pVTZ-level of theory. IR intensity in km/mol and Raman intensity in $\text{\AA}^4/\text{u}$. Abbreviations for IR intensities: vs = very strong, s = strong, m = medium, w = weak. Experimental Raman activity is stated to a scale of 1 to 100. Experimental frequencies are scaled with an empirical factor of 0.95. [b] M = As/Sb, X = O/D.

$[\text{C}_3\text{H}_2\text{D}_4\text{O}_4]^{2+}$ are listed. The complete tables are attached in the Supporting Information (Table S1 and S2).

Vibrational Spectra of $[\text{HOOCCH}_2\text{C}(\text{OH})_2][\text{AsF}_6]$ (**1**) and $[\text{DOOCCH}_2\text{C}(\text{OD})_2][\text{AsF}_6]$ (**5**)

As a consequence of the C_1 symmetry, 30 fundamental vibrations are expected for the cations $[\text{C}_3\text{H}_5\text{O}_4]^+$ and $[\text{C}_3\text{H}_2\text{D}_3\text{O}_4]^+$, with all of them being Raman and IR active. The assignment of the vibrational modes was carried out by analyzing the Cartesian displacement vectors of the calculated vibrational modes.^[10]

The CH stretching vibrations of both compounds are in good agreement with the literature values of malonic acid and are not affected by the protonation. The Infrared spectrum of $[\text{HOOCCH}_2\text{C}(\text{OH})_2][\text{AsF}_6]$ (**1**) exhibits a $\nu(\text{OH})$ vibration at

3450 cm^{-1} . This red-shift of the $\nu(\text{OH})$ vibration, compared to malonic acid is an indication for a protonation of the oxygen atom of the carboxyl group. This assumption is supported by the $\nu(\text{OD})$ vibration of the deuterated species **5**. The $\nu(\text{OD})$ vibrations are detected at 2491 cm^{-1} , 2389 cm^{-1} and 2313 cm^{-1} in the Raman spectra and at 2486 cm^{-1} , 2390 cm^{-1} and 2294 cm^{-1} in the IR spectra. These values are consistent with the Teller-Redlich rule for an H/D isotopic effect.^[11] The calculated $\nu(\text{C}3\text{O}3\text{--H})$ vibration at 1895 cm^{-1} is extraordinarily shifted to lower wavenumbers, compared to regular O-H stretching vibrations.^[12] This is caused by the six-membered ring-like bonding of the C3O3–H proton.

Based on the vibrational spectroscopic results, the deuterated cation could not unambiguously be assigned to any of the three conformers obtained by the quantum chemical calcula-

tions. A comparison of the experimental frequencies of the salts of monodeuterated malonic acid with the according conformers is listed in the Supporting Information (Table S2).

For the anions $[MF_6]^-$ ($M = \text{As}, \text{Sb}$) more vibrations are observed than expected for an ideal octahedral symmetry. This implies a lower symmetry for the anions, which is in agreement with the crystal structure analysis.

Vibrational Spectra of $[(\text{HO})_2\text{CCH}_2\text{C}(\text{OH})_2][\text{AsF}_6]_2$ (**3**) and $[(\text{DO})_2\text{CCH}_2\text{C}(\text{OD})_2][\text{SbF}_6]_2$ (**8**)

In accordance with the quantum chemical calculations, C_1 symmetry is predicted for the cations $[\text{C}_3\text{H}_6\text{O}_4]^{2+}$ and $[\text{C}_3\text{H}_2\text{D}_4\text{O}_4]^{2+}$ with 33 fundamental vibrations. All of them are Raman and IR active. The assignment of the vibrational modes is based on the analysis of the Cartesian displacement vectors of the calculated vibrational modes.^[10]

Due to moisture condensed on the IR plate during measurement, no meaningful Infrared bands for the $\nu(\text{OH})$ vibrations of $[(\text{HO})_2\text{CCH}_2\text{C}(\text{OH})_2][\text{AsF}_6]_2$ are observable. The $\nu(\text{OD})$ vibrations are observed between 2350 cm^{-1} and 2125 cm^{-1} in the Raman spectrum and as a broad band at 2159 cm^{-1} in the Infrared spectrum. These $\nu(\text{OD})$ vibrations are shifted to lower wavenumbers in comparison of those of the monoprotonated species. The CH stretching vibrations of $[(\text{HO})_2\text{CCH}_2\text{C}(\text{OH})_2][\text{AsF}_6]_2$ are with 2998 cm^{-1} and 2971 cm^{-1} (Raman) similar to those of monoprotonated malonic acid and malonic acid. The same applies to the deuterated isotopologue.^[11] Compared to the experimental $\nu_{\text{as}}(\text{CO}_2)$ vibrations of the monoprotonated species, the experimental $\nu_{\text{as}}(\text{CO}_2)$ of $[(\text{HO})_2\text{CCH}_2\text{C}(\text{OH})_2][\text{AsF}_6]_2$ are shifted to lower wavenumbers by 54 cm^{-1} (IR) and by 42 cm^{-1} , respectively 62 cm^{-1} (Raman). Analogous shifts are noticeable for $[(\text{DO})_2\text{CCH}_2\text{C}(\text{OD})_2][\text{SbF}_6]_2$.

For the anions $[MF_6]^-$ ($M = \text{As}, \text{Sb}$) with an ideal octahedral symmetry, two bands in the Infrared spectrum and three lines in the Raman spectrum are expected. In both cases, more than five vibrations are observed. This indicates a lower symmetry, which is in accordance with the crystal structure analysis.

In general, the calculated vibrations of $[(\text{HO})_2\text{CCH}_2\text{C}(\text{OH})_2]^{2+}$ and $[(\text{DO})_2\text{CCH}_2\text{C}(\text{OD})_2]^{2+}$ are in good accordance with the experimental vibrations, with exception of the O–H stretching vibrations, caused by intermolecular hydrogen bonding. Experimental values of the OH stretching vibrations are observed at lower wavenumbers.

Crystal Structures

Crystal Structure of $[\text{HOOCCH}_2\text{C}(\text{OH})_2][\text{AsF}_6]$ (**1**)

The salt of monoprotonated malonic acid $[\text{HOOCCH}_2\text{C}(\text{OH})_2][\text{AsF}_6]$ (**1**) crystallizes in the orthorhombic space group $Pbca$ with eight formula units per unit cell. An illustration of the asymmetric unit of **1** is shown in Figure 3. Table 3 contains selected geometric parameters.

The C–C bond lengths in the cation of **1** are with $1.503(3)\text{ \AA}$ and $1.491(3)\text{ \AA}$ similar to the those of malonic acid as reported in the literature [$1.503(2)\text{ \AA}$ and $1.499(3)\text{ \AA}$].^[13] The C–O bond lengths C1–O2 [$1.289(3)\text{ \AA}$] and C3–O4 [$1.277(3)\text{ \AA}$] range be-

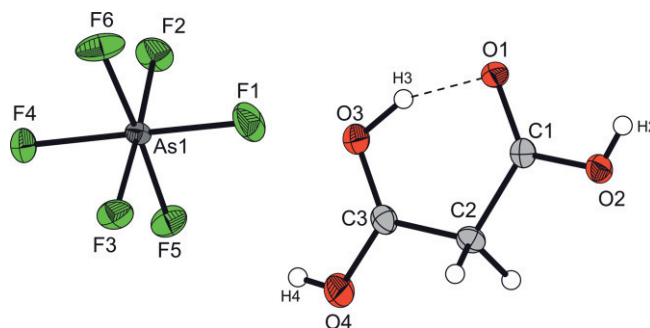


Figure 3. Asymmetric unit of **1** (50 % probability displacement ellipsoids).

Table 3. Selected bond lengths [\AA] and angles [$^\circ$] of **1** with estimated standard deviations in parentheses. Symmetry codes: $i = -0.5 + x$, $0.5 - y$, $1 - z$; $ii = -1 + x$, y , z .

Bond lengths [\AA]			
C1–C2	1.503(3)	C1–O2	1.289(3)
C2–C3	1.491(3)	C3–O3	1.251(3)
C1–O1	1.234(2)	C3–O4	1.277(3)
Bond angles [$^\circ$]			
C1–C2–C3	112.5(2)	C2–C3–O3	122.8(2)
C2–C1–O1	122.5(2)	C2–C3–O4	116.1(2)
C2–C1–O2	113.6(2)	O3–C2–O4	121.1(2)
O1–C1–O2	123.9(2)		
Torsion angles [$^\circ$]			
C3–C2–C1–O1	0.9(3)	C1–C2–C3–O3	–3.8(3)
C3–C2–C1–O2	–178.8(2)	C1–C2–C3–O4	175.8(2)
Interatomic distances D...A [\AA]			
O3–(H3)...O1	2.444(2)	O2–(H2)...F4 $_{ii}$	2.655(2)
O4–(H4)...O1 i	3.012(2)		

tween a formal single and double bond (C–O: 1.43 \AA and C=O: 1.19 \AA).^[14,15] In comparison with the starting material, no significant difference in the lengths of the C–OH bonds [$1.288(2)\text{ \AA}$ and $1.292(2)\text{ \AA}$] is observable.^[13]

The C3–O3 bond length is approximately 32 pm shorter than the other C–OH bond lengths, but 17 pm longer than the C1–O1 bond. The C1–O1 bond length is, with $1.234(2)\text{ \AA}$, the shortest C–O bond length in **1**, but slightly longer than the bond lengths of the unprotonated C=O groups of malonic acid [$1.227(2)\text{ \AA}$ and $1.219(2)\text{ \AA}$]. The geometry of the cation is nearly planar, due to the strong intramolecular hydrogen bond O3–(H3)...O1. It should be noted, that the localization of protons by X-ray diffraction is not meaningful, but the electron density between O1 and O3 indicates a high probability of presence of the proton at this position of the six-membered ring-like structure.

The As–F bond lengths of the $[\text{AsF}_6]^-$ anion are in the range of $1.697(1)\text{ \AA}$ – $1.757(1)\text{ \AA}$. Compared to the literature, these values are typical for an $[\text{AsF}_6]^-$ anion, displaying a slightly distorted octahedral coordination.^[16] The As1–F4 bond, which is involved in hydrogen bonding, is slightly longer than the other As–F bonds.

In the crystal structure of **1**, the ions are connected by a network of moderate O–(H)...O and O–(H)...F hydrogen bonds

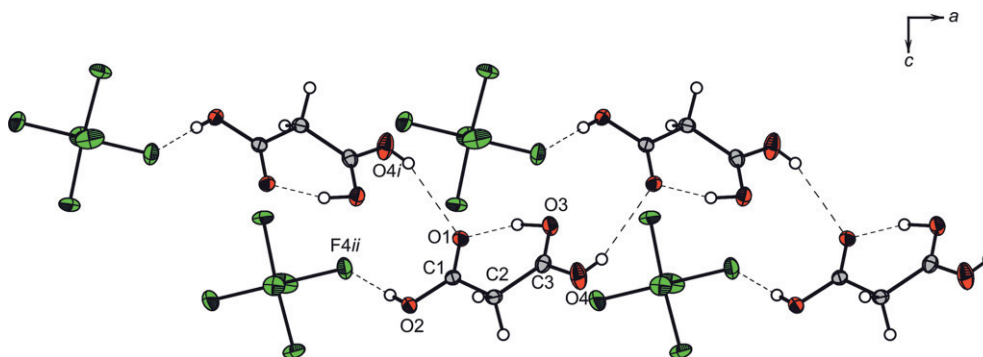


Figure 4. Illustration of the crystal packing along the *b*-axis (50 % probability displacement ellipsoids). Hydrogen bonds are drawn as dashed lines. Symmetry codes: *i* = $-0.5 + x, 0.5 - y, 1 - z$; *ii* = $-1 + x, y, z$.

(Figure 4). Table 3 lists the interatomic distances. The cations and anions form a chain along the *a*-axis involving the O4-(H4)⋯O1*i* hydrogen bonds. The anions and cations are further connected via the hydrogen bonds O2-(H2)⋯F4*ii*.^[17]

All geometric parameters of the calculated Conformer A are in good agreement with the results obtained for the [HOOCCH₂C(OH)₂]⁺ cation by single-crystal X-ray structure analysis. In Figure 5 selected calculated and experimental bond lengths and angles of the [HOOCCH₂C(OH)₂]⁺ cation are compared.

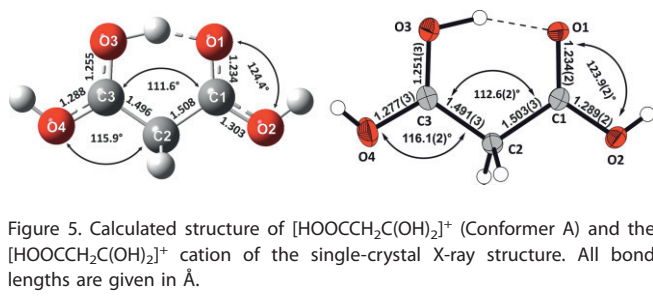


Figure 5. Calculated structure of [HOOCCH₂C(OH)₂]⁺ (Conformer A) and the [HOOCCH₂C(OH)₂]⁺ cation of the single-crystal X-ray structure. All bond lengths are given in Å.

Crystal Structure of [(HO)₂CCH₂C(OH)₂][AsF₆]₂ (**3**)

The [AsF₆][−] salts of diprotonated malonic acid [(HO)₂CCH₂C(OH)₂][AsF₆]₂ (**3**) crystallizes in the monoclinic space group *P*2₁/*c* with four formula units per unit cell. An illustration of the asymmetric unit is shown in Figure 6. Table 4 contains selected geometric parameters.

The C–C bond lengths in the cation of **3** are, with 1.502(4) Å and 1.494(4) Å, in the same range as in the monoprotonated compound **1**. The C–OH bond lengths of **3** [1.246(4) Å–1.265(3) Å] are all between a formal single and double bond.^[14,15]

In comparison to the starting material, these values are larger than the C=O bond lengths and smaller than the C–OH distances. The two C(OH)₂ groups have a dihedral angle of approximately 83° between the plane, containing the three carbon atoms. With respect to this plane, one of the C(OH)₂ groups is twisted by −93°, while the other group is rotated by about 10°.

The As–F bond lengths of the [AsF₆][−] anion range between 1.678(2) Å and 1.768(2) Å, which are typical for an [AsF₆][−] anion. Examining the structure, the anions form slightly distorted octa-

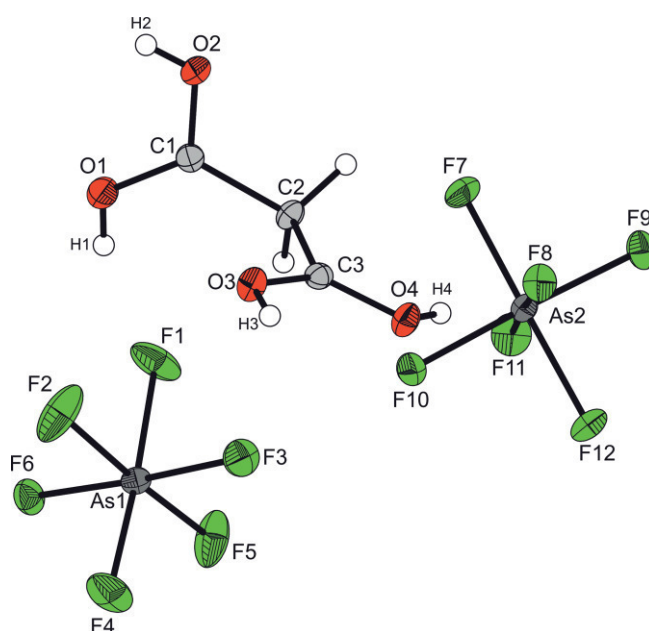


Figure 6. Asymmetric unit of **1** (50 % probability displacement ellipsoids).

Table 4. Selected bond lengths [Å] and angles [°] of **3** with estimated standard deviations in parentheses. Symmetry codes: *i* = $x, -1 + y, z$; *ii* = $-1 + x, y, z$.

Bond length [Å]			
C1–C2	1.502(4)	C1–O2	1.246(4)
C2–C3	1.494(4)	C3–O3	1.260(3)
C1–O1	1.257(4)	C3–O4	1.265(3)
Bond angles [°]			
C1–C2–C3	111.1(2)	C2–C3–O3	117.4(3)
C2–C1–O1	124.4(3)	C2–C3–O4	122.8(3)
C2–C1–O2	116.8(3)	O3–C2–O4	119.8(3)
O1–C1–O2	118.9(3)		
Torsion angles [°]			
C3–C2–C1–O1	−92.8(4)	C1–C2–C3–O3	10.0(4)
C3–C2–C1–O2	87.1(3)	C1–C2–C3–O4	−170.8(3)
Interatomic distances D⋯A [Å]			
O1–(H1)⋯F1	2.806(3)	O2–(H2)⋯F12 <i>i</i>	2.592(3)
O1–(H1)⋯F2	2.912(4)	O3–(H3)⋯F6 <i>ii</i>	2.583(3)
O4–(H4)⋯F8	2.599(3)		

hedrons.^[16] The As–F bonds, involved in hydrogen bonding (As1–F1, As1–F2, As1–F6, As2–F8 and As2–F12) are slightly longer than the other As–F bonds.

In the crystal structure of **3**, the ions are connected by a three-dimensional network of moderate O–(H)⋯F hydrogen bonds (Figure 7). The interatomic distances are summarized in Table 4. The cations and anions form chains along the *b*-axis via the strong hydrogen bonds O4–(H4)⋯F8 and O2–(H2)⋯F12*i*. Along the *a*-axis the moderate hydrogen bonds O1–(H1)⋯F1 and O1–(H1)⋯F2 as well as the strong hydrogen bond O3–(H3)⋯F6*ii* form chains, with every second connection being a five-membered ring-like structure.^[17]

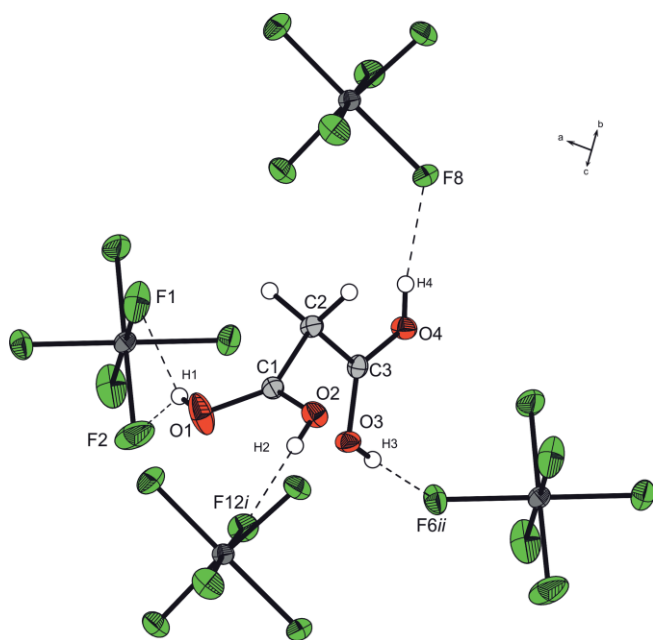


Figure 7. Hydrogen bonds of the cation with neighbored anions in the cell of **3** (50 % probability displacement ellipsoids). Hydrogen bonds are drawn as dashed lines. Symmetry codes: *i* = *x*, *−1* + *y*, *z*; *ii* = *−1* + *x*, *y*, *z*.

Comparing the experimentally obtained geometric parameters of the $[(\text{HO})_2\text{CCH}_2\text{C}(\text{OH})_2]^{2+}$ cation with those, obtained from quantum chemical calculations, it can be stated, that all bond lengths and angles are in good agreement with the calculated structure. A comparison of selected calculated and experimental bond lengths and angles of the $[(\text{HO})_2\text{CCH}_2\text{C}(\text{OH})_2]^{2+}$ cation is illustrated in Figure 8.

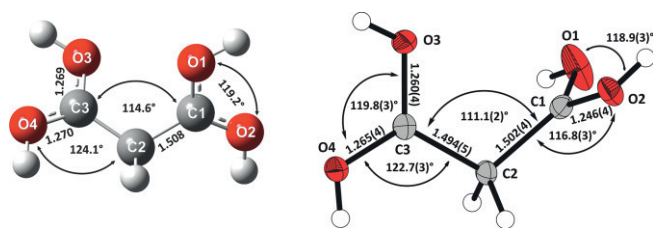


Figure 8. Calculated structure of $[(\text{HO})_2\text{CCH}_2\text{C}(\text{OH})_2]^{2+}$ and the $[(\text{HO})_2\text{CCH}_2\text{C}(\text{OH})_2]^{2+}$ cation of the single-crystal X-ray structure. All bond lengths are given in Å.

Conclusions

The diprotonated malonic acid $[(\text{HO})_2\text{CCH}_2\text{C}(\text{OH})_2][\text{AsF}_6]_2$ was synthesized in superacidic media using at least a two-to-one ratio of Lewis acid in relation to malonic acid. Diprotonated malonic acid was characterized by vibrational spectroscopy and a single-crystal X-ray structure analysis.

Furthermore, the existence of the monoprotonated malonic acid was confirmed by vibrational spectroscopy and a single-crystal X-ray structure analysis of $[\text{HOOCCH}_2\text{C}(\text{OH})_2][\text{AsF}_6]$. Salts of monoprotonated malonic acid were obtained by reacting malonic acid with an equimolar ratio of Lewis acid in anhydrous hydrogen fluoride. After the protonation, the additional proton is located between the two carbonyl oxygen atoms and forms an intermolecular hydrogen bond, explaining the nearly planar structure of $[\text{HOOCCH}_2\text{C}(\text{OH})_2][\text{AsF}_6]$.

Experimental Section

General: Caution! Avoid contact with any of these compounds. Note that hydrolysis of these salts might form HF, which burns skin and causes irreparable damage. Safety precautions should be taken when using and handling these materials.

Apparatus and Materials: All reactions were performed by employing standard Schlenk techniques using a stainless-steel vacuum line. Syntheses were carried out in FEP/PFA reactors, closed with a stainless-steel valve. In advance of usage, all reaction vessels and the stainless-steel line were dried with fluorine. For IR measurements, a cooled cell with a single-crystal CsBr plate coated with a small amount of the sample was used. IR spectra were recorded at a temperature of -196°C with a Bruker Vertex 70 V FTIR spectrometer. Raman measurements were carried out in a cooled glass cell with a Bruker MultiRAM FT-Raman spectrometer with Nd:YAG laser excitation ($\lambda = 1064\text{ nm}$) in vacuo at -196°C . The low-temperature X-ray diffraction of **1** and **3** was performed with an Oxford XCalibur3 diffractometer equipped with a Spellman generator (voltage 50 kV, current 40 mA) and a KappaCCD detector, operating with Mo- K_α radiation ($\lambda = 0.7107\text{ \AA}$). Data collection at 123 K was performed using the CrysAlis CCD software,^[18] the data reductions were carried out using the CrysAlis RED software.^[19] The solution and refinement of the structure was performed with the programs SHELXS^[20] and SHELXL-97^[21] implemented in the WinGX software package and finally checked with the PLATON software.^[22] The absorption correction was performed with the SCALE3 ABSPACK multi-scan method.^[23] Selected data and parameters of the X-ray analysis are given in Table S4. All quantum chemical calculations were performed on the MP2/aug-cc-pVTZ-level of theory by Gaussian 09.^[7]

CCDC 1582028 (for **1**), and 1582029 (for **3**) contain the supplementary crystallographic data for this paper. These data can be obtained free of charge from The Cambridge Crystallographic Data Centre.

Synthesis of $[\text{HOOCCH}_2\text{C}(\text{OH})_2][\text{AsF}_6]$ (1**), $[\text{DOOCCH}_2\text{C}(\text{OD})_2][\text{AsF}_6]$ (**5**) and $[(\text{HO})_2\text{CCH}_2\text{C}(\text{OH})_2][\text{AsF}_6]_2$ (**3**), $[(\text{DO})_2\text{CCH}_2\text{C}(\text{OD})_2][\text{AsF}_6]_2$ (**7**):** For the formation of the required superacid, arsenic pentafluoride (1.00 mmol or 3.00 mmol, 170 mg or 510 mg) and anhydrous hydrogen fluoride (150 mmol, 3 mL) were condensed into a 7 mL FEP tube-reactor. The temperature of the reaction mixture was reduced to -196°C and subsequently raised to -40°C in order to form the superacidic system. Hereafter, the temperature of the reaction vessel was again reduced to -196°C . Following this, malonic acid (1.00 mmol, 104 mg) was added to the superacid un-

der inert gas atmosphere. In order to enable the protonation of malonic acid, the temperature of the reaction mixture was again raised to $-30\text{ }^{\circ}\text{C}$ for 5 min and then reduced to $-78\text{ }^{\circ}\text{C}$. Keeping this temperature, the remaining aHF was removed in a dynamic vacuum, yielding in quantitative amounts $[\text{HOOCCH}_2\text{C}(\text{OH})_2][\text{AsF}_6]$ and $[(\text{HO})_2\text{CCH}_2\text{C}(\text{OH})_2][\text{AsF}_6]_2$ as colorless crystalline solids. $[\text{DOOCCH}_2\text{C}(\text{OD})_2][\text{AsF}_6]$ and $[(\text{DO})_2\text{CCH}_2\text{C}(\text{OD})_2][\text{AsF}_6]_2$ were prepared analogously, by using deuterium fluoride, DF, instead of aHF.

Synthesis of $[\text{HOOCCH}_2\text{C}(\text{OH})_2][\text{SbF}_6]$ (2), $[\text{DOOCCH}_2\text{C}(\text{OD})_2][\text{SbF}_6]$ (6) and $[(\text{HO})_2\text{CCH}_2\text{C}(\text{OH})_2][\text{SbF}_6]_2$ (4) and $[(\text{DO})_2\text{CCH}_2\text{C}(\text{OD})_2][\text{SbF}_6]_2$ (8): Initially, the antimony pentafluoride (1.00 mmol or 2.00 mmol, 217 mg or 434 mg) was condensed into a 7 mL FEP-tube-reactor together with aHF at $-196\text{ }^{\circ}\text{C}$. The reaction was warmed up to $0\text{ }^{\circ}\text{C}$ in order to ensure a thorough mixing of the components. Following this, the temperature was reduced to $-196\text{ }^{\circ}\text{C}$ again and malonic acid (1.00 mmol, 104 mg) was added to the superacid under inert gas atmosphere. To form the protonated species, the reaction mixture was warmed to $-40\text{ }^{\circ}\text{C}$. After 5 min the reaction vessel was cooled to $-78\text{ }^{\circ}\text{C}$ and the excess of anhydrous hydrogen fluoride was removed in a dynamic vacuum. The deuterated species were obtained by changing the solvent from aHF to deuterium fluoride aDF. All products were obtained as a colorless crystalline solid in quantitative yield.

Acknowledgments

We are grateful to the Department of Chemistry of the Ludwig-Maximilian University, the Deutsche Forschungsgemeinschaft (DFG), and F-Select GmbH for the support of this work.

Keywords: Ab initio calculations · Protonated malonic acid · Superacidic systems · Structure elucidation

[1] J. Falbe, M. Regitz in *Römpf Chemie Lexikon*, 9th ed., Vol. 4 (Ed.: E. Hillen-Maske), Georg Thieme Verlag, Stuttgart **1989**, p. 2619.

[2] V. Dessaignes, *Ann. Chem. Pharm.* **1858**, 107, 251–254.

- [3] M. Schickinger, Y. Morgenstern, K. Stierstorfer, A. Kornath, *Z. Anorg. Allg. Chem.* **2017**, 643, 1431–1435.
- [4] E. Braude, F. Nachod in *Determination of Organic Structures by Physical Methods*, Academic Press, New York, **1955**.
- [5] W. Matthews, J. Bares, J. Bartmess, F. Bordwell, F. Cornforth, G. Drucker, Z. Margolin, R. McCallum, G. McCollum, N. Vanier, *J. Am. Chem. Soc.* **1975**, 97, 7006–7014.
- [6] G. Olah, A. White, *J. Am. Chem. Soc.* **1967**, 89, 4752–4756.
- [7] *Gaussian 09*, revision a.02: M. Frisch et al., Gaussian Inc., Pittsburgh (PA, USA), **2003**.
- [8] T. Steiner, *Angew. Chem. Int. Ed.* **2002**, 41, 48–76; *Angew. Chem.* **2002**, 114, 50–80.
- [9] T. Soltner, N. Goetz, A. Kornath, *Eur. J. Inorg. Chem.* **2011**, 2011, 5429–5435.
- [10] D. Bougeard, J. de Villepin, A. Novak, *Spectrochim. Acta* **1988**, 44A, 1281–1286.
- [11] J. Weidlein, U. Müller, K. Dehnicke in *Schwingungsspektroskopie*, Georg Thieme Verlag, Stuttgart, **1988**, pp. 29–30.
- [12] N. Jagannathan, S. Rajan, E. Subramanian, *J. Chem. Crystallogr.* **1994**, 24, 75–78.
- [13] A. F. Holleman, E. Wiberg, *Lehrbuch der anorganischen Chemie* (Ed.: N. Wiberg), 102. ed., de Gruyter, Berlin **2007**, p. 2006.
- [14] F. Allen, O. Kennard, D. Watson, L. Brammer, A. Orpen, R. Taylor, *J. Chem. Soc., Perkin Trans. 2* **1987**, 1–19.
- [15] R. Minkwitz, F. Neikes, U. Lohmann, *Eur. J. Inorg. Chem.* **2002**, 27–30.
- [16] G. Jeffrey, *An Introduction to Hydrogen Bonding*, Oxford University Press, Oxford **1997**.
- [17] *CrysAlisCCD*, Version 1.171.35.11 (release 16–05–2011 CrysAlis 171.NET), Oxford Diffraction Ltd. **2011**.
- [18] *CrysAlisRED*, Version 1.171.35.11 (release 16–05–2011 CrysAlis 171.NET), Oxford Diffraction Ltd. **2011**.
- [19] G. Sheldrick, *SHELXS-97, Program for Crystal Structure Solution*, University of Göttingen (Germany), **1997**.
- [20] G. Sheldrick, *SHELXL-97, Programm for the Refinement of Crystal Structures*, University of Göttingen, Germany, **1997**.
- [21] L. Farrugia, *J. Appl. Crystallogr.* **1999**, 32, 837–838.
- [22] A. Spek, *PLATON, A Multipurpose Crystallographic Tool*, Utrecht University, Utrecht (The Netherlands), **1999**.
- [23] *SCALE3 ABSPACK* – An Oxford Diffraction program, Oxford Diffraction Ltd. **2005**.

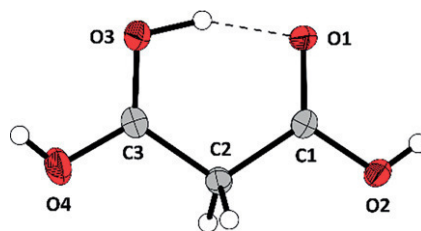
Received: September 12, 2018

Superacid Chemistry

M. Schickinger, F. Zischka,
K. Stierstorfer, A. Kornath* 1–8



Investigation of Malonic Acid in Superacidic Solutions



The structure of monoprotonated malonic acid contains an intramolecular hydrogen bond forming a six-membered ring-like structure. Mono- and diprotonated salts of malonic acid were isolated and characterized by vibrational spectroscopy and single-crystal structure analysis.

DOI: 10.1002/ejoc.201801382



Supporting Information

Investigation of Malonic Acid in Superacidic Solutions

Manuel Schickinger, Florian Zischka, Karin Stierstorfer, and Andreas Kornath*

[ejoc201801382-sup-0001-SupMat.pdf](#)

Table S1. Experimental vibrational frequencies (in cm^{-1}) of $[\text{HOOCCH}_2\text{C}(\text{OH})_2][\text{AsF}_6]$, $[(\text{HO})_2\text{CCH}_2\text{C}(\text{OH})_2][\text{AsF}_6]_2$, $[\text{DOOCCH}_2\text{C}(\text{OD})_2][\text{AsF}_6]$ and $[(\text{DO})_2\text{CCH}_2\text{C}(\text{OD})_2][\text{SbF}_6]_2$ and calculated vibrational frequencies (in cm^{-1}) of $[\text{C}_3\text{H}_5\text{O}_4]^+$ $[\text{C}_3\text{H}_2\text{D}_3\text{O}_4]^+$ $[\text{C}_3\text{H}_6\text{O}_4]^{2+}$ and $[\text{C}_3\text{H}_2\text{D}_4\text{O}_4]^{2+}$.

$[\text{HOOCCH}_2\text{C}(\text{OH})_2][\text{AsF}_6]$		$[(\text{HO})_2\text{CCH}_2\text{C}(\text{OH})_2][\text{AsF}_6]_2$		$[\text{DOOCCH}_2\text{C}(\text{OD})_2][\text{AsF}_6]$		$[(\text{DO})_2\text{CCH}_2\text{C}(\text{OD})_2][\text{SbF}_6]_2$		$[\text{C}_3\text{H}_5\text{O}_4]^+$	$[\text{C}_3\text{H}_2\text{D}_3\text{O}_4]^+$	$[\text{C}_3\text{H}_6\text{O}_4]^{2+}$	$[\text{C}_3\text{H}_2\text{D}_4\text{O}_4]^{2+}$	Assignment
IR	Raman	IR	Raman	IR	Raman	IR	Raman	calc. ^[a]	calc. ^[a]	calc. ^[a]	calc. ^[a]	
3450(m)				2486(vw)	2491(17)		2350-2125(5)	3496(210/96)	2544(120/48)	3457(365/88)	2523(1951/38)	$\nu(\text{OX})$
				2390(vw)	2389(6)		2350-2125(5)	3475(277/81)	2530(168/37)	3453(371/27)	2520(218/12)	$\nu(\text{OX})$
							2350-2125(5)			3366(500/79)	2452(303/35)	$\nu(\text{OX})$
				2294(vw)	2313(10)	2159s, br	2350-2125(5)	1895(566/9)	1268(442/11)	3362(424/41)	2449(231/20)	$\nu(\text{OX})$
	2988(20)		2998(20)	2986vw	2990(22)	2981w	2984(11)	2984(27/37)	2984(27/37)	2953(40/29)	2953(41/30)	$\nu_{\text{as}}(\text{CH}_2)$
	2967(5),		2971(4)	2963vw,	2967(5),	2938w	2943(13)	2939(32/99)	2939(31/101)	2901(40/29)	2902(45/87)	$\nu_{\text{s}}(\text{CH}_2)$
	2701(3)				2703(2)	2741w	2741(5)					$2\text{-}\delta(\text{CH}_2)$
1705(s,br)	1704(5)	1651m	1662(4)	1689m	1664(5)	1656(m)		1693(253/12)	1685(362/9)	1639(328/2)	1624(328/1)	$\nu_{\text{as}}(\text{CO}_2)$
	1622(9)	1541m	1561(30)	1519w	1525(25)	1625(s)		1610(248/1)	1627(97/2)	1601(273/1)	1588(346/1)	$\nu_{\text{as}}(\text{CO}_2)$
	1489(5)		1417(2)	1443m	1446(2)	1506(s)	1522(13)	1487(626/7)	1471(171/5)	1497(321/2)	1468(202/6)	$\nu_{\text{s}}(\text{CO}_2)$
1409m		1395w	1398(14)	1395sh	1393(9)			1420(5/8)	1421(330/1)	1496(4/16)	1465(5/18)	$\nu_{\text{s}}(\text{CO}_2)$
1357m	1360(50)	1353w	1313(4)	1349m	1361(24)	1390(m)	1395(5)	1345(66/7)	1345(66/7)	1354(42/5)	1354(44/5)	$\delta(\text{CH}_2)$
1266m	1285(6)	1310w		1248w	1249(3)	1302w		1245(92/1)	1209(51/1)	1287(93/0)	1281(67/0)	$\omega(\text{CH}_2)$
1231vw	1237(5)							1186(55/1)	842(15/0)			$\gamma(\text{OX})$
	1208(2)	1216m	1215(18)	1217w	1208(11)	1221w	1224(6)	1170(6/1)	1172(1/2)	1219(14/2)	1217(20/2)	$\tau(\text{CH}_2)$
1189m				1059vw	1062(4)	1024s	1025(12)	1163(108/3)	1029(102/1)	1145(176/4)	974(40/1)	$\delta(\text{COX})$
				1024w	1030(29)	978m		1151(39/5)	993(17/9)	1139(63/1)	965(53/11)	$\delta(\text{COX})$
			964(8)	959m	946(3)	940s	943(2)	1107(1435/3)	906(321/7)	1094(24/9)	863(6/6)	$\delta(\text{COX})$
										1086(405/2)	809(104/2)	$\delta(\text{COX})$
961vw	954(3)	942vw	944(15)			955m		928(8/1)	941(27/0)	917(6/1)	920(7/0)	$\rho(\text{CH}_2)$
	914(3)	890m	918(37)	893vw	891(1)	897m	899(4)	891(2/1)	849(36/1)	890(1/1)	847(80/1)	$\nu_{\text{as}}(\text{CC})$
866w	903(74)	824m		849w	853(12)	874m	878(4)	867(10/15)	804(85/5)	871(4/8)	811(4/1)	$\nu_{\text{s}}(\text{CC})$
			752(14)			643vs	640(10)			739(7/1)	654(5/3)	$\gamma(\text{CO})$
	722(2)	668vs		673vs	671(5)	608vs	606(2)	680(61/1)	630(1/1)	732(97/0)	603(39/0)	$\gamma(\text{OX})$
			632	600m	594(4)	543vs	541(9)	666(346/4)	601(319/5)	663(109/4)	559(73/2)	$\delta(\text{CCC})$
				559w	556(7)	421s	425(3)	661(198/1)	542(94/1)	609(348/0)	455(125/1)	$\gamma(\text{OX})$
			601(6)							603(53/1)	440(45/0)	$\gamma(\text{OX})$
	626(26)		530(11)	434w	430(5)			575(1/2)	453(1/1)	520(21/1)	467(4/1)	$\gamma(\text{CO})$

444w	552(17)	524w	553(7)				543(1/6)	504(4/6)	562(11/1)	499(36/1)	$\delta(\text{OCO})$
	433(12)						439(20/1)	396(55/1)			$\gamma(\text{OX})$
			451(5)			393s	391(3)		487(8/0)	433(48/0)	$\gamma(\text{CO})$
	407(5)							403(51/1)	394(27/0)		$\delta(\text{CCO})$
			439(2)	393vs		364s		386(104/1)	363(108/0)	372(1/4)	$\delta(\text{CCO})$
	236(6)				268(2)			263(230/1)	240(215/1)	343(1/4)	$\delta(\text{CCO})$
			141(36)							177(0/1)	$\delta(\text{CCC})$
697vs	177(11)						154(3)	138(0/1)	138(0/0)	46(2/2)	$\gamma(\text{CO})$
	113(70)				112(45)		127(5)	76(1/1)	73(1/1)	29(1/0)	$\gamma(\text{CC})$
	709(48)		719(31)		723(20)		721(38)				$[\text{MF}_6]^-$
	690(15)	704vs	706(17)	705vs	710(49)	653vs	657(100)				$[\text{MF}_6]^-$
	677(100)		687(100)		680(100)						$[\text{MF}_6]^-$
545w	579(33)	571w	571(32)	573vw	581(19)	568vs	575(5)				$[\text{MF}_6]^-$
	373(86)	396s	369(65)		372(64)		294(14)				$[\text{MF}_6]^-$

[a] Calculated at the MP2/aug-cc-pVTZ-level of theory. IR intensity in km/mol and Raman intensity in $\text{\AA}^4/\text{u}$. Abbreviations for IR intensities: v = very, s = strong, m = medium, w = weak. Experimental Raman activity is stated to a scale of 1 to 100: Calculated frequencies are scaled with an empirical factor of 0.95 [b] X = H, D, M = Sb, As.

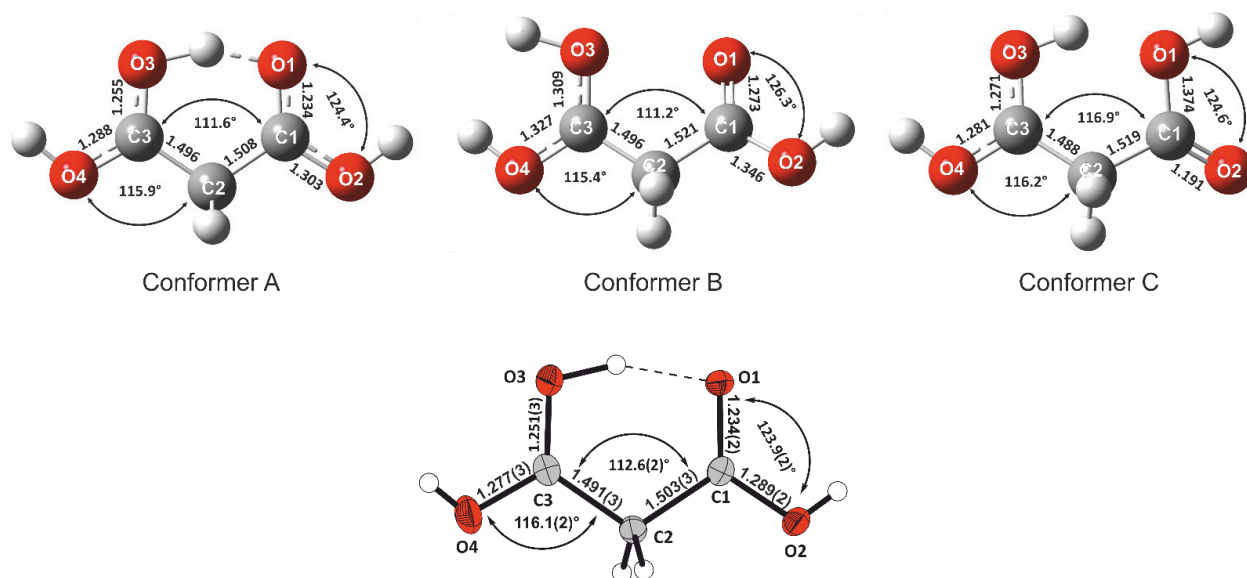


Figure S1. Comparison of the three different conformers of the $[\text{DOOCCH}_2\text{C}(\text{OD})_2]^+$ cation (first row) with the $[\text{HOOCCH}_2\text{C}(\text{OH})_2]^+$ cation of the single-crystal X-ray structure

Table S2. Experimental vibrational frequencies (in cm^{-1}) of, $[\text{DOOCCH}_2\text{C}(\text{OD})_2][\text{AsF}_6]$ and the calculated vibrational frequencies (in cm^{-1}) of the Conformers A, B and C of the $[\text{C}_3\text{H}_2\text{D}_3\text{O}_4]^+$ cation.

$\text{DOOCCH}_2\text{C}(\text{OD})_2[\text{AsF}_6]$		$[\text{C}_3\text{H}_2\text{D}_3\text{O}_4]^+$	$[\text{C}_3\text{H}_2\text{D}_3\text{O}_4]^+$	$[\text{C}_3\text{H}_2\text{D}_3\text{O}_4]^+$	Assignment
IR	Raman	calc. ^[a]	calc. ^[a]	calc. ^[a]	
2486(vw)	2491(17)	2553(118/45)	2510(109/40)	2544(120/48)	$\nu(\text{OD})$
2390(vw)	2389(6)	2520(169/40)	2446(113/49)	2530(168/37)	$\nu(\text{OD})$
2294(vw)	2313(10)	2161(492/19)	1605(88/62)	1268(442/11)	$\nu(\text{OD})$
2986vw	2990(22)	3007(24/42)	2802(20/60)	2984(27/37)	$\nu_{\text{as}}(\text{CH}_2)$
2963vw,	2967(5),	2908(38/91)	2708(38/106)	2939(31/101)	$\nu_{\text{s}}(\text{CH}_2)$
	2703(2)				$2\cdot\delta(\text{CH}_2)$
1689m	1664(5)	1774(253/15)	1436(287/11)	1685(362/9)	$\nu_{\text{as}}(\text{CO}_2)$
1519w	1525(25)	1589(438/1)	1404(216/5)	1627(97/2)	$\nu_{\text{as}}(\text{CO}_2)$
1443m	1446(2)	1477(199/11)	1374(34/3)	1471(171/5)	$\nu_{\text{s}}(\text{CO}_2)$
1395sh	1393(9)	1153(25/2)	1308(49/1)	1421(330/1)	$\nu_{\text{s}}(\text{CO}_2)$
1349m	1361(24)	1348(52/6)	1362(164/10)	1345(66/7)	$\delta(\text{CH}_2)$
1248w	1249(3)	1254(9/1)	1190(104/2)	1209(51/1)	$\omega(\text{CH}_2)$
		656(16/0)	815(45/2)	842(15/0)	$\gamma(\text{OD})$
1217w	1208(11)	1197(63/2)	1174(83/3)	1172(1/2)	$\tau(\text{CH}_2)$
1059vw	1062(4)	1004(102/4)	1043(90/5)	1029(102/1)	$\delta(\text{COD})$
1024w	1030(29)	959(52/2)	950(51/4)	993(17/9)	$\delta(\text{COD})$
959m	946(3)	946(58/1)	886(54/4)	906(321/7)	$\delta(\text{COD})$
		906(18/1)	586(5/1)	941(27/0)	$\rho(\text{CH}_2)$
893vw	891(1)	842(17/1)	839(5/1)	849(36/1)	$\nu_{\text{as}}(\text{CC})$
849w	853(12)	798(29/9)	795(45/9)	804(85/5)	$\nu_{\text{s}}(\text{CC})$
673vs	671(5)	656(16/0)	621(16/3)	630(1/1)	$\gamma(\text{OX})$
600m	594(4)	575(27/3)	935(19/3)	601(319/5)	$\delta(\text{CCC})$
559w	556(7)	433(6/0)	500(46/1)	542(94/1)	$\gamma(\text{OD})$
434w	430(5)	617(15/1)	658(11/6)	453(1/1)	$\gamma(\text{CO})$
		543(68/1)	541(74/3)	504(4/6)	$\delta(\text{OCO})$
		404(43/1)	420(47/0)	396(55/1)	$\gamma(\text{OD})$
		374(13/3)	374(3/2)	394(27/0)	$\delta(\text{CCO})$
393vs		351(14/0)	361(7/0)	363(108/0)	$\delta(\text{CCO})$
	268(2)	251(24/1)	263(8/0)	240(215/1)	$\delta(\text{CCO})$
		90(1/0)	144(3/1)	138(0/0)	$\gamma(\text{CO})$
	112(45)	53(2/0)	157(1/0)	73(1/1)	$\gamma(\text{CC})$

	723(20)	[AsF ₆] [−]
705vs	710(49)	[AsF ₆] [−]
	680(100)	[AsF ₆] [−]
573vw	581(19)	[AsF ₆] [−]
	372(64)	[AsF ₆] [−]

[a] Calculated at the MP2/aug-cc-pVTZ-level of theory. IR intensity in km/mol and Raman intensity in Å⁴/u. Abbreviations for IR intensities: v = very, s = strong, m = medium, w = weak. Raman activity is stated to a scale of 1 to 100. Frequencies are scaled with an empirical factor of 0.95

Table S3. Comparison of selected geometric parameters of the cations of **1** and **3** and malonic acid.

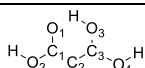
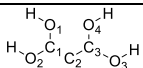
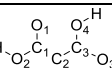
			
Bond distances [Å]			
C1-C2	1.503(3)	1.502(4)	1.503(2)
C2-C3	1.491(3)	1.494(4)	1.499(3)
C1-O1	1.234(2)	1.257(4)	1.227(2)
C1-O2	1.289(3)	1.246(4)	1.288(2)
C3-O3	1.251(3)	1.260(3)	1.219(2)
C3-O4	1.277(3)	1.265(3)	1.292(2)
Bond angles [°]			
C1-C2-C3	112.5(2)	111.1(2)	111.3(1)
C2-C1-O1	122.5(2)	124.4(3)	121.7(2)
C2-C1-O2	113.6(2)	116.8(3)	113.5(1)
O1-C1-O2	123.9(2)	118.9(3)	124.8(1)
C2-C3-O3	122.8(2)	117.4(3)	121.8(1)
C2-C3-O4	116.1(2)	122.8(3)	115.0(1)
O3-C2-O4	121.1(2)	119.8(3)	123.3(2)
Torsions angles [°]			
C3-C2-C1-O1	0.9(3)	-92.8(4)	-7.3
C3-C2-C1-O2	-178.8(2)	87.1(3)	173.2
C1-C2-C3-O3	-3.8(3)	10.0(4)	87.0
C1-C2-C3-O4	175.8(2)	-170.8(3)	-91.9

Table S4. X-ray data and parameters of **1** and **3**

	[HOOCCH ₂ C(OH) ₂][AsF ₆]	[(HO) ₂ CCH ₂ C(OH) ₂][AsF ₆] ₂
formula	C ₃ H ₅ AsF ₆ O ₄	C ₃ H ₆ As ₂ F ₁₂ O ₄
M _r [g mol ⁻¹]	293.99	483.92
crystal size, [mm ³]	0.25 x 0.2 x 0.15	0.30 x 0.25 x 0.2
crystal system	orthorhombic	monoclinic
space group	<i>Pbca</i>	<i>P2₁/n</i>
<i>a</i> [Å]	9.6739(4)	7.3348(2)
<i>b</i> [Å]	11.8355(5)	9.8437(3)
<i>c</i> [Å]	13.9826(6)	16.6903(6)
α [deg]	90.0	90.0
β [deg]	90.0	97.818(3)
γ [deg]	90.0	90.0
<i>V</i> [Å ³]	1600.94(12)	1193.86(7)
<i>Z</i>	8	4
ρ _{calcd} , [g cm ⁻³]	2.439	2.692
μ(MoK _α), [cm ⁻¹]	0.71073	0.71073
<i>F</i> (000)	1136	920
<i>T</i> [K]	173(2)	173(2)
<i>hkl</i> range	-12:11; -14:9; -17:17	-9:9; -12:12; -20:11
refl. measured	7871	5110
refl. unique	1624	2436
<i>R</i> _{int}	0.0250	0.0220
parameters	139	202
<i>R</i> (<i>F</i>)/ <i>wR</i> (<i>F</i> ²) [^a] (all reflexions)	0.0235/0.0496	0.0317/0.0652
weighting scheme ^[b]	0.0245/0.9033	0.0347/0.3359
<i>S</i> (GooF) ^[c]	1.047	1.031
residual density [e Å ⁻³]	0.274/-0.452	0.959/-0.844
device type	Oxford XCalibur	Oxford XCalibur
solution	SHELXS-97 ^[1]	SHELXS-97 ^[1]
refinement	SHELXL-97 ^[2]	SHELXL-97 ^[2]
CCDC	1582028	1582029

[a] $R_1 = \sum ||F_o| - |F_c|| / \sum |F_o|$; [b] $wR_2 = [\sum [w(F_o^2 - F_c^2)^2] / \sum [w(F_o^2)^2]]^{1/2}$; $w = [\sigma_c^2(F_o^2) + (xP)^2 + yP]^{-1}$; $P = (F_o^2 + 2F_c^2)/3$ [c] GooF = $\{\sum [w(F_o^2 - F_c^2)^2] / (n-p)\}^{1/2}$ (*n* = number of reflections; *p* = total number of parameters)

[1] G. Sheldrick, *SHELXS-97, Program for Crystal Structure Solution*, University of Göttingen (Germany), **1997**.

[2] G. Sheldrick, *SHELXL-97, Programm for the Refinement of Crystal Structures*, University of Göttingen, Germany, **1997**.

Organic & Supramolecular Chemistry

The Tetrahydroxydicarbenium Cation $[(\text{HO})_2\text{CC}(\text{OH})_2]^{2+}$:
Synthesis and StructureManuel Schickinger, Thomas Saal, Florian Zischka, Joachim Axhausen, Karin Stierstorfer,
Yvonne Morgenstern, and Andreas J. Kornath^{*[a]}

Oxalic acid forms in superacidic solutions HF/MF_5 ($M = \text{As}, \text{Sb}$) its corresponding mono- and diprotonated salts $[\text{HOOCC}(\text{OH})_2][\text{MF}_6]$ and $[(\text{HO})_2\text{CC}(\text{OH})_2][\text{MF}_6]_2$ ($M = \text{As}, \text{Sb}$). The number of protonations is strongly dependent on the stoichiometric ratio of the Lewis acid with regard to oxalic acid. Mono- and diprotonated salts were characterized by vibrational spectroscopy and in the case of $[\text{HOOCC}(\text{OH})_2][\text{AsF}_6]$ (1) and $[(\text{HO})_2\text{CC}(\text{OH})_2][\text{SbF}_6]_2$ (4) by a single-crystal X-ray structure analysis. The salts crystallize in the monoclinic space groups $P2_1/c$ and $P2_1/n$ with eight, respectively

four, formula units per unit cell. The vibrational spectra were compared to quantum chemical calculations of the cations $[\text{HOOCC}(\text{OH})_2]^+$ and $[(\text{HO})_2\text{CC}(\text{OH})_2]^{2+} \cdot 4\text{HF}$. In addition to this, an MEP analysis together with the NPA charges of $[(\text{HO})_2\text{CC}(\text{OH})_2]^{2+}$, $[(\text{HO})_2\text{CC}(\text{OH})_2]^{2+} \cdot 6\text{HF}$ and oxalic acid were calculated to locate the positive charge. The protonation of oxalic acid does not lead to a remarkable change of the C-C bond length, which is discussed for the entire series of the oxalic skeleton, starting with the dianion and ending with the tetrahydroxy dication.

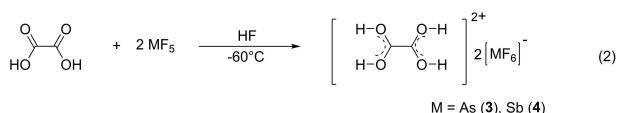
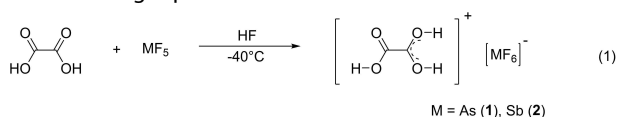
Introduction

Oxalic acid is the simplest representative of dicarboxylic acids. With its structure containing no CH bonds, it is at the interface of organic and inorganic chemistry. In 1769, oxalic acid was isolated by *Johann Christian Wiegleb* for the first time from *Oxalis acetosella* (wood sorrel), for which it is named.^[1] In 1953, *Wiles* studied the behavior of *n*-aliphatic dicarboxylic acids in sulfuric acid. He found that oxalic acid decomposes while all other examined acids remain stable.^[2] *Olah* reported in 1957 the existence of mono- and diprotonated oxalic acid in "magic acid", proven by ^1H - and ^{13}C -NMR spectroscopy.^[3,4] An intriguing structural feature of the diprotonated oxalic acid is the vicinal position of its positive charges, which had previously only been known for the nitrogen framework structure of diprotonated hydrazine.^[5] Thus, the described positioning of the vicinal positive charges was found for the first time for a carbon framework. In 1999 a crystal structure of the diprotonated oxalic acid co-crystallized with four molecules of water was already reported.^[6] This crystal structure raises general questions, since it is unlikely that in a superacidic medium the molecule of lower basicity (oxalic acid) is protonated before the more basic water. Consequently, we examined the behavior of oxalic acid in superacidic media.

Results and Discussion

Synthesis and Properties of $[\text{HOOCC}(\text{OH})_2][\text{MF}_6]$ and $[(\text{HO})_2\text{CC}(\text{OH})_2][\text{MF}_6]_2$ ($M = \text{As}, \text{Sb}$)

The preparations of the salts containing the mono- and dications were carried out as two-step syntheses according to the following Equations 1 and 2:



Initially, the superacidic medium was prepared. For this, the Lewis acid, SbF_5 or AsF_5 , was mixed with an excess of hydrogen fluoride at a low temperature. Complete solvation was achieved by homogenizing the superacid solution at -20°C . Following this, oxalic acid was added to the frozen superacidic system under inert gas atmosphere. After warming the reaction mixture slowly to -40°C , the protonated species were formed immediately. Excess *a*HF was removed at -78°C *in vacuo*. All products were obtained as colorless salts in quantitative yield with the monoprotonated salts of oxalic acid $[\text{HOOCC}(\text{OH})_2][\text{AsF}_6]$ (1) and $[\text{HOOCC}(\text{OH})_2][\text{SbF}_6]$ (2) being stable up to -20°C and the diprotonated salts $[(\text{HO})_2\text{CC}(\text{OH})_2][\text{AsF}_6]_2$ (5) as well as $[(\text{HO})_2\text{CC}(\text{OH})_2][\text{SbF}_6]_2$ (6) being stable up to -50°C .

The corresponding deuterated salts, $[\text{DOOCC}(\text{OD})_2][\text{AsF}_6]$ (5), $[\text{DOOCC}(\text{OD})_2][\text{SbF}_6]$ (6), $[(\text{DO})_2\text{CC}(\text{OD})_2][\text{AsF}_6]_2$ (7) and $[(\text{DO})_2\text{CC}(\text{OD})_2][\text{SbF}_6]_2$ (8), are obtained by changing the superacidic system from HF/MF_5 to DF/MF_5 ($M = \text{As}, \text{Sb}$). The hydroxyl hydrogens are entirely replaced by deuterium, as deuterium

[a] M. Schickinger, T. Saal, F. Zischka, J. Axhausen, K. Stierstorfer, Y. Morgenstern, Prof. A. J. Kornath
Department Chemie, Ludwig-Maximilians-Universität München, Butenandtstr. 5–13(D), 81377 München, Germany
Fax: +49-89-2180-77867
E-mail: andreas.kornath@cup.uni-muenchen.de

Supporting information for this article is available on the WWW under <https://doi.org/10.1002/slct.201802456>

fluoride is used in large excess. The degree of deuteration approximates 96%.

Vibrational Spectra

The infrared and Raman spectra of $[\text{HOOCC}(\text{OH})_2][\text{AsF}_6]$ (**1**), $[\text{DOOCC}(\text{OD})_2][\text{AsF}_6]$ (**3**), $[(\text{HO})_2\text{CC}(\text{OH})_2][\text{AsF}_6]_2$ (**5**), $[(\text{DO})_2\text{CC}(\text{OD})_2][\text{AsF}_6]_2$ (**7**) and oxalic acid are illustrated in Figure 1. Tables 1 and

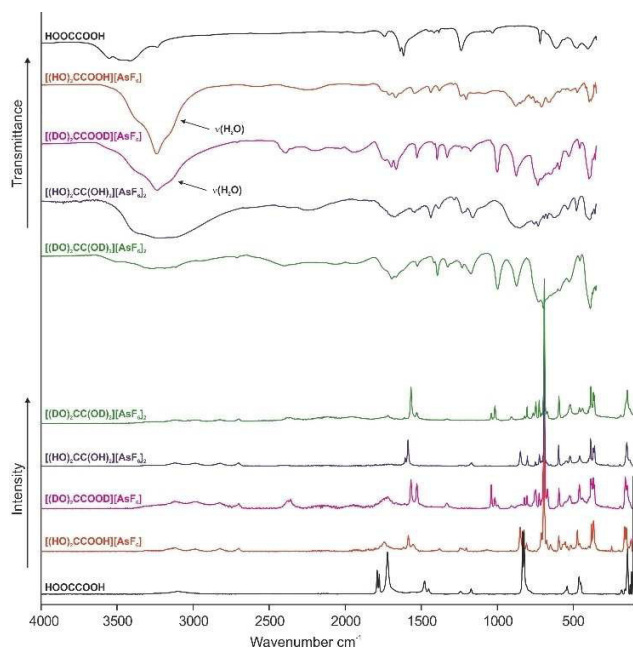


Figure 1. Low temperature Raman and IR spectra of oxalic acid, [HOCC(OH)₂][AsF₆] (1), [DOCC(OD)₂][AsF₆] (3), [(HO)₂CC(OH)₂][AsF₆] (5), and [(HO)₂CC(OH)₂][AsF₆] (7).

2 summarize selected experimental infrared and Raman frequencies together with the quantum chemically calculated frequencies of the cations $[\text{C}_2\text{H}_3\text{O}_4]^+$, $[\text{C}_2\text{D}_3\text{O}_4]^+$, $[\text{C}_2\text{H}_4\text{O}_4]^{2+} \cdot 4\text{HF}$, and $[\text{C}_2\text{D}_4\text{O}_4]^{2+}$. The complete tables are attached in the Supporting Information.

Vibrational Spectra of the monoprotonated salts of oxalic acid 1 and 3

According to quantum chemical calculations, C_1 -symmetry is predicted for the $[\text{HOOCC}(\text{OH})_2]^+$ and $[\text{DOOCC}(\text{OD})_2]^+$ cations, with 21 fundamental vibrations. All of them are IR and Raman active. The assignment is based on an analysis of the Cartesian displacement vectors of the calculated vibrational modes and on a comparison with the vibrations described in literature for oxalic acid.^[7]

In the IR spectrum of **1**, the OH stretching vibrations are overlaid by the $\nu(\text{OH})$ vibrations of water. The existence of condensed water as a broad band at 3240 cm^{-1} for the IR spectra of **1** and **3** is caused by the measuring method. As a result of the poor polarizability of the OH group, corresponding Raman lines usually are of low intensity. This is not the case for the OD stretching vibrations. The OD stretching vibrations of $[\text{DOOCC}(\text{OD})_2][\text{AsF}_6]$ are observed at 2392 cm^{-1} in the IR spectrum and at 2376 cm^{-1} , respectively 2360 cm^{-1} in the Raman spectrum.^[8]

The broad band at 1744 cm^{-1} in the IR spectrum of **3** can be assigned to the CO stretching vibration by a comparison with the quantum chemical calculations. An indication for a successful O-protonation is the disappearance of the antisymmetric C=O stretching vibration of oxalic acid at 1793 cm^{-1} and 1780 cm^{-1} .^[7] Compared to the starting material, the remaining CO stretching vibration has a lower intensity and is blue-shifted by 19 cm^{-1} . The lines at 1585 cm^{-1} and 1552 cm^{-1} for $[\text{HOOC}(\text{OH})_2][\text{AsF}_6]$ are determined as CO stretching vibrations. In contrast to oxalic acid, they are blue-shifted by 103 cm^{-1} and 98 cm^{-1} respectively. The CO stretching vibration is splitted into two lines for **1**, this is probably caused by packing effects or crystal field splitting. Coincidentally, a similar effect is observed for oxalic acid.^[7] The CO stretching vibrations at 1438 cm^{-1} and 1382 cm^{-1} (IR) are in good agreement with the quantum chemical calculations. The COH deformation vibrations are not affected by the protonation and are in accordance with the ones found for oxalic acid. Similar results are found for the CC stretching vibration, which appears at 879 cm^{-1} (IR) and 850 cm^{-1} (Ra) and is thus in good agreement with frequencies observed for oxalic acid.

Table 1. Selected experimental vibrational frequencies (in cm^{-1}) of $[\text{HOOC}(\text{OH})_2][\text{AsF}_6]$ (1), $[\text{DOOCCH}_2\text{C}(\text{OD})_2][\text{AsF}_6]$ (3), $[\text{HOOC}(\text{OH})_2][\text{AsF}_6]^{[\text{a}]}$ and calculated vibrational frequencies (in cm^{-1}) of $[\text{C}_7\text{H}_5\text{O}_4]^+$ and $[\text{C}_7\text{D}_5\text{O}_4]^+$.

[HOOC(OH) ₂][AsF ₆] ^[a]		[HOOC(OH) ₂][AsF ₆]		[DOOC(OD) ₂][AsF ₆]		[C ₂ H ₃ O ₄] ⁺ ·	[C ₂ D ₃ O ₄] ⁺	Assignment ^[c]
IR	Raman	IR	Raman	IR	Raman	calc. ^[b] (IR/Raman)	calc. ^[b] (IR/Raman)	
				2394(m)	2376(19)	3555(242/85)	2588(140/43)	ν(OX)
3156(br)					2360(22)	3486(202/90)	2540(109/42)	ν(OX)
1704(br)						3464(390/18)	2522(233/8)	ν(OX)
1667(br)	1588(23)	1712(s)	1744(7)	1697(s), 1666(s)	1721(8)	1820(233/24)	1818(230/23)	ν _{as} (CO)
1443(m)		1543(m)	1585(13), 1552(5)		1560(21), 1529(17)	1625(218/2)	1608(284/2)	ν _{as} (CO)
1236(m)		1438(m), 1382(m)	1383(2)	1396(s), 1330(s)	1332(4)	1479(238/8)	1441(133/11)	ν _s (CO)
875(s)	846(20)	1240(s)	1245(3)	1176(w)		1279(100/4)	1195(165/3)	ν _s (CO)
		879(m)	850(18)		750(14)	749(17/9)	661(10/6)	ν(CC)

[a] reported in reference 6 [b] Calculated at the B3LYP/aug-cc-pVTZ level of theory. IR intensity in km/mol and Raman intensity in Å⁴/u. Abbreviations for IR intensities: v = very, s = strong, m = medium, w = weak, br = broad. Raman activity is stated to a scale of 1 to 100: Frequencies are scaled with an empirical factor of 0.965. [c] X = H, D.

Table 2. Selected experimental vibrational frequencies (in cm^{-1}) of $[(\text{HO})_2\text{CC}(\text{OH})_2][\text{AsF}_6]_2$ (**5**) and $[(\text{DO})_2\text{CC}(\text{OD})_2][\text{AsF}_6]_2$ (**7**), $[(\text{HO})_2\text{CC}(\text{OH})_2][\text{SbF}_6]_2$ ^[a] and calculated vibrational frequencies (in cm^{-1}) of $[\text{C}_2\text{H}_4\text{O}_4]^{2+} \cdot 4\text{HF}$ and $[\text{C}_2\text{D}_4\text{O}_4]^{2+}$.

$[(\text{HO})_2\text{CC}(\text{OH})_2][\text{SbF}_6]_2$ ^[a]	$[(\text{HO})_2\text{CC}(\text{OH})_2][\text{AsF}_6]_2$	$[(\text{DO})_2\text{CC}(\text{OD})_2][\text{AsF}_6]_2$	$[\text{C}_2\text{H}_4\text{O}_4]^{2+} \cdot 4\text{HF}$	$[\text{C}_2\text{D}_4\text{O}_4]^{2+}$	Assignment ^[c]
IR	Raman	IR	Raman	calc. ^[b] (IR/Raman)	
			2350-2450	2762(1/226)	$\nu(\text{OX})$
				2725(3619/0)	$\nu(\text{OX})$
			2350-2450	2630(70/166)	$\nu(\text{OX})$
		2406(w)		2610(6012/2)	$\nu(\text{OX})$
1731(s)	1699(m)	1695(m)		1678(601/0)	$\nu_{\text{as}}(\text{CO})$
1671(sh)			1721(3)	1677(22/3)	$\nu_{\text{as}}(\text{CO})$
	1607(5), 1592(9)	1607(5), 1588(16)	1586(23), 1531(5)	1656(553/0)	$\nu_{\text{s}}(\text{CO})$
1386(w)	1437(m)	1395(m), 1327(w)		1517(0/22)	$\nu_{\text{s}}(\text{CO})$
	851(11)	849(14)	673(5)	1415(348/0)	$\nu_{\text{s}}(\text{CO})$
				1352(179/0)	$\nu(\text{CC})$
				828(0/10)	$\nu(\text{CC})$
				656(0/5)	

[a] reported in reference 6 [b] Calculated at the B3LYP/aug-cc-pVTZ level of theory. IR intensity in km/mol and Raman intensity in $\text{\AA}^4/\text{u}$. Abbreviations for IR intensities: ν = very, s = strong, m = medium, w = weak, br = broad. Raman activity is stated to a scale of 1 to 100: Frequencies are scaled with an empirical factor of 0.965. [c] $X = \text{H, D}$; $M = \text{As, Sb}$.

For the anions $[\text{MF}_6]^-$ ($M = \text{As, Sb}$) with an ideal octahedral symmetry, two bands in the infrared spectrum and three lines in the Raman spectrum are expected. In both cases, more than five vibrations are observed. This indicates a lower symmetry, which is in accordance with the results of the crystal structure analysis.

The vibrational spectroscopic data for monoprotonated oxalic acid, reported by Minkwitz *et al.*, was included in our assignment of the vibrations and is in accordance with our results.^[6]

Vibrational Spectra of the diprotonated salts of oxalic acid **5** and **7**

For the $[(\text{HO})_2\text{CC}(\text{OH})_2]^{2+} \cdot 4\text{HF}$ and $[(\text{DO})_2\text{CC}(\text{OD})_2]^{2+}$ cations, C_1 -symmetry is predicted according to quantum chemical calculations, with 24 fundamental vibrations. Higher symmetries, like C_2 , C_{2h} or C_s , would be expected, but the protons being slightly out of the oxalic backbone plane lead to C_1 -symmetry. The assignment of the vibrations was performed by analyzing the Cartesian displacement coordinates of the calculated vibrational modes and by a comparison with the corresponding vibrations of oxalic acid.^[7]

The infrared spectrum of $[(\text{DO})_2\text{CC}(\text{OD})_2][\text{AsF}_6]_2$ (**7**) exhibits a $\nu(\text{OD})$ vibration at 2406 cm^{-1} , which deviates by 22 cm^{-1} to lower wavenumbers compared to the quantum chemical calculation (2438 cm^{-1}). In the Raman spectra of **7**, the $\nu(\text{OD})$ vibrations, visible in the region around 2400 cm^{-1} , are weak and broad. The disappearance of all $\text{C}=\text{O}$ stretching vibrations of oxalic acid at 1793 cm^{-1} , 1780 cm^{-1} and 1725 cm^{-1} indicates a successful diprotonation.^[7] The $\nu(\text{CO})$ vibration of $[(\text{HO})_2\text{CC}(\text{OH})_2][\text{AsF}_6]_2$ at 1699 cm^{-1} (IR) is blue-shifted by 61 cm^{-1} compared to oxalic acid (1638 cm^{-1} , and 1617 cm^{-1}).^[7] Similar to $[\text{HOOCC}(\text{OH})_2][\text{AsF}_6]$, the CO stretching vibration at 1588 cm^{-1} is blue-shifted by 106 cm^{-1} compared to the starting material. The vibrational frequency of $[(\text{HO})_2\text{CC}(\text{OH})_2][\text{AsF}_6]_2$ at 1437 cm^{-1} (Raman) can be determined, according to the quantum chemical calculation, as a CO stretching vibration. All COH , CCO and OCO deformation vibrations are in good agreement with the calculated values. The CC stretching vibration of **5** is slightly red-shifted by 24 cm^{-1}

compared to oxalic acid, possibly resulting from charge repulsion, which is discussed later.

An ideal octahedral symmetry for the anions $[\text{AsF}_6]^-$ leads to two bands in the infrared spectrum and three lines in the Raman spectrum. Combining Raman and IR spectra of **5** and **7**, more than five vibrations are observed. This suggests a lower symmetry, which is in good agreement with the crystal structure analysis. The lower symmetry can be explained by a distortion of the anion in the solid state. Again, this assumption is confirmed by the crystal structure.

The vibrational spectra previously reported for $[(\text{HO})_2\text{CC}(\text{OH})_2][\text{SbF}_6]_2$ only partially correspond to ours. In this context, it is possible to find a correspondence for the CO and CC stretching vibrations, but not for vibrational frequencies below 1100 wavenumbers .^[6]

Crystal Structure of $[\text{HOOCC}(\text{OH})_2][\text{AsF}_6]$

The $[\text{AsF}_6]^-$ salt of monoprotonated oxalic acid, $[\text{HOOCC}(\text{OH})_2][\text{AsF}_6]$ (**1**), crystallizes in the monoclinic space group $P2_1/c$ with eight formula units per unit cell, containing two symmetrically independent formula units. Having slightly different geometric parameters, both symmetrically independent formula units are discussed. Illustrations of the asymmetric unit are shown in Figure 2. Selected geometric parameters of **1** are listed in Table 3 together with the geometric parameters reported in the literature for $[\text{HOOCC}(\text{OH})_2][\text{SbF}_6]$ (**2**).^[6]

The $\text{C}-\text{C}$ bond distances of monoprotonated oxalic acid are, with $1.538(6) \text{ \AA}$ and $1.555(6) \text{ \AA}$, in the range of a formal $\text{C}-\text{C}$ single bond and similar to that found in oxalic acid ($1.537(1) \text{ \AA}$).^[9] Comparing the $\text{C}=\text{O}$ bond lengths of anhydrous oxalic acid ($1.222(1)^\circ \text{ \AA}$ or $1.207(1)^\circ \text{ \AA}$) with **1** ($\text{C}1-\text{O}2$ $1.207(6) \text{ \AA}$ or $\text{C}3-\text{O}6$ $1.213(6) \text{ \AA}$), it can be stated that they are in good agreement and still in the region of a formal $\text{C}=\text{O}$ bond.^[9,10] The $\text{C}1-\text{O}1$ ($1.315(6) \text{ \AA}$) and the $\text{C}3-\text{O}6$ distance ($1.296(6) \text{ \AA}$) of **1** are in accordance with the literature values of oxalic acid ($1.290(1) \text{ \AA}$ or $1.306(1) \text{ \AA}$).^[6,9] These $\text{C}-\text{O}$ distances are all between a formal CO single and double bond.^[10] The same applies to the $\text{C}-\text{O}$ bond distances (**1**) of $\text{C}2-\text{O}3$ ($1.268(5)^\circ \text{ \AA}$), $\text{C}2-\text{O}4$ ($1.259(6)^\circ \text{ \AA}$), $\text{C}4-\text{O}7$ ($1.266(6)^\circ \text{ \AA}$) and

C4–O8 (1.253(6) Å).^[10] The difference in bond length of the former CO double bond and the CO single bond decreases, caused by the delocalized positive charge.^[6] This delocalization is observed for all protonated carboxyl groups, as, for instance, for protonated formic acid [HC(OH)₂][AsF₆] (9).^[11] Differences in the C–O(H) bond lengths of **1** can be explained by hydrogen bonding. The O=C=O angles are, with 127.6(4)° and 128.1(4)°, slightly widened compared to the starting material (126.9(1)° and 126.7(1)°).^[9] With a maximum deviation of 5.6° to the plane, the [HOOCC(OH)₂]⁺ cation has an almost planar geometry.

The As–F bond lengths of the [AsF₆][−] anion are range from 1.710(3) Å to 1.750(3) Å. These values are typical for an [AsF₆][−] anion.^[12] The anions form slightly distorted octahedrons. The As–F bonds, which are involved in hydrogen bonding (As1–F3, As1–F5 and As2–F10 and As2–F11), are slightly longer than the other As–F bonds.

In the crystal packing of **1**, the ions are connected by a network of moderate O–H...F hydrogen bonds (Figure 3), with the bond lengths and angles being summarized in Table 3.

The cations, connected by hydrogen bonding (O4*iii*–H4*iii*...O2 and O7–H7...O6*iii*), form chains along the *c*-axis.^[6] Cations and anions build hydrogen bonds (O1–H1...F5*i*, O3–H3...F11 and O5–H5...F10*iv*, O8–H8...F3) forming a two-dimensional layer structure along the *ac*-plane. These layers are stacked alternately, with no bonds connecting the individual layers along the *b*-axis.^[13,14]

The geometric parameters for the cation of [HOOCC(OH)₂][SbF₆] (**2**), reported by Minkwitz *et al.*, are in good accordance with the experimental data for **1**. In contrast to our structure the C=O bond distance of **2** (1.187(3) Å) is slightly shortened compared to **1** (1.207(6) Å and 1.213(6) Å).^[6]

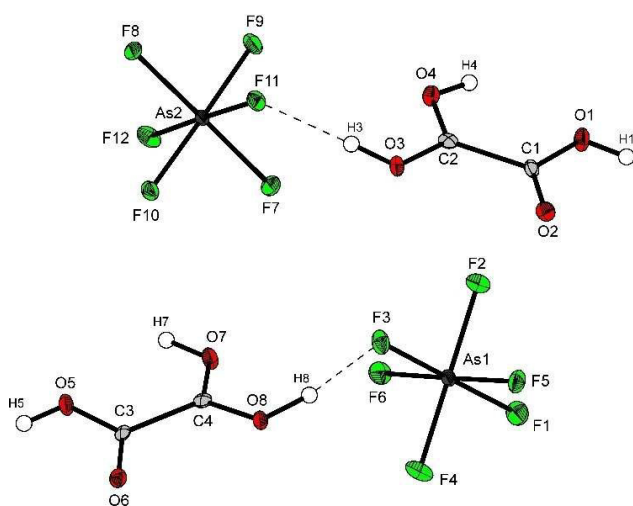


Figure 2. Projection of the asymmetric unit of [HOOCC(OH)₂][AsF₆] (50% probability displacement ellipsoids). Hydrogen bonds are drawn as dashed lines.

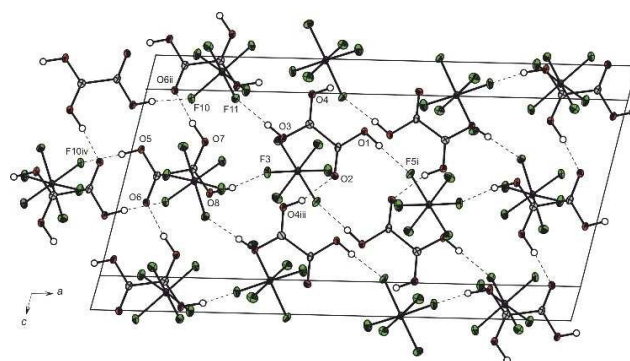


Figure 3. Projection of the interionic contacts between anion and cation of [HOOCC(OH)₂][AsF₆] (50% probability displacement ellipsoids). Hydrogen bonds are drawn as dashed lines. Symmetry codes: *i* = 1−*x*, 1−*y*, 1−*z*, *ii* = *x*, 0.5−*y*, −0.5 + *z*, *iii* = *x*, 1.5−*y*, 0.5 + *z* and *iv* = −*x*, −0.5 + *y*, 0.5−*z*.

Crystal Structure of [(HO)₂CC(OH)₂][SbF₆]₂

The [SbF₆][−] salt of diprotonated oxalic acid, [(HO)₂CC(OH)₂][SbF₆]₂ (**4**) crystallizes in the monoclinic space group *P*2₁/*c* with two formula units per unit cell. A formula unit of **4** is displayed in Figure 4. Table 4 contains selected geometric parameters.

The [(HO)₂CC(OH)₂]²⁺ cation possesses centrosymmetry, which is located on the C–C bond. Moreover, for the entire carbon oxygen skeleton a planar structure is observed.

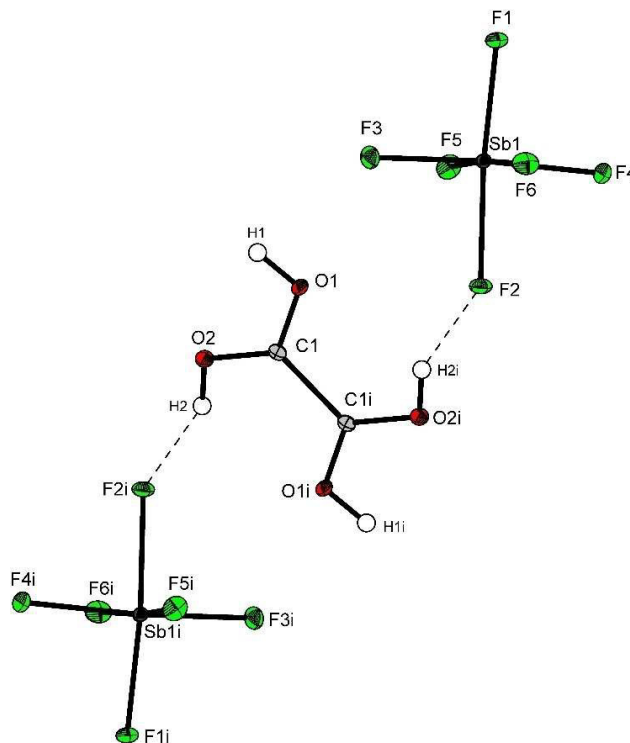


Figure 4. Projection of the formula unit of [(HO)₂CC(OH)₂][SbF₆]₂ (50% probability displacement ellipsoids). Hydrogen bonds are drawn as dashed lines. Symmetry code: *i* = 1−*x*, −*y*, 1−*z*.

Table 3. Selected bond lengths (in Å) and angles (in deg) of 1 and the literature values for 2 ^[6] with estimated standard deviations in parentheses. Symmetry codes: <i>i</i> = 1-x, 1-y, 1-z, <i>ii</i> = x, 0.5-y, -0.5+z, <i>iii</i> = x, 1.5-y, 0.5+z, <i>iv</i> = -x, -0.5+y, 0.5-z.		
Bond length [Å]	[HOOCC(OH) ₂][AsF ₆]	[HOOCC(OH) ₂][SbF ₆] ^[6]
C1-C2	1.538(6)	1.530(3)
C1-O1	1.315(6)	1.313(3)
C1-O2	1.207(6)	1.187(3)
C2-O3	1.268(5)	1.270(3)
C2-O4	1.259(6)	1.259(3)
C3-C4	1.555(6)	
C3-O5	1.295(6)	
C3-O6	1.213(6)	
C4-O7	1.253(6)	
C4-O8	1.266(6)	
Bond angles [°]		
C1-C2-O3	113.7(4)	118.1(2)
C1-C2-O4	124.1(4)	124.2(2)
C2-C1-O1	110.5(4)	109.5(2)
C2-C1-O2	122.0(4)	119.9(2)
O1-C1-O2	127.6(4)	130.6(2)
O3-C2-O4	122.2(4)	117.5(2)
C3-C4-O7	123.5(4)	
C3-C4-O8	114.1(4)	
C4-C3-O5	110.1(4)	
C4-C3-O6	122.4(4)	
O5-C3-O6	128.1(4)	
O7-C4-O8	122.4(4)	
Dihedral angles [°]		
O2-C1-C2-O4	179.5(4)	
O2-C1-C2-O3	1.3(6)	
O6-C3-C4-O7	174.5(4)	
O6-C3-C4-O8	-5.2(6)	
Interatomic distances D-A [Å]		
O1-(H1)---F5 <i>i</i>	2.639(4)	2.689(3)
O3-(H3)---F11	2.668(4)	2.601(3)
O5-(H5)---F10 <i>iv</i>	2.666(4)	
O8-(H8)---F3	2.616(4)	
O4 <i>iii</i> -(H4 <i>iii</i>)---O2	2.552(5)	
O7-(H7)---O6 <i>ii</i>	2.540(5)	

Surprisingly, when comparing the C-C bond distance of **4** (1.528(3) Å), **1** (1.538(6) Å) and anhydrous oxalic acid (1.537(1) Å), no significant difference is found. with the C-C bond distances being in the range of a formal C-C single bond.^[10] The C-O bond lengths of [(HO)₂CC(OH)₂][SbF₆]₂ (1.257(2) Å and 1.259(2) Å) are fairly similar and between a formal C-O single (1.43 Å) and double bond (1.19 Å).^[10] Reasonably similar C-O bond distances can be found for other protonated carboxylic acids, like [HOOCC(OH)₂][AsF₆]**(1)** (1.259(6) Å/1.253(6) Å and 1.268(5) Å/1.266(6) Å) and [HC(OH)₂][AsF₆]**(2)** (1.255(5) Å and 1.239(6) Å).^[9] The O-C-O and O-C-O angles are in good agreement with those observed for **1**, **9** and **10**.^[6,9]

The Sb-F bond lengths of the [SbF₆]⁻ anions range from 1.857(1) Å to 1.921(1) Å. Compared to the values reported in the literature, they are typical for an [SbF₆]⁻ anion, with it displaying a slightly distorted octahedral coordination.^[15-18] The

Table 4. Selected bond lengths (in Å) and angles (in deg) of 4 and [(HO) ₂ CC(OH) ₂][SbF ₆] ₂ ·4H ₂ O with estimated standard deviations in parentheses. Symmetry codes: <i>i</i> = -1+x, y, z; <i>ii</i> = 1-x, -y, 1-z, <i>v</i> = 1-x, -y, 1-z and <i>vi</i> = 1.5x, -0.5+y, 0.5-z. ^[6]		
Bond lengths [Å]	[(HO) ₂ CC(OH) ₂][SbF ₆] ₂	[(HO) ₂ CC(OH) ₂][SbF ₆] ₂ ·4H ₂ O
C1-C1 <i>i</i>	1.528(3)	1.521(8)
C1-O1	1.257(2)	1.256(4)
C1-O2	1.259(2)	1.256(4)
Bond angles [°]		
C1 <i>i</i> -C1-O1	114.2(2)	114.7(3)
C1 <i>i</i> -C1-O2	122.4(2)	122.0(3)
O1-C1-O2	123.4(2)	123.3(3)
Interatomic distances D-A [Å]		
O1-(H1)---F4 <i>i</i>	2.485(2)	
O2-(H2)---F2 <i>ii</i>	2.500(2)	2.495(2)
C1 <i>v</i> ---F6 <i>vi</i>	2.531(3)	
C1---F6 <i>vi</i>	2.472(2)	
O1---O3		2.457(3)
O3---O4		2.440(3)

Sb1-F2 and Sb1-F2*i* bonds, which are involved in hydrogen bonding, are slightly longer than the other Sb-F bonds.

In the crystal structure of [(HO)₂CC(OH)₂][SbF₆]₂, the ions are connected by a network of strong hydrogen bonds (Figure 5).^[13] Each [(HO)₂CC(OH)₂]²⁺ cation forms hydrogen bonds with four different [SbF₆]⁻ anions, causing a zigzag-like chain structure. All the individual [SbF₆]⁻ anions form hydrogen bonds to two different [(HO)₂CC(OH)₂]²⁺ cations. There are also strong interactions between carbon and fluorine (C1*v*---F6*vi* with 2.531(3) Å and C1---F6*vi* with 2.472(2) Å), stabilizing the C-C bond. These interactions are within the van-der-Waals radii (3.17 Å).^[14]

The surprising feature of the structure of diprotonated oxalic acid is that the C-C bond distance does not change significantly compared to oxalic acid. In Table 5, the C-C bond distances of some selected protonated and deprotonated salts containing oxalic acid are listed. Surprisingly, irrespective of the oxalic acid's charge, no significant difference in the C-C bond length is observable. Seemingly, the C-C bond length is not affected by the charge of the oxalic acid's backbone. This presumption is supported by the results of the quantum chemical calculations, discussed later.

Minkwitz *et al.* reported in 1999 the crystal structure of [(HO)₂CC(OH)₂][SbF₆]₂·4H₂O, which raised general questions, since it is unlikely that in a superacidic medium the molecule of lower basicity (oxalic acid) is protonated before the more basic water. At first sight, the previously reported^[6] bond distances of the [(HO)₂CC(OH)₂]²⁺ cation are in good agreement with our findings for this cation. The location of the protons in the X-ray structure analysis is not meaningful, but taking a closer look at the interatomic contacts leads us to the assumption, that a different interpretation of the crystal structure is possible. The four hydrate molecules form pairs via O...O contacts of 2.457(3) Å and 2.440(3) Å. Such contacts are found for the [H₃O]⁺ cation (2.400(3) Å, 2.418(8) Å and 2.40(1) Å). Assuming

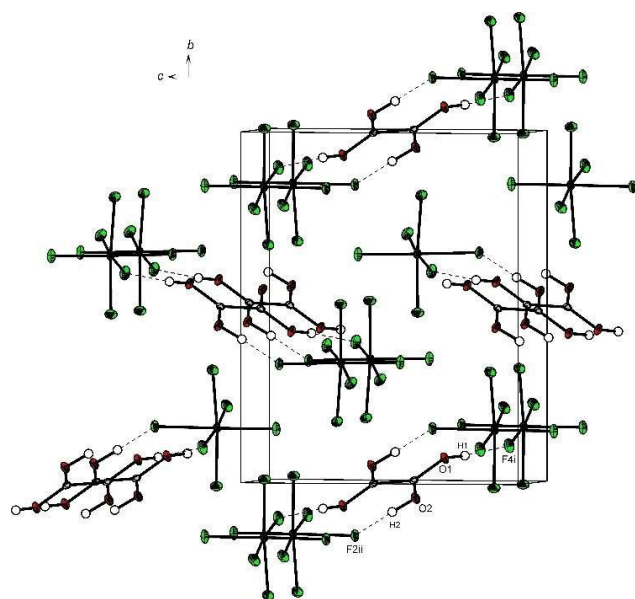


Figure 5. Projection of the interionic contacts between anion and cation of $[(\text{HO})_2\text{CC}(\text{OH})_2][\text{SbF}_6]_2$ (50% probability displacement ellipsoids). Symmetry codes: $i = -1 + x, y, z$; $ii = 1 - x, -y, 1 - z$.

the cations actually are $[\text{H}_3\text{O}_2]^+$ cations, this crystal structure would be better interpreted as $2[\text{H}_3\text{O}_2][\text{SbF}_6] \cdot \text{C}_2\text{O}_4\text{H}_2$. From this point of view, different C-O bond lengths should be obtained for the oxalic acid backbone, which cannot be observed. The reason for this most likely is intermolecular charge repulsion, like it is reported for $\text{Na}_2\text{C}_2\text{O}_4$ ^[19] (C-O: 1.534(3) Å and 1.654(3) Å). Combining this charge repulsion with intermolecular hydrogen bonding, which is for instance reported for $\text{CaC}_2\text{O}_4 \cdot \text{H}_2\text{O}$, all four C-O bond distances are equal (1.253(4) Å).^[22] This special case also applies to $[(\text{HO})_2\text{CC}(\text{OH})_2][\text{SbF}_6]_2 \cdot 4\text{H}_2\text{O}$ described by *Min- kwitz et al.*, resulting in four equal C-O bond distances.

Quantum chemical calculations

All calculations were performed at the B3LYP/aug-cc-pVTZ-level of theory with the Gaussian program package.^[34] Bond lengths and angles of the $[\text{HOCC}(\text{OH})_2]^+$ and the $[(\text{HO})_2\text{CC}(\text{OH})_2]^{2+} \cdot 6\text{HF}$ cation are shown in Figure 6 and 7. The hydrogen fluoride molecules added to the gas phase structure of the $[(\text{HO})_2\text{CC}(\text{OH})_2]^{2+}$ simulate hydrogen bonding in the solid state. This method already is established in the literature.^[35] For the $[\text{HOCC}(\text{OH})_2]^+$ cation this method does not lead to satisfying results.

Comparing the experimentally obtained geometric parameters of the $[\text{HOCC}(\text{OH})_2]^+$ cation, with those obtained from quantum chemical calculations, it can be stated, that all bond lengths and angles are in good agreement with the calculated structure. The sole exception is the C1-O2 bond distance which, compared to the experimental value, is slightly elongated in the calculation. This is probably due to hydrogen bonding observed in the solid state, but not considered in quantum chemical calculations.

Table 5. Summary of C-C and C-O distances of some selected oxalic acid derivatives.

Charge of the oxalate backbone	Compound	C-C distance [Å]	C1-O1/2 distance [Å]	C2-O3/4 distance [Å]
− 2	$\text{Na}_2\text{C}_2\text{O}_4$ ^[19]	1.568(4)	1.253(4), 1.265(4)	
	$\text{Na}_2\text{C}_2\text{O}_4 \cdot \text{H}_2\text{O}_2$ ^[20]	1.570(11)	1.270(7), 1.259(7)	
	$\text{Na}_2\text{C}_2\text{O}_4 \cdot \text{H}_2\text{O}_2$ ^[21]	1.564(10)	1.267(1), 1.245(1)	
	$\text{CaC}_2\text{O}_4 \cdot \text{H}_2\text{O}$ ^[22]	1.530(8)	1.247(8), 1.229(8)	
	$\text{CaC}_2\text{O}_4 \cdot \text{H}_2\text{O}$ ^[22]	1.550(4)	1.253(4), 1.253(4)	
	$(\text{NH}_4)_2\text{C}_2\text{O}_4 \cdot \text{H}_2\text{O}$ ^[23]	1.565(14)	1.254(5), 1.248(9)	
	$(\text{NH}_4)_2\text{C}_2\text{O}_4 \cdot \text{H}_2\text{O}$ ^[23]	1.557(2)	1.248(2), 1.254(3)	
− 1	$\text{NaHC}_2\text{O}_4 \cdot 2\text{H}_2\text{O}$ ^[24]	1.552(3)	1.210(1), 1.307(1)	1.245(1), 1.249(1)
	$(\text{NH}_4)\text{HC}_2\text{O}_4$ ^[25]	1.587(13)	1.30(1), 1.20(1)	1.24(1), 1.22(1)
	KHC_2O_4 ^[26]	1.547(2)	1.309(3), 1.214(3)	1.256(3), 1.239(3)
	KHC_2O_4 ^[27]	1.543(10)	1.297(9), 1.218(9)	1.267(9), 1.229(9)
	KHC_2O_4 ^[28]	1.552(2)	1.234(2), 1.256(2)	1.211(2), 1.308(2)
− 0.5	$(\text{NH}_4)\text{H}_3(\text{C}_2\text{O}_4)_2 \cdot 2\text{H}_2\text{O}$ ^[29]	1.549(5)	1.211(4), 1.288(4)	
	$(\text{NH}_4)\text{H}_3(\text{C}_2\text{O}_4)_2 \cdot 2\text{H}_2\text{O}$ ^[29]	1.544(5)	1.206(4), 1.296(4)	
	$(\text{NH}_4)\text{H}_3(\text{C}_2\text{O}_4)_2 \cdot 2\text{H}_2\text{O}$ ^[29]	1.549(3)	1.212(4), 1.291(4)	1.247(4), 1.230(4)
0	$\alpha\text{-H}_2\text{C}_2\text{O}_4$ ^[9]	1.537(1)	1.207(1), 1.306(1)	
	$\beta\text{-H}_2\text{C}_2\text{O}_4$ ^[9]	1.537(1)	1.222(1), 1.290(1)	
	$\alpha\text{-H}_2\text{C}_2\text{O}_4 \cdot 2\text{H}_2\text{O}$ ^[30]	1.544(1)	1.289(1), 1.223(1)	
	$\alpha\text{-H}_2\text{C}_2\text{O}_4 \cdot 2\text{H}_2\text{O}$ ^[31]	1.536(3)	1.212(4), 1.291(5)	
+ 1	$[\text{C}_2\text{O}_4\text{H}_3][\text{SbF}_6]$ ^[6]	1.530(3)	1.187(3), 1.313(3)	1.270(3), 1.259(3)
	$[\text{C}_2\text{O}_4\text{H}_3][\text{AsF}_6]$	1.538(6)	1.207(6), 1.315(6)	1.259(6), 1.268(6)
	$[\text{C}_2\text{O}_4\text{H}_3][\text{AsF}_6]$	1.555(6)	1.213(6), 1.295(6)	1.253(6), 1.266(6)
+ 2	$[\text{C}_2\text{O}_4\text{H}_4][\text{SbF}_6] \cdot 4\text{H}_2\text{O}$ ^[6]	1.521(8)	1.256(4), 1.256(4)	
	$[\text{C}_2\text{O}_4\text{H}_4][\text{SbF}_6]_2$	1.528(3)	1.257(2), 1.259(2)	

Compared to our experimental data for $[(\text{HO})_2\text{CC}(\text{OH})_2]^{2+}$, all bond lengths and angles are in good accordance with the calculated structure, except the CCO angle, which differs slightly. The method of adding four HF molecules only is an approximation to the solid state interactions, which, however, leads to satisfying results for almost all geometrical and vibrational values.

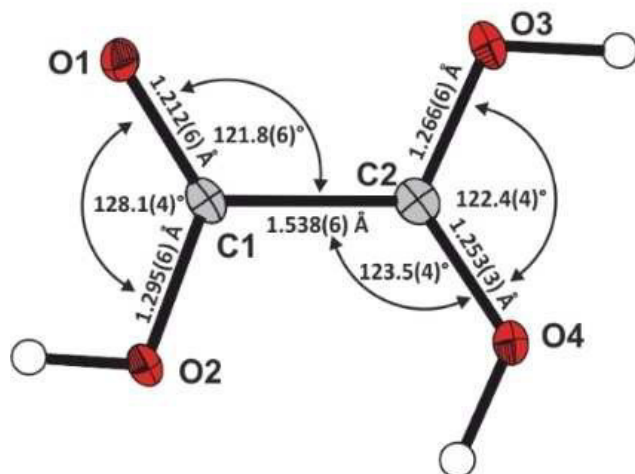
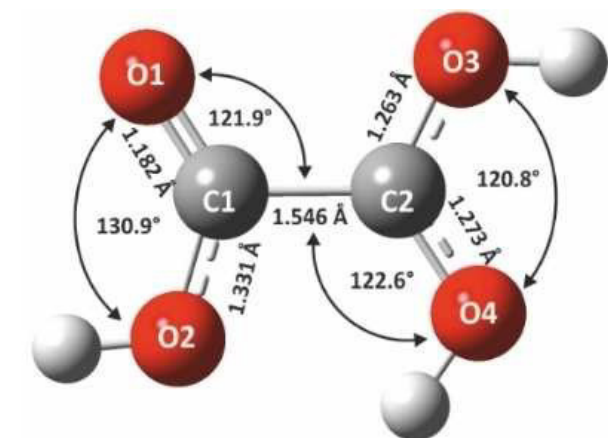


Figure 6. Calculated structure of $[\text{HOOCC}(\text{OH})_2]^+$ and the $[\text{HOOCC}(\text{OH})_2]^+$ cation of the single-crystal X-ray structure.

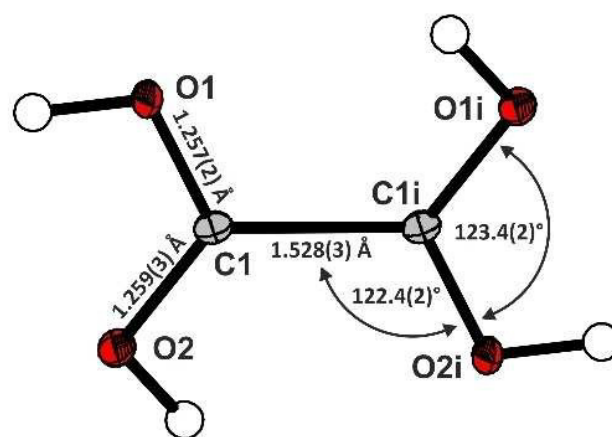
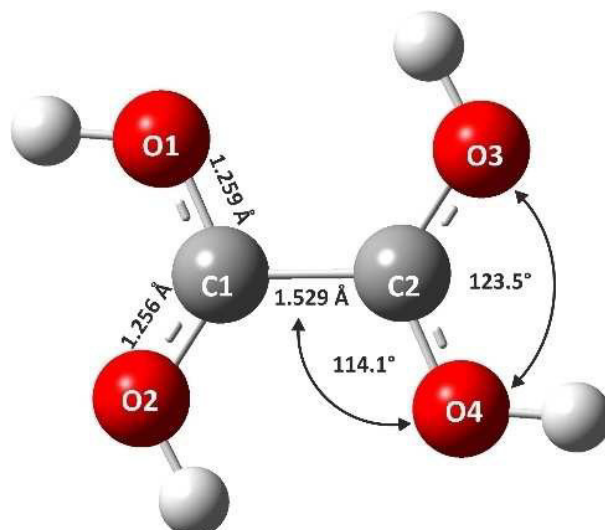


Figure 7. Calculated structure of $[(\text{HO})_2\text{CC}(\text{OH})_2]^{2+}$ and the $[(\text{HO})_2\text{CC}(\text{OH})_2]^{2+} \cdot 6\text{HF}$ cation of the single-crystal X-ray structure

Figures 8, 9 and 10 depict the Mapped Electrostatic Potentials (MEPs) together with Natural Population Analysis charges (NPA) of oxalic acid, $[(\text{HO})_2\text{CC}(\text{OH})_2]^{2+}$ and $[(\text{HO})_2\text{CC}(\text{OH})_2]^{2+} \cdot 6\text{HF}$. A positive electrostatic potential between the two carbon atoms in the MEP is observed for all three structures. The relative distribution of the electrostatic potential in the oxalic acid backbone remains unchanged despite the different charges of the molecules and hydrogen bonding. Comparing the NPA charges of oxalic acid (Figure 8) with the charges of the free diprotonated cation of oxalic acid (Figure 9), the positive charges at the carbon atoms increase, whereas the negative charges of the oxygen atoms decrease. This applies in particular to the oxygen atoms (O2 and O3) of former hydroxyl groups. The positive charge is delocalized over the individual OCO groups.

The simulation of the solid state effects using four HF molecules (Figure 10) results in an even slightly stronger delocalization of the positive charge. This is probably the reason for the similar C-C bond distances in oxalic acid with different stages of protonation.

As a result of these calculations, it is obvious that salts of diprotonated oxalic acid have two vicinal positive charges at the carbon atoms. Similarities have already been observed with hydrazine. The N-N bond distance of diprotonated hydrazine (1.438(5) Å) and non-protonated hydrazine (1.447(9) Å) do not differ significantly.^[5,36] To our best knowledge, this is the first time that a molecule with a carbon backbone has been isolated with two positive charges at the vicinal carbon atoms.

Conclusion

Salts of the monoprotinated oxalic acid $[\text{HOOCC}(\text{OH})_2][\text{MF}_6]$, were synthesized in the superacidic media HF/MF_5 ($M = \text{As}, \text{Sb}$) and characterized by Raman and IR spectroscopy. The results obtained by a single-crystal X-ray analysis of $[\text{HOOCC}(\text{OH})_2][\text{AsF}_6]$, supported by quantum chemical calculations, are in good agreement with the geometric parameters published by Minkwitz *et al.* in 1999 for $[\text{HOOCC}(\text{OH})_2][\text{SbF}_6]$.^[6]

Salts of diprotonated oxalic acid, $[(\text{HO})_2\text{CC}(\text{OH})_2][\text{MF}_6]_2$, were obtained by reacting oxalic acid in superacidic media HF/MF_5 ($M = \text{As}, \text{Sb}$). These were characterized by vibrational spectroscopy and in the case of $[(\text{HO})_2\text{CC}(\text{OH})_2][\text{SbF}_6]_2$ additionally by a single-crystal X-ray structure analysis, supported by quantum chemical calculations.

A former crystal structure of diprotonated oxalic acid, $[(\text{HO})_2\text{CC}(\text{OH})_2][\text{SbF}_6]_2 \cdot 4\text{H}_2\text{O}$, raised general questions, since it is

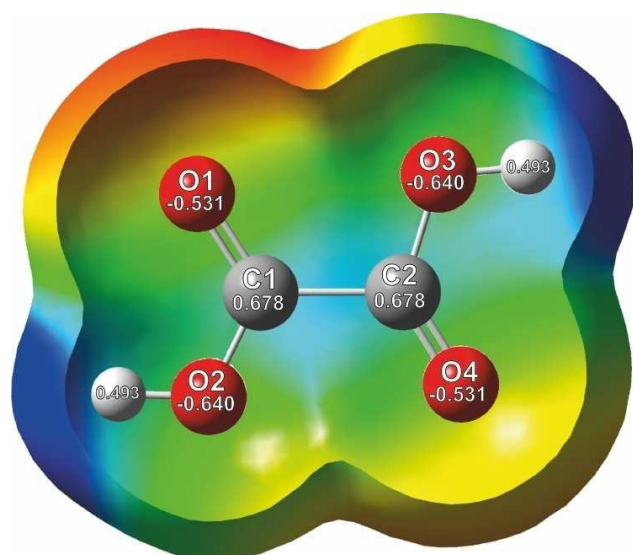


Figure 8. Molecular 0.0004 bohr^{-3} 3D isosurfaces with mapped electrostatic potential as a color scale ranging from -0.05 a.u. (red) to 0.05 a.u. (blue). The electrostatic potential isosurfaces and the NPA charges have been calculated for HOOCCOOH .

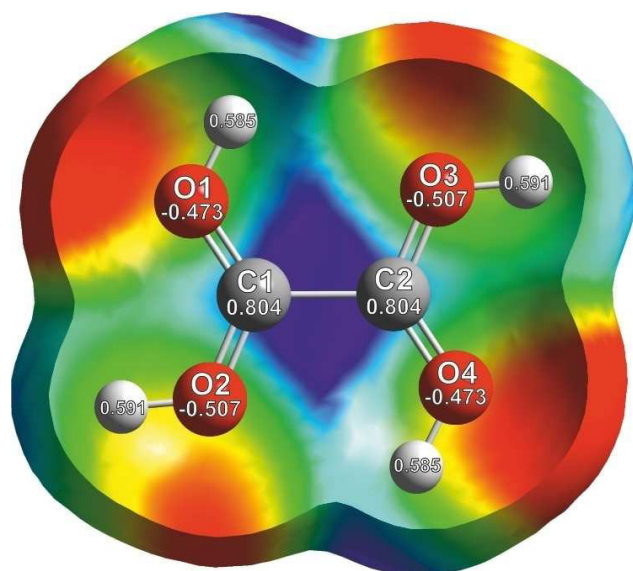


Figure 9. Molecular 0.0004 bohr^{-3} 3D isosurfaces with mapped electrostatic potential as a color scale ranging from 0.32 a.u. (red) to 0.40 a.u. (blue). The electrostatic potential isosurfaces and the NPA charges have been calculated for $[(\text{HO})_2\text{CC}(\text{OH})_2]^{2+}$.

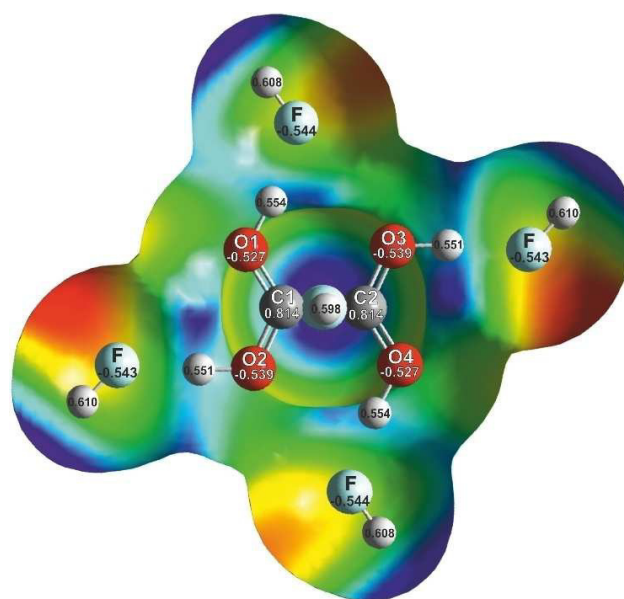


Figure 10. Molecular 0.0004 bohr^{-3} 3D isosurfaces with mapped electrostatic potential as a color scale ranging from 0.20 a.u. (red) to 0.28 a.u. (blue). The electrostatic potential isosurfaces and the NPA charges have been calculated for $[(\text{HO})_2\text{CC}(\text{OH})_2]^{2+} \cdot 6\text{HF}$.

unlikely that in a superacidic medium the molecule of lower basicity (oxalic acid) is protonated before the more basic water.

This structure is more correctly described as $[\text{H}_5\text{O}_2]_2[\text{SbF}_6]_2 \cdot \text{C}_2\text{O}_4\text{H}_2$.^[6,32,33]

Surprisingly, the C-C-bond distance does not change significantly for oxalic acid in different stages of protonation. This is confirmed by our experimental results and supported by quantum chemical calculations of the geometric parameters, MEP analysis and NPA charges. The calculations support that, for the first time, a dication has been isolated containing two vicinal positive charges in the carbon backbone.

Supporting Information Summary

The Supporting Information section contains two tables with the complete vibrational frequencies of the mono- and diprotonated salts of oxalic acid, the experimental section and a table summarizing the X-ray data of **1** and **4**.

Acknowledgements

We are grateful to the Department of Chemistry of the Ludwig-Maximilian University, Munich, the Deutsche Forschungsgemeinschaft (DFG) and the F-Select GmbH for the support of this work.

Conflict of Interest

The authors declare no conflict of interest.

Keywords: protonated oxalic acid · quantum chemical calculations · superacidic systems · vibrational spectroscopy · X-ray diffraction

- [1] M. Yamaguchi, S. Matsuyama, K. Yamaji, *Appl Entomol Zool* **2016**, 51(1), 91–98.
- [2] L. Wiles, J. Goulden, *J. Am. Chem. Soc.* **1953**, 0, 996–998.
- [3] G. Olah, A. White, *J. Am. Chem. Soc.* **1967**, 89(18), 4752–4756.
- [4] G. Olah, J. Bausch, H. George, G. Prakash, *J. Am. Chem. Soc.* **1993**, 115(18), 8060–8065.
- [5] T. Klapötke, P. White; I. Tornieporth-Oetting, *Polyhedron* **1996**, 15(15), 2579–2582.
- [6] R. Minkwitz, N. Hartfeld, C. Hirsch, *Z. anorg. allg. Chem.* **1999**, 625, 1479–1485.
- [7] J. De Villepin, A. Novak, D. Bougeard, *Chem Phys* **1982**, 73, 291–312.
- [8] J. Weidlein, U. Müller, K. Dehnicke in *Schwingungsspektroskopie*, Georg Thieme Verlag, Stuttgart, **1988**, pp 29–30.
- [9] J. Derissen, P. H. Smit, *Acta Cryst. B* **1974**, 30, 2240–2242.
- [10] A. Holleman, E. Wiberg, *Lehrbuch der anorganischen Chemie*, (Ed.: N. Wiberg), 102. ed., de Gruyter, Berlin **2007**, p. 2006.
- [11] R. Minkwitz, S. Schneider, M. Seifert, H. Hartl, *Z. anorg. allg. Chem.* **1996**, 622, 1404–1410.
- [12] R. Minkwitz, F. Neikes, U. Lohmann, *Eur. J. Inorg. Chem.* **2002**, 27–30.
- [13] A. Bondi, *J. Phys. Chem.* **1964**, 68(3), 441–451.
- [14] G. Jeffrey, *An Introduction to Hydrogen Bonding*, Oxford University Press, Oxford **1997**.
- [15] R. Minkwitz, G. Nowicki, H. Preut, *Z. anorg. allg. Chem.* **1992**, 611, 23–27.
- [16] K. Christe, W. Wilson, D. Dixon, S. Khan, R. Bau, T. Metzenthin, R. Lu, *J. Am. Chem. Soc.* **1993**, 115(5), 1836–1842.
- [17] R. Minkwitz, S. Schneider, *Angew. Chem.* **1999**, 111, 229–231.
- [18] R. Minkwitz, C. Hirsch, T. Berends, *Eur. J. Inorg. Chem.* **1999**, 1999, 2249–2254.
- [19] D. Reed, M. Olmstead, *Acta Cryst. B* **1981**, 37, 938–939.
- [20] B. Pedersen, B. F. Pedersen, *Acta Chem. Scand.* **1964**, 18(6), 1454–1468.
- [21] B. Pedersen, Å. Kvick, *Acta Cryst. C* **1989**, 45, 1727–1730.
- [22] S. Deganello, *Acta Cryst. B* **1981**, 37, 826–829.
- [23] J. Taylor, T. Sabine, *Acta Cryst. B* **1972**, 28, 3340–3351.
- [24] R. Tellgren, J. Thomas, I. Olovsson, *Acta Cryst. B* **1977**, 33, 3500–3504.
- [25] H. Audebrand, D. Louër, *Z. Kristallogr.* **2002**, 217, 35–40.
- [26] F. Moore, L. Power, *Inorg. Nucl. Chem. Letters* **1971**, 7, 873–875.
- [27] B. Pedersen, *Acta Chem. Scand.* **1968**, 22, 2953–2964.
- [28] H. Elinspahr, R. Marsh, J. Donohue, *Acta Cryst. B* **1972**, 28, 2194–2198.
- [29] M. Currie, J. Speakman N. Curry, *J. Chem. Soc. A* **1967**, 0, 1862–1869.
- [30] E. Stevens, P. Coppens, *Acta Cryst. B* **1980**, 36, 1864–1876.
- [31] T. Sabine, G. Cox, B. Craven, *Acta Cryst. B* **1969**, 25, 2437–2441.
- [32] R. Minkwitz, C. Hirsch, *Acta Cryst. C* **1999**, 55, 703–705.
- [33] R. Minkwitz, S. Schneider, A. Kornath, *Inorg. Chem.* **1998**, 37, 4662–4665.
- [34] Gaussian 09, revision a.02: M. Frisch, Gaussian Inc., Pittsburgh (PA, USA), **2003**.
- [35] T. Soltner, N. Goetz, A. Kornath, *Eur. J. Inorg. Chem.* **2011**, 20, 5429–5435.
- [36] R. Liminga, I. Olovsson, *Acta Cryst. C* **1964**, 17, 1523–1528.

Submitted: August 3, 2018

Accepted: October 31, 2018



Supporting Information

© Copyright Wiley-VCH Verlag GmbH & Co. KGaA, 69451 Weinheim, 2018

The Tetrahydroxydicarbenium Cation $[(\text{HO})_2\text{CC}(\text{OH})_2]^{2+}$: Synthesis and Structure

Manuel Schickinger, Thomas Saal, Florian Zischka, Joachim Axhausen, Karin Stierstorfer, Yvonne Morgenstern, and Andreas J. Kornath*

Table S1. Experimental vibrational frequencies (in cm^{-1}) of $[\text{HOCC}(\text{OH})_2][\text{AsF}_6]$ (**1**), $[\text{DOCCCH}_2\text{C}(\text{OD})_2][\text{AsF}_6]$ (**3**), $[\text{HOCC}(\text{OH})_2][\text{AsF}_6]^{[\text{a}]}$ and calculated vibrational frequencies (in cm^{-1}) of $[\text{C}_2\text{H}_3\text{O}_4]^+$ and $[\text{C}_2\text{D}_3\text{O}_4]^+$.

$[\text{HOCC}(\text{OH})_2][\text{AsF}_6]^{[\text{a}]}$		$[\text{HOCC}(\text{OH})_2][\text{AsF}_6]$		$[\text{DOCC}(\text{OD})_2][\text{AsF}_6]$		$[\text{C}_2\text{H}_3\text{O}_4]^+$	$[\text{C}_2\text{D}_3\text{O}_4]^+$	Assignment ^[\text{c}]
IR	Raman	IR	Raman	IR	Raman	calc. ^[\text{b}] (IR/Raman)	calc. ^[\text{b}] (IR/Raman)	
				2394(m)	2376(19)	3555(242/85)	2588(140/43)	$\nu(\text{OX})$
					2360(22)	3486(202/90)	2540(109/42)	$\nu(\text{OX})$
3156(br)						3464(390/18)	2522(233/8)	$\nu(\text{OX})$
1704(br)		1712(s)	1744(7)	1697(s), 1666(s)	1721(8)	1820(233/24)	1818(230/23)	$\nu_{\text{as}}(\text{CO})$
1667(br)	1588(23)	1543(m)	1585(13), 1552(5)		1560(21), 1529(17)	1625(218/2)	1608(284/2)	$\nu_{\text{as}}(\text{CO})$
1443(m)		1438(m), 1382(m)	1383(2)	1396(s), 1330(s)	1332(4)	1479(238/8)	1441(133/11)	$\nu_{\text{s}}(\text{CO})$
1236(m)		1240(s)	1245(3)	1176(w)		1279(100/4)	1195(165/3)	$\nu_{\text{s}}(\text{CO})$
1163(m)		1206(s)	1205(3)		1040(18)	1157(127/2)	972(1/6)	$\delta(\text{COX})$
				1001(s)	1018(8)	1135(102/6)	964(147/1)	$\delta(\text{COX})$
		1083(m)		876(s)	822(8), 805(9)	1106(248/3)	871(53/2)	$\delta(\text{COX})$
						792(0/0)	790(0/0)	$\gamma(\text{CO})$
875(s)	846(20)	879(m)	850(18)		750(14)	749(17/9)	661(10/6)	$\nu(\text{CC})$
		778(m)		592(m)		732(4/1)	586(62/0)	$\gamma(\text{OX})$
	668(11)	659(m)				680(296/1)	510(132/0)	$\gamma(\text{OX})$
623(s)				530(m)	524(9)	600(100/0)	538(17/1)	$\delta(\text{OCO})$
531(s)		521(m)	517(5)			587(121/1)	457(9/1)	$\gamma(\text{OX})$
477(s)		475(m)	474(16)	459(m)	461(18)	511(8/1)	491(36/1)	$\delta(\text{CCO})$
			460(6)			399(10/0)	339(29/0)	$\gamma(\text{CO})$
				356(m)		390(8/2)	371(9/2)	$\delta(\text{OCO})$
						237(1/0)	225(1/0)	$\delta(\text{CCO})$
						70(0/0)	68(0/0)	$\gamma(\text{CO})$
708(s)		709(s)	710(14)	733(s)	725(12)			$[\text{AsF}_6]^-$
	702(100)		695(100)	678(s)	692(100)			$[\text{AsF}_6]^-$
			678(8)	654(s)	671(14)			$[\text{AsF}_6]^-$
			651(5)					$[\text{AsF}_6]^-$
398(s)	595(14)	396(s)	597(12)	392(s)				$[\text{AsF}_6]^-$
			381(20)		384(29)			$[\text{AsF}_6]^-$
	374(18)		368(23)	356(m)	366(20)			$[\text{AsF}_6]^-$

[a] reported in reference 1 [b] Calculated at the B3LYP/aug-CC-pVTZ level of theory. IR intensity in km/mol and Raman intensity in $\text{\AA}^4/\text{u}$. Abbreviations for IR intensities: ν = very, s = strong, m = medium, w = weak, br = broad. Raman activity is stated to a scale of 1 to 100: Frequencies are scaled with an empirical factor of 0.965. [c] $X = \text{H, D}$.

Table S2. Experimental vibrational frequencies (in cm^{-1}) of $[(\text{HO})_2\text{CC}(\text{OH})_2][\text{AsF}_6]_2$ (**5**) and $[(\text{DO})_2\text{CC}(\text{OD})_2][\text{AsF}_6]_2$ (**7**), $[(\text{HO})_2\text{CC}(\text{OH})_2][\text{SbF}_6]_2$ ^[a] and calculated vibrational frequencies (in cm^{-1}) of $[\text{C}_2\text{H}_4\text{O}_4]^{2+}\cdot 4\text{HF}$ and $[\text{C}_2\text{D}_4\text{O}_4]^{2+}$.

$[(\text{HO})_2\text{CC}(\text{OH})_2][\text{SbF}_6]_2$ ^[a]		$[(\text{HO})_2\text{CC}(\text{OH})_2][\text{AsF}_6]_2$		$[(\text{DO})_2\text{CC}(\text{OD})_2][\text{AsF}_6]_2$		$[\text{C}_2\text{H}_4\text{O}_4]^{2+}\cdot 4\text{HF}$	$[\text{C}_2\text{D}_4\text{O}_4]^{2+}$	Assignment ^[c]
IR	Raman	IR	Raman	IR	Raman	calc. ^[b] (IR/Raman)	calc. ^[b] (IR/Raman)	
					2350-2450	2762(1/226)	2492(0/45)	$\nu(\text{OX})$
						2725(3619/0)	2491(436/0)	$\nu(\text{OX})$
					2350-2450	2630(70/166)	2442(0/48)	$\nu(\text{OX})$
				2406(w)		2610(6012/2)	2438(6663/0)	$\nu(\text{OX})$
1731(s)		1699(m)		1695(m)		1678(601/0)	1669(0/4)	$\nu_{\text{as}}(\text{CO})$
1671(sh)					1721(3)	1677(22/3)	1656(553/0)	$\nu_{\text{as}}(\text{CO})$
	1607(5), 1592(9)		1607(5), 1588(16)		1586(23), 1531(5)	1517(0/22)	1473(0/24)	$\nu_{\text{s}}(\text{CO})$
1386(w)		1437(m)		1395(m), 1327(w)		1415(348/0)	1352(179/0)	$\nu_{\text{s}}(\text{CO})$
	1266(2)		1245(2)		822(2)	1282(0/2)	823(0/4)	$\delta(\text{COX})$
1298(w), 1242(m)		1233(m)		998(s)		1264(247/0)	943(193/0)	$\delta(\text{COX})$
	1195(4)		1170(3)		1041(5), 1016(10)	1177(0/11)	961(0/7)	$\delta(\text{COX})$
1058(sh)		1164(m)		843(s)		1163(874/0)	787(166/0)	$\delta(\text{COX})$
1046(sh)		934(m)		591(m)		964(47/0)	610(90/0)	$\gamma(\text{OX})$
1027(s)					523(10)	963(39/0)	530(0/1)	$\gamma(\text{OX})$
						910(0/0)	457(0/0)	$\gamma(\text{OX})$
877(w)		855(w)				907(304/0)	456(247/0)	$\gamma(\text{OX})$
	851(11)		849(14)		673(5)	828(0/10)	656(0/5)	$\nu(\text{CC})$
	798(13)		803(7)		805(9)	800(0/1)	789(0/1)	$\gamma(\text{CO})$
					766(3)			$2\cdot[\text{AsF}_6]^-$
728(w)					747(12)			$2\cdot[\text{AsF}_6]^-$
	633(69)							?
		619(s)		529(m)		685(6/0)	515(99/0)	$\delta(\text{OCO})$
529(vw)								?
521(vw)								?
	553(8)		548(5)		461(7)	562(0/3)	491(0/2)	$\delta(\text{CCO})$
	497(5)							?
	456(10)							?
470(vw), 457(vw)		510(s)		458(w)		466(24/0)	359(2/0)	$\gamma(\text{CO})$
372(m)		479(w)	459(8)		440(7)	335(98/0)	356(0/2)	$\delta(\text{OCO})$
	302(8)							?
						196(24/0)	214(12/0)	$\delta(\text{CCO})$
						74(0/1)	70(2/0)	$\gamma(\text{CO})$
	692(22)		724(8)	731(s)	725(14)			$[\text{MF}_6]^-$
	678(100)							$[\text{MF}_6]^-$
656(vs)	670(44)	700(s)	692(100)	698(s)	692(100)			$[\text{MF}_6]^-$
	661(11)		669(3)					$[\text{MF}_6]^-$
	583(5)		598(16)		596(16)			$[\text{MF}_6]^-$
	571(6)	392(s)	388(20)	389(s)	387(23)			$[\text{MF}_6]^-$
	285(29)		381(10)					$[\text{MF}_6]^-$
276(s)	274(18)		370(14)		369(29)			$[\text{MF}_6]^-$
			361(14)					$[\text{MF}_6]^-$

[a] reported in reference 1 [b] Calculated at the B3LYP/aug-CC-pVTZ level of theory. IR intensity in km/mol and Raman intensity in $\text{\AA}^2/\text{u}$. Abbreviations for IR intensities: ν = very, s = strong, m = medium, w = weak, br = broad. Raman activity is stated to a scale of 1 to 100: Frequencies are scaled with an empirical factor of 0.965. [c] $X = \text{H, D}$; $M = \text{As, Sb}$

Experimental Section

General:

Caution! Any contact with the components must be avoided. HF may be released by hydrolysis of the salts, burning skin and causing irreparable damage. Appropriate safety precautions must be implemented when handling these materials.

Apparatus and Materials

All reactions were performed by employing standard Schlenk techniques using a stainless-steel vacuum line. Syntheses were carried out in FEP/PFA reactors, closed with a stainless-steel valve. In advance of usage, all reaction vessels and the stainless-steel line were dried with fluorine. IR spectra were recorded with a Bruker Vertex 80V FTIR spectrometer. Raman measurements were carried out with a Bruker MultiRAM FT-Raman spectrometer with Nd:YAG laser excitation ($\lambda = 1064$ nm). The low-temperature X-ray diffraction of $[\text{HOCC}(\text{OH})_2][\text{AsF}_6]$ and $[(\text{HO})_2\text{CC}(\text{OH})_2][\text{SbF}_6]_2$ was performed with an Oxford XCalibur3 diffractometer equipped with a Spellman generator (voltage 50 kV, current 40 mA) and a KappaCCD detector, operating with Mo-K α radiation ($\lambda = 0.7107$ Å). Data collection at 123 K was performed using the CrysAlis CCD software,^[2] the data reductions were carried out using the CrysAlis RED software.^[3] The solution and refinement of the structure was performed with the programs SHELXS^[4] and SHELXL-97^[5] implemented in the WinGX software package^[6] and finally checked with the PLATON software.^[7] The absorption correction was performed with the SCALE3 ABSPACK multi-scan method.^[8] Selected data and parameters of the X-ray analysis are given in Table 5. All quantum chemical calculations were performed on the MP2/aug-cc-pVTZ-level of theory by Gaussian 09.^[9] Crystallographic data (excluding structure factors) for the structure in this paper have been deposited with the Cambridge Crystallographic Data Centre, CCDC, 12 Union Road, Cambridge CB21EZ, UK. Copies of the data can be obtained free of charge on quoting the depository numbers CCDC-1827283 and 1827284 (Fax: +44-1223-336-033; E-Mail: deposit@ccdc.cam.ac.uk, <http://www.ccdc.cam.ac.uk>).

Synthesis of $[\text{HOCC}(\text{OH})_2][\text{AsF}_6]$ (1), $[\text{DOCC}(\text{OD})_2][\text{AsF}_6]$ (5) and $[(\text{HO})_2\text{CC}(\text{OH})_2][\text{AsF}_6]_2$ (3), $[(\text{DO})_2\text{CC}(\text{OD})_2][\text{AsF}_6]_2$ (7)

First, the superacid had to be synthesized. For this, a 7 mL FEP tube-reactor was filled with arsenic pentafluoride and anhydrous hydrogen fluoride via condensation. Consequently, the temperature was cooled to -196°C and thereafter allowed to warm up to -40°C . In doing so, the superacidic media was formed. For the addition of oxalic acid (1.00 mmol, 90 mg), conducted under inert gas atmosphere, the mixture was again cooled to -196°C . In order to allow for the protonation of the reagent, the temperature was raised to -30°C for a period of five minutes and subsequently lowered to -78°C . Finally, the excess of aHF was removed in a dynamic vacuum. A quantitative yield of $[\text{HOCC}(\text{OH})_2][\text{AsF}_6]$ and $[(\text{HO})_2\text{CC}(\text{OH})_2][\text{AsF}_6]_2$ as colorless crystalline solids was received. The synthesis of the respective deuterated species, $[\text{DOCC}(\text{OD})_2][\text{AsF}_6]$ and $[(\text{DO})_2\text{CC}(\text{OD})_2][\text{AsF}_6]_2$, was conducted in an analogous way by the use of deuterium fluoride, instead of aHF.

Synthesis of $[\text{HOCC}(\text{OH})_2][\text{SbF}_6]$ (2), $[\text{DOCC}(\text{OD})_2][\text{SbF}_6]$ (6) and $[(\text{HO})_2\text{CC}(\text{OH})_2][\text{SbF}_6]_2$ (4) and $[(\text{DO})_2\text{CC}(\text{OD})_2][\text{SbF}_6]_2$ (8)

The initial step of the synthesis constitutes the condensation of antimony pentafluoride (1.00 mmol or 2.00 mmol, 217 mg or 434 mg) into a 7 mL FEP-tube-reactor together with aHF at a temperature of -196°C . In order to allow for a thorough mixing of the reagents, the mixture's temperature was raised to 0°C and subsequently lowered to -196°C again. Following this, oxalic acid (1.00 mmol, 90 mg) was added to the superacidic medium under inert gas atmosphere. After allowing the mixture to warm up to -40°C for five minutes, in order to enable the protonation of the oxalic acid, the reaction mixture was again cooled to -78°C . Excessive aHF was removed in a dynamic vacuum. The products were obtained as colorless crystalline solids in quantitative yield. For the formation of the deuterated species, aDF was used instead of aHF.

Table S3. X-ray data and parameters of **1** and **4**

	[HOOC(OH) ₂][AsF ₆] (1)	[(HO) ₂ CC(OH) ₂][SbF ₆] ₂ (4)
formula	C ₂ H ₃ AsF ₆ O ₄	CH ₂ SbF ₆ O ₂
M _r [g mol ⁻¹]	279.96	281.78
crystal size, mm ³	0.27 x 0.22 x 0.15	0.28 x 0.24 x 0.22
crystal system	monoclinic	monoclinic
space group	<i>P</i> 2 ₁ / <i>c</i>	<i>P</i> 2 ₁ / <i>n</i>
<i>a</i> [Å]	20.2574(12)	6.3855(3)
<i>b</i> [Å]	7.5371(4)	10.6761(5)
<i>c</i> [Å]	9.7329(6)	9.1290(5)
α [deg]	90.0	90.0
β [deg]	103.263(6)	103.706(6)
γ [deg]	90.0	90.0
<i>V</i> [Å ³]	1446.40(12)	604.62(7)
<i>Z</i>	8	4
ρ _{calcd.} [g cm ⁻³]	2.571	3.095
μ [mm ⁻¹]	4.803	4.635
λ(MoK _α), [Å]	0.71073	0.71073
<i>F</i> (000)	1072	516
<i>T</i> [K]	100(2)	100(2)
hkl range	−25:33; −8:9; −12:12	−7:7; −13:13; −11:11
refl. measured	7444	5977
refl. unique	2951	1229
<i>R</i> _{int}	0.0304	0.0216
parameters	259	94
<i>R</i> (<i>F</i>)/ <i>wR</i> (<i>F</i> ²) [^a] (all reflexions)	0.0448/0.0906	0.0118/0.0285
weighting scheme ^[b]	0.0198/6.0000	0.0131/0.2832
<i>S</i> (GooF) ^[c]	1.234	1.122
residual density [e Å ⁻³]	1.049/−0.648	0.473/−0.399
device type	Oxford XCalibur	Oxford XCalibur
solution	SHELXS-97 ^[4]	SHELXS-97 ^[4]
refinement	SHELXL-97 ^[5]	SHELXL-97 ^[5]
CCDC	1827283	1827284

[a] $R_1 = \sum ||F_o| - |F_c|| / \sum |F_o|$; [b] $wR_2 = [\sum (w(F_o^2 - F_c^2)^2) / \sum (w(F_o^2))]^{1/2}$; $w = [\sigma_c^2(F_o^2) + (xP)^2 + yP]^{-1}$; $P = (F_o^2 + 2F_c^2)/3$ [c] GooF = $\{\sum (w(F_o^2 - F_c^2)^2) / (n-p)\}^{1/2}$ (*n* = number of reflections; *p* = total number of parameters)

- [1] R. Minkwitz, N. Hartfeld, C. Hirsch, *Z. anorg. allg. Chem.* **1999**, 625, 1479-1485.
- [2] CrysAlisCCD, Version 1.171.35.11 (release 16-05-2011 CrysAlis 171.NET), Oxford Diffraction Ltd., **2011**.
- [3] CrysAlisRED, Version 1.171.35.11 (release 16-05-2011 CrysAlis 171.NET), Oxford Diffraction Ltd., **2011**.
- [4] G. Sheldrick, *SHELXS-97, Program for Crystal Structure Solution*, University of Göttingen (Germany), **1997**.
- [5] G. Sheldrick, *SHELXL-97, Programm for the Refinement of Crystal Structures*, University of Göttingen, Germany, **1997**.
- [6] L. Farrugia, *J. Appl. Crystallogr.* **1999**, 32, 837–838.
- [7] A. Spek, *PLATON, A Multipurpose Crystallographic Tool*, Utrecht University, Utrecht (The Netherlands), **1999**.
- [8] *SCALE3 ABSPACK – An Oxford Diffraction program*, Oxford Diffraction Ltd., **2005**.
- [9] Gaussian 09, revision a.02: M. Frisch et al., Gaussian Inc., Pittsburgh (PA, USA), **2003**.

Protonation of *p*-Benzoquinone in Superacidic Solutions

Manuel Schickinger,^[a] Markus Siegert,^[a] Yvonne Morgenstern,^[a] Florian Zischka,^[a] Karin Stierstorfer,^[a] and Andreas Kornath*^[a]

Abstract. The reaction of *p*-benzoquinone in the binary superacidic systems XF/MF_5 ($M = \text{As}, \text{Sb}; X = \text{H}, \text{D}$) leads to the formation of the corresponding salts $[\text{OC}_6\text{H}_4(\text{OX})][\text{MF}_6]$ ($M = \text{As}, \text{Sb}; X = \text{H}, \text{D}$). Threefold excess of Lewis acid in relation to *p*-benzoquinone is required to form these salts quantitatively. The salts are characterized by infrared spectroscopy and in the case of $[\text{OC}_6\text{H}_4(\text{OH})][\text{SbF}_6]$ (**2**) by a

single-crystal X-ray structure analysis, according to which it is more correctly described as a double hemi-protonated salt of *p*-benzoquinone. The salt crystallizes in the triclinic space group $P\bar{1}$ with one formula unit per unit cell. In the solid state the cations are arranged in chains, linked via $\text{O}\cdots(\text{H})\cdots\text{O}$ bonds. The vibrational spectra were compared to quantum chemical calculations of the cation $[\text{OC}_6\text{H}_4(\text{OH})]^+$.

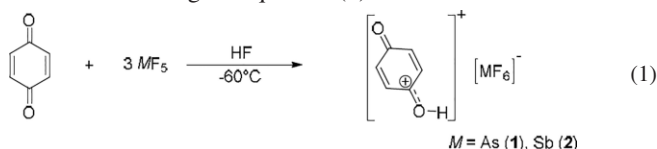
Introduction

p-Benzoquinone was first synthesized in 1838 by Alexander Voskresenskij.^[1] The chemistry of quinones is dominated by its electron acceptor character.^[2] Furthermore, *p*-benzoquinone is used as a dienophile in Diels-Alder reactions and as a proton acceptor in organic syntheses, like the Thiele-Winter reaction.^[3,4] In 1972, Olah already discovered the possibility of an *O*-protonation of *p*-benzoquinone in the superacidic system $\text{FSO}_3\text{H}/\text{SbF}_5$.^[5,6] Only the monoprotonated species was characterized by ^{13}C -NMR studies. However, no further structural information is reported. This lack of structural information leads us to a reinvestigation of *p*-benzoquinone in the binary superacidic systems HF/AsF_5 and HF/SbF_5 with the aim to isolate and structurally characterize protonated salts of *p*-benzoquinone. Especially the isolation of the diprotonated species in the case of squaric acid raised the question, if it is possible to diprotonate *p*-benzoquinone in the superacidic systems HF/AsF_5 and HF/SbF_5 .^[7]

Results and Discussion

Synthesis and Properties of $[\text{OC}_6\text{H}_4(\text{OH})][\text{AsF}_6]$ and $[\text{OC}_6\text{H}_4(\text{OH})][\text{SbF}_6]$

In the following reaction equation, the synthesis of double hemi-protonated *p*-benzoquinone, $[\text{OC}_6\text{H}_4(\text{OH})][\text{MF}_6]$ ($M = \text{As}, \text{Sb}$) is shown. The preparation was realized in a two-step reaction according to Equation (1):



* Prof. Dr. A. Kornath
Fax: +49-89-2180-77867
E-Mail: andreas.kornath@cup.uni-muenchen.de

[a] Department Chemie
Ludwig-Maximilians-Universität München
Butenandtstr. 5–13(D)
81377 München, Germany

Firstly, the superacidic system (HF/AsF_5 or HF/SbF_5) was formed, using an excess of anhydrous hydrogen fluoride. In order to ensure a complete homogenization, the binary super acid was warmed to -20°C and stirred. Following this, *p*-benzoquinone was added to the frozen superacidic system under inert gas atmosphere. For a complete protonation, a three-fold excess of the Lewis acid in relation to *p*-benzoquinone was used. The reaction mixture was slowly warmed to -40°C , resulting in an immediate formation of the protonated species. After the removal of excess αHF and, in the case of AsF_5 , the Lewis acid at -78°C in vacuo, the air and temperature sensitive salts remained as green solids in quantitative yield (when assuming that the nonvolatile excess of SbF_5 remained as $[\text{H}_2\text{F}][\text{SbF}_6]$). The protonated salts of *p*-benzoquinone, $[\text{OC}_6\text{H}_4(\text{OH})][\text{AsF}_6]$ (**1**) and $[\text{OC}_6\text{H}_4(\text{OH})][\text{SbF}_6]$ (**2**) are stable up to -60°C . At temperatures above -60°C the salts start to decompose, changing their color from dark green to deep purple. Due to their sensitivity to lasers, salts of the protonated *p*-benzoquinone could only be characterized by IR spectroscopy and in the case of **2** by single-crystal X-ray structure analysis. Even twenty-fold excess of Lewis acid in relation to *p*-benzoquinone did not lead to salts with a higher degree of protonation.

Using the superacidic system DF/AsF_5 instead of HF/AsF_5 leads to the corresponding salts, $[\text{OC}_6\text{H}_4(\text{OD})][\text{AsF}_6]$ (**3**) and $[\text{OC}_6\text{H}_4(\text{OD})][\text{SbF}_6]$ (**4**), respectively. The hydroxyl hydrogen atoms are entirely replaced by deuterium, as deuterium fluoride is used in large excess. The degree of deuteration approximates 96%. The CH protons remain unaffected.

Infrared Spectra of $[\text{OC}_6\text{H}_4(\text{OH})][\text{SbF}_6]$ and $[\text{OC}_6\text{H}_4(\text{OD})][\text{AsF}_6]$

The infrared spectra of $[\text{OC}_6\text{H}_4(\text{OH})][\text{SbF}_6]$ (**2**) and $[\text{OC}_6\text{H}_4(\text{OD})][\text{AsF}_6]$ (**3**) are illustrated in Figure 1 and the observed frequencies are summarized in Table 1 together with the quantum chemically calculated frequencies. According to the calculated structure of the $[\text{OC}_6\text{H}_4(\text{OX})]^+$ ($X = \text{H}, \text{D}$) cation of C_1 symmetry, 33 fundamental vibrations are expected. The

assignment of the vibrational modes is based on the analysis of the Cartesian displacement vectors of the calculated vibrational modes and on a comparison with the vibrations described in literature for *p*-benzoquinone and quinhydrone.^[8–13]

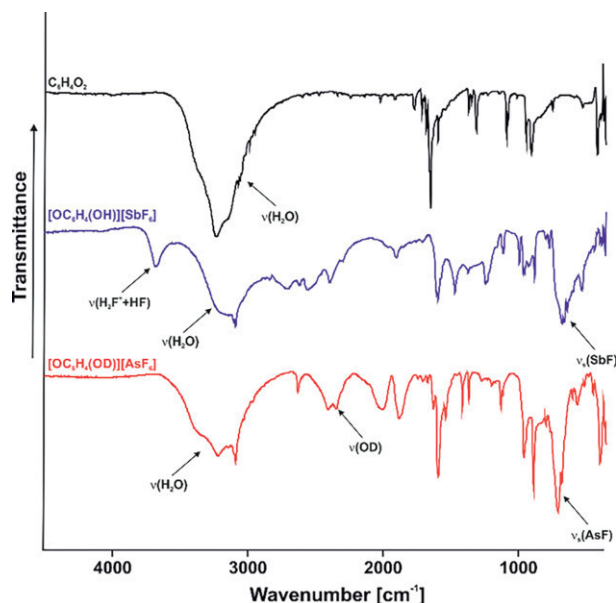


Figure 1. Low temperature IR spectra of $C_6H_4O_2$, $[OC_6H_4(OH)][SbF_6]$, and $[OC_6H_4(OD)][AsF_6]$.

In the IR spectrum of $[OC_6H_4(OH)][SbF_6]$, the OH stretching vibrations are overlaid by $\nu(OH)$ vibrations of water. The occurrence of condensed water as a broad band at around 3250 cm^{-1} in the IR spectra of **2** and **3** is caused by the measuring method. A successful *O*-protonation is assumed due to the $\nu(OD)$ vibration of the deuterated species (**3**). The $\nu(OD)$ band is split and detected at 2408 cm^{-1} and 2348 cm^{-1} , respectively.^[14]

The $\nu_{as}(CO)$ vibrations of **2** and **3** deviate to higher wavenumbers by 176 cm^{-1} and 155 cm^{-1} compared to the quantum chemical calculations. This great deviation is caused by coupling effects of the ring $[\nu(CC)]$ and the carbonyl group $[\nu_{as}(CO)]$.^[15] Compared to the starting material, the $\nu_s(CO)$ of $[OC_6H_4(OH)][SbF_6]$ is red-shifted by 35 cm^{-1} and the $\nu_s(CO)$ of $[OC_6H_4(OD)][AsF_6]$ is blue-shifted by 34 cm^{-1} .^[12] The frequencies for the $\nu(CC)$ vibrations of **2** (1605 , 1591 , and 796 cm^{-1}) and **3** (1630 , 1594 , 1414 , and 797 cm^{-1}) are in good agreement with the values described in literature for *p*-benzoquinone (1613 , 1592 , 1393 , and 770 cm^{-1}) and are not affected by the protonation.^[12]

Crystal Structure of $[OC_6H_4(OH)][SbF_6]$ (**2**)

The $[SbF_6]^-$ salt of monoprotonated *p*-benzoquinone $[OC_6H_4(OH)][SbF_6]$ (**2**) crystallizes in the triclinic space group $P\bar{1}$ with one formula unit per unit cell. The formula unit is illustrated in Figure 2 and the geometric parameters are listed in Table 2.

The C–C bond lengths of $1.327(4)$, $1.453(5)$, and $1.467(5)\text{ Å}$ are slightly shorter, than those reported for *p*-benzoquinone

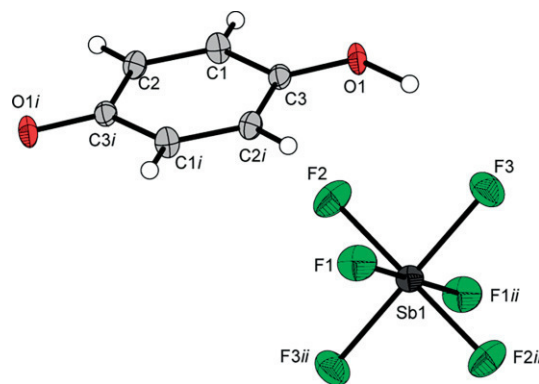


Figure 2. Asymmetric unit of the double hemi-protonated *p*-benzoquinone. Symmetry codes: $i = 1 -x, 1 -y, 1 -z$; $ii = -x, -y, -z$.

[$1.312(6)$, $1.469(3)$, and $1.479(3)\text{ Å}$].^[16] The C1–C2 bond length is in the range of a formal C–C double bond, the other C–C bond lengths are between a formal single and double bond.^[17] In contrast to the starting material, the C1–C3 and C2–C3 bonds of **2** differ in length, resulting in a slight distortion of the six-membered ring structure compared to *p*-benzoquinone. In contrast to *p*-benzoquinone [$1.222(3)\text{ Å}$], the C–O bond is elongated to $1.248(4)\text{ Å}$. Only the C2i–C3–C1 angle is slightly widened compared to the neutral compound. The structure of the $[OC_6H_4(OH)]^+$ cation is approximately planar.^[16] It should be noted, that the localization of protons by X-ray diffraction is not meaningful, but the electron density between O1 and O1i indicates a high probability of presence of the proton at this point of the structure.

The Sb–F bond lengths of the $[SbF_6]^-$ anion are in the range of $1.868(12)$ and $1.873(2)\text{ Å}$. These values are typical for an $[SbF_6]^-$ anion. The bond angles differ only by 0.3° from an ideal octahedral angle.^[18]

In the crystal structure of **2**, the cations are connected by strong $O1\cdots(H)\cdots O1$ hydrogen bonds (Figure 3), with the geo-

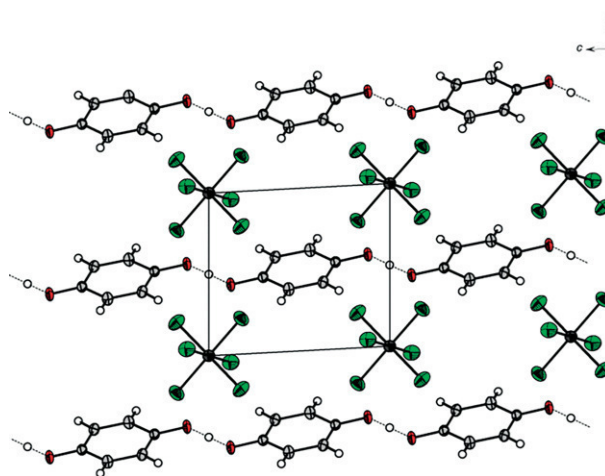


Figure 3. Crystal packing of $[OC_6H_4(OH)][SbF_6]$. Hydrogen bonds are drawn as dashed lines. (50% probability displacement ellipsoids). Symmetry codes: $i = 1 -x, 1 -y, 1 -z$; $ii = -x, -y, -z$.

Table 1. Experimental vibrational frequencies /cm⁻¹ of [OC₆H₄(OH)][SbF₆] (**2**) and [OC₆H₄(OD)][AsF₆] (**3**), and calculated vibrational frequencies /cm⁻¹ of [OC₆H₄(OH)]⁺ and [OC₆H₄(OD)]⁺.

2 IR	3 IR	[OC ₆ H ₄ (OH)] ⁺ calcd. (IR/Raman) ^{a)}	[OC ₆ H ₄ (OD)] ⁺ calcd. (IR/Raman) ^{a)}	Assignment ^{c)}
3683(m)				v(H ₂ F ⁺)+v(HF)
	2408(s), 2348(s)	3624 (306/117)	2640 (181/57)	v(OX)
3109(m)	3147(m)	3115 (17/141)	3115 (17/141)	v(CH)
3092(s)	3094(s)	3109 (19/78)	3109 (19/77)	v(CH)
		3103 (6/48)	3103 (6/48)	v(CH)
	3027(m)	3078 (3/77)	3078 (2/75)	v(CH)
2838(m)				b)
2711(m)				b)
	2632(m)			b)
2558(m)				b)
2396(m)				b)
	2004(m)			b)
1903(w)	1884(m)	1727 (53/146)	1727 (53/146)	v _{as} (CO)
1605(vs)	1630(m)	1647 (198/69)	1646 (205/68)	v(CC)
1591(vs)	1594(vs)	1576 (63/8)	1575 (70/8)	v(CC)
1469(s)	1539(m)	1496 (283/5)	1490 (352/5)	v _s (CO)
	1414(m)	1448 (188/7)	1419 (103/8)	v(CC)
1371(m)	1368(m)	1349 (18/6)	1344 (6/4)	δ(CH)
		1336 (4/4)	1331 (8/3)	v(CC)
1245(s)		1222 (27/3)	1211 (1/4)	δ(CCH)
1127(w)	1132(w)	1140 (50/22)	1139 (25/25)	δ(CCH)
1112(s)		1135 (105/7)	895 (91/1)	δ(COX)
1023(s)		1067 (36/2)	1076 (19/2)	δ(CCH)
		1001 (0/1)	1001 (0/1)	γ(CH)
979(s)	960(s)	982 (1/0)	982 (1/0)	γ(CH)
946(s)		931 (25/3)	931 (17/3)	δ(CCC)
887(s)	889(s)	877 (81/0)	877 (80/0)	γ(CO)
796(w)	797(w)	791 (0/21)	783 (3/21)	v(CC)
		768 (26/1)	750 (1/1)	γ(CC)
		759 (1/1)	760 (2/1)	γ(CO)
	565(w)	728 (1/4)	726 (0/4)	δ(CCC)
619(m)	450(s)	651 (81/1)	489 (53/0)	γ(OX)
579(m)	602(w)	583 (5/2)	578 (5/2)	δ(CCO)
518(m)	512(w)	507 (14/0)	519 (5/1)	γ(CO)
		438 (1/12)	434 (0/11)	δ(CCC)
442(s)		428 (4/0)	424 (5/1)	δ(CCO)
368(s)		383 (15/0)	366 (16/0)	δ(CCO)
		308 (3/0)	304 (4/0)	γ(CC)
		216 (5/1)	214 (5/1)	γ(CC)
		88 (4/0)	87 (4/0)	γ(CO)
676(vs)	710(vs)			[MF ₆] ⁻
662(vs)	679(vs)			[MF ₆] ⁻

a) Calculated at the PBE1PBE/6-311G++(3df,3pd) level of theory. IR intensity in km·mol⁻¹. Abbreviations for IR intensities: v = very, s = strong, m = medium, w = weak. b) Combination modes. c) X = H, D; M = As, Sb.

Table 2. Selected bond lengths /Å and angles /° of **2** with estimated standard deviations in parentheses. Symmetry codes: *i* = 1–x, 1–y, 1–z; *ii* = –x, –y, –z.

Bond lengths			
C1–C2	1.327(4)	C1–C3	1.453(5)
C2–C3 <i>i</i>	1.467(5)	C3–O1	1.248(4)
Bond angles			
C1–C2–C3 <i>i</i>	119.4(3)	C3–C1–C2	120.3(3)
C2–C3–C1	120.3(3)	C1–C3–O1	118.0(3)
C2–C3–O1	121.7(3)		
Dihedral angle			
C2–C1–C3–O1	179.5(3)		
Interatomic distances D···A			
O1–(H3)···F1	3.173(3)	O1–(H3)···F3	3.034(4)
O1···(H)···O1 <i>i</i>	2.461(4)		

metric parameters being summarized in Table 2.^[19] The cations form chains along the *c*-axis. The donor-acceptor distance is, with 2.461(4) Å, considerably shorter than the van der Waals radii (3.00 Å).^[20] In this context, the [OC₆H₄(OH)]⁺ cation shows a similarly short O···(H)···O distance like the [H₅O₂]⁺ cation.^[21,22] Therefore, the monoprotonated *p*-benzoquinone in the solid state is better described as a double hemiprotonated species.

During the reaction, a color change of the solution from colorless to deep green occurred after addition of *p*-benzoquinone. The change of color of the solid from bright yellow (*p*-benzoquinone) to deep green ([OC₆H₄(OH)][MF₆], M = As, Sb) reminds of the synthesis of quinhydrone, without double hemi-protonated *p*-benzoquinone exhibiting the metallic gloss of quinhydrone.^[23]

Theoretical Calculations

Quantum chemical calculations were performed at the PBE1PBE/6-311G++(3df,3pd) level of theory with the Gaussian program package.^[24] The experimental and the calculated structures, together with bond length and angles, are illustrated in Figure 4.

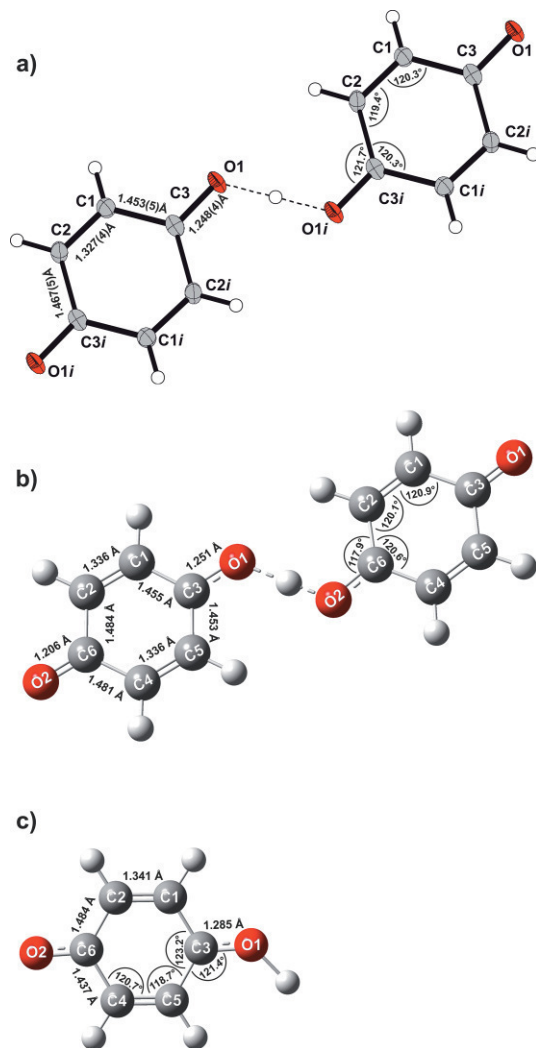


Figure 4. a) $[\text{OC}_6\text{H}_4(\text{OH})]^+$ dimer of the single-crystal X-ray structure. b) Calculated structure of $[\text{OC}_6\text{H}_4(\text{OH})]^+$ dimer. c) Calculated structure of $[\text{OC}_6\text{H}_4(\text{OH})]^+$ cation.

Due to the hemi-protonation, the monoprotonated cation of *p*-benzoquinone was calculated as a dimer, resulting in two different stationary points in the energy isosurface. The global minimum does not reflect the experimental result of the X-ray structure analysis as it differs in the $\text{O1}\cdots(\text{H})\cdots\text{O1}$ angle and thus in the entire structure. The difference in energy of the global and the local minimum is $0.0136 \text{ kJ}\cdot\text{mol}^{-1}$. Due to the very small energetic difference and the better agreement with our experimental results, we used the local minimum structure for the calculations of the geometric parameters.

The calculation of the vibrational frequencies was carried out for the monoprotonated free cation of *p*-benzoquinone, due to a simpler assignment of the vibration modes (Figure 4c).

The experimentally observed vibrational frequencies are deviated to lower wavenumbers compared to the calculated vibrations. This is explained by hydrogen bonding in the solid state.

Conclusions

Protonated *p*-benzoquinone was synthesized and isolated for the first time in the binary superacidic systems XF/MF_5 ($M = \text{As}, \text{Sb}$; $X = \text{H}, \text{D}$). The salts display a very low thermal stability up to -60°C under inert gas atmosphere. The existence of the double hemi-protonated structure of $[\text{OC}_6\text{H}_4(\text{OH})][\text{SbF}_6]$ is confirmed by IR spectroscopy and single-crystal X-ray structure analysis. Further species of protonated *p*-benzoquinone with a higher degree of protonation, like the diprotonated species, could not be observed.

Experimental Section

Caution! Avoid contact with any of these compounds. Note that hydrolysis of these salts might form HF, which burns skin and causes irreparable damage. Safety precautions should be taken when using and handling these materials.

Apparatus and Materials: All reactions were performed by employing standard Schlenk techniques using a stainless-steel vacuum line. Syntheses were carried out in FEP/PFA reactors, closed with a stainless-steel valve. In advance of usage, all reaction vessels and the stainless-steel line were dried with fluorine. IR spectra were recorded with a Bruker Vertex 80V FTIR spectrometer. As a result of the measuring method, there is the possibility that the remaining moisture, condensed on the cooled CsBr-plates, is observed in the IR spectra. The low-temperature X-ray diffraction of **1** was performed with an Oxford XCalibur3 diffractometer equipped with a Spellman generator (voltage 50 kV, current 40 mA) and a KappaCCD detector, operating with Mo-K_α radiation ($\lambda = 0.7107 \text{ \AA}$). Data collection at 123 K was performed using the CrysAlis CCD software,^[25] the data reductions were carried out using the CrysAlis RED software.^[26] The solution and refinement of the structure was performed with the programs SHELXS^[27] and SHELXL-97^[28] implemented in the WinGX software package^[29] and finally checked with the PLATON software.^[30] The absorption correction was performed with the SCALE3 ABSPACK multi-scan method.^[31] Selected data and parameters of the X-ray analysis are given in Table 3. All quantum chemical calculations were performed with the PBE1PBE/6311G++(3df, 3pd) level of theory by Gaussian 09.^[24]

Crystallographic data (excluding structure factors) for the structure in this paper have been deposited with the Cambridge Crystallographic Data Centre, CCDC, 12 Union Road, Cambridge CB21EZ, UK. Copies of the data can be obtained free of charge on quoting the depository number CCDC-1825986 for $[\text{OC}_6\text{H}_4(\text{OH})][\text{SbF}_6]\cdot(2)$ (Fax: +44-1223-336-033; E-Mail: deposit@ccdc.cam.ac.uk, <http://www.ccdc.cam.ac.uk>).

Synthesis of $[\text{OC}_6\text{H}_4(\text{OH})][\text{AsF}_6]$ (1**) and $[\text{OC}_6\text{H}_4(\text{OHD})][\text{AsF}_6]$ (**3**):** For the formation of the required superacid, arsenic pentafluoride (1.50 mmol, 255 mg) and anhydrous hydrogen fluoride (150 mmol, 3 mL) were condensed into a 7 mL FEP tube-reactor. The temperature of the reaction mixture was reduced to -196°C and subsequently raised to -40°C in order to form the superacidic system. Hereafter,

Table 3. X-ray data and parameters of [OC₆H₄(OH)][SbF₆].

	[OC ₆ H ₄ (OH)][SbF ₆] (2)
Formula	C ₆ H ₅ O ₂ SbF ₆
M _r /g·mol ⁻¹	344.85
Crystal size /mm ³	0.18 × 0.15 × 0.05
Crystal system	triclinic
Space group	P $\bar{1}$
a /Å	6.2042(7)
b /Å	6.2586(5)
c /Å	6.8257(5)
a /°	90.690(6)
β /°	98.458(7)
γ /°	105.003(8)
V /Å ³	252.87(4)
Z	1
ρ _{calcd} /g·cm ⁻³	2.662
μ(Mo-K α) /cm ⁻¹	0.71073
F(000)	162
T /K	173(2)
hkl range	−7:7; −7:7; −6:8
Refl. measured	1813
Refl. unique	1037
Parameters	79
R(F)/wR(F ²) ^a (all reflexions)	0.0258/ 0.0470
Weighting scheme ^b	0.0131/0.00
S (GooF) ^c	1.015
Residual density /e·Å ⁻³	−0.568/0.685
Device type	Oxford XCalibur
Solution	SHELXS-97 [27]
Refinement	SHELXL-97 [28]

a) $R_1 = \sum |F_o| - |F_c| / \sum |F_o|$. b) $wR_2 = [\sum [w(F_o^2 - F_c^2)^2] / \sum [w(F_o^2)]]^{1/2}$; $w = [\sigma_c^2(F_o^2) + (xP)^2 + yP]^{-1}$; $P = (F_o^2 + 2F_c^2)/3$. c) GooF = $\{\sum [w(F_o^2 - F_c^2)^2] / (n - p)\}^{1/2}$ (n = number of reflections; p = total number of parameters).

the temperature of the reaction vessel was again reduced to −196 °C. Following this, *p*-benzoquinone (0.50 mmol, 54 mg) was added to the superacid in an inert gas atmosphere. In order to enable the protonation of *p*-benzoquinone, the temperature of the reaction mixture was again raised to −60 °C for 5 min and finally reduced to −78 °C. Keeping this temperature, the remaining *a*HF was removed in a dynamic vacuum, yielding in quantitative amount [OC₆H₄(OH)][AsF₆] as green crystalline solids. [OC₆H₄(OD)][AsF₆] were prepared analogously, by using deuterium fluoride, DF, instead of *a*HF.

Synthesis of [OC₆H₄(OH)][SbF₆] (2) and [OC₆H₄(OD)][SbF₆] (4): Anhydrous hydrogen fluoride, *a*HF, (150 mmol, 3 mL) was added to a 7 mL FEP-tube-reactor in which, prior to this, antimony pentafluoride, SbF₅, (1.50 mmol, 326 mg) had been condensed in at −196 °C. To form the superacidic system the mixture was warmed up to 0 °C. The reaction vessel was cooled to −196 °C again and *p*-benzoquinone (0.50 mmol, 54 mg) was added in an inert gas atmosphere. The reaction vessel was warmed up to −60 °C for 5 min and cooled to −78 °C afterwards. The excess of *a*HF was removed in a dynamic vacuum at −78 °C. [OC₆H₄(OH)][SbF₆] was obtained as green crystalline solids in quantitative yield. [OC₆H₄(OD)][SbF₆] was prepared analogously, by using deuterium fluoride, DF, instead of *a*HF.

Acknowledgements

We are grateful to the Department of Chemistry of the Ludwig-Maximilian University, Munich and the Deutsche Forschungsgemeinschaft (DFG) for the support of this work.

Keywords: Superacidic systems; Vibrational spectroscopy; X-ray diffraction; Protonated *p*-benzoquinone; Quantum chemical calculations

References

- [1] A. Voskresenskij, *Annalen der Pharmacie* **1838**, 27, 257.
- [2] S. Patai (Ed.) *The Chemistry of Functional Groups: The Chemistry of the Quinonoid Compounds*, Wiley: New York, **1974**.
- [3] M. Oda, T. Kawase, T. Okada, T. Enomoto, *Org. Synth.* **1996**, 73, 253.
- [4] B. Mundy, M. Ellerd, F. Favaloro Jr., *Name Reactions and Reagents in Organic Synthesis*, John Wiley & Sons, Inc., New Jersey, **2005**, 644–645.
- [5] G. Olah, Y. Halpern, Y. Mo, G. Liang, *J. Am. Chem. Soc.* **1972**, 94, 3554–3556.
- [6] G. Olah, D. Donovan, *J. Org. Chem.* **1978**, 43, 1743–1750.
- [7] M. Schickinger, D. Cibu, F. Zischka, K. Stierstorfer, C. Jessen, A. Kornath, *Chem. Eur. J.* **2018**, 24, 13355–13361.
- [8] M. Kubinyi, G. Keresztury, *Spectrochim. Acta Part A* **1989**, 45, 421–429.
- [9] I. Kanesaka, H. Nagami, K. Kobayashi, K. Ohno, *Bull. Chem. Soc. Jpn.* **2006**, 79, 406–412.
- [10] Y. Yamakita, M. Tasumi, *J. Phys. Chem.* **1995**, 99, 8524–8534.
- [11] D. Döpp, H. Musso, *Spectrochim. Acta Part A* **1966**, 22, 1813–1822.
- [12] P. Mohandas, S. Umapathy, *J. Phys. Chem. A* **1997**, 101, 4449–4459.
- [13] C.-G. Zhan, S. Iwata, *Chem. Phys.* **1998**, 230, 45–56.
- [14] J. Weidlein, U. Müller, K. Dehnicke, in *Schwingungsspektroskopie*, Georg Thieme Verlag, Stuttgart **1988**, 29–30.
- [15] J. Weidlein, U. Müller, K. Dehnicke, in *Schwingungsspektroskopie*, Georg Thieme Verlag, Stuttgart, **1988**, pp 146–147.
- [16] J. Trotter, *Acta Crystallogr.* **1960**, 13, 86–95.
- [17] A. Holleman, E. Wiberg, N. Wiberg, *Lehrbuch der anorganischen Chemie*, 102. ed., Walter de Gruyter, Berlin – New York, **2007**.
- [18] R. Minkwitz, F. Neikes, U. Lohmann, *Eur. J. Inorg. Chem.* **2002**, 27–30.
- [19] G. Jeffrey, *An Introduction to Hydrogen Bonding*, Oxford University Press, Oxford **1997**.
- [20] A. Bondi, *J. Phys. Chem.* **1964**, 68, 441–451.
- [21] R. Minkwitz, C. Hirsch, *Acta Crystallogr., Sect. C* **1999**, 55, 703–705.
- [22] R. Minkwitz, S. Schneider, A. Kornath, *Inorg. Chem.* **1998**, 37, 4662–4665.
- [23] G. Desiraju, D. Curtin, I. Paul, *J. Org. Chem.* **1977**, 42, 4071–4075.
- [24] M. Frisch, G. Scuseria, M. Robb, J. Cheeseman, J. Montgomery, T. K. Kudin Jr., J. Burant, J. Millam, S. Iyengar, J. Tomasi, V. Barone, B. Mennucci, M. Cossi, G. Scalmani, N. Rega, G. Petersson, H. Nakatsuji, M. Hada, M. Ehara, K. Toyota, R. Fukuda, J. Hasegawa, M. Ishida, T. Nakajima, Y. Honda, O. Kitao, H. Nakai, M. Klene, X. Li, J. Knox, H. Hratchian, J. B. Cross, C. Adamo, J. Jaramillo, R. Gomperts, R. E. Stratmann, O. Yazyev, A. Austin, R. Cammi, C. Pomelli, J. Ochterski, P. Ayala, K. Morokuma, G. Voth, P. Salvador, J. Dannenberg, V. Zakrzewski, S. Dapprich, A. Daniels, M. Strain, O. Farkas, D. Malick, A. Rabuck, K. Raghavachari, J. Foresman, J. Ortiz, Q. Cui, A. Baboul, S. Clifford, J. Cioslowski, B. Stefanov, G. Liu, A. Liashenko, P. Piskorz, I. Komaromi, R. Martin, D. Fox, T. Keith, M. Al-Laham, C. Peng, A. Nanayakkara, M. Challacombe, P. Gill, B. Johnson, W. Chen, M. Wong, C. Gonzalez, J. Pople, Gaussian, Inc. **2003**, Pittsburgh PA.
- [25] CrysAlisCCD, Version 1.171.35.11 (release 16–05–2011 CrysAlis 171.NET), Oxford Diffraction Ltd., **2011**.
- [26] CrysAlisRED, Version 1.171.35.11 (release 16–05–2011 CrysAlis 171.NET), Oxford Diffraction Ltd., **2011**.

- [27] G. Sheldrick, *SHELXS-97*, Program for Crystal Structure Solution, University of Göttingen, Germany, **1997**.
- [28] G. Sheldrick, *SHELXL-97*, Program for the Refinement of Crystal Structures, University of Göttingen, Germany, **1997**.
- [29] L. Farrugia, *J. Appl. Crystallogr.* **1999**, 32, 837–838.
- [30] A. Spek, *PLATON, A Multipurpose Crystallographic Tool*, Utrecht University, Utrecht, The Netherlands, **1999**.
- [31] SCALE3 ABSPACK – An Oxford Diffraction Program, Oxford Diffraction Ltd., **2005**.

Received: September 9, 2018

Published online: October 22, 2018

Croconic Acid | Very Important Paper |

VIP Investigations on Croconic Acid in Superacidic Media

Manuel Schickinger,^[a] Christoph Jessen,^[a] Yvonne Morgenstern,^[a] Katharina Muggli,^[a] Florian Zischka,^[a] and Andreas Kornath^{*[a]}

Abstract: Croconic acid reacts in superacidic solutions HF/MF₅ (M = As, Sb) to yield its corresponding salts [H₃O₅C₅][MF₆] and [(H₃O₅C₅)H(H₃O₅C₅)](MF₆)₃·2HF (M = As, Sb). The degree of protonation is strongly dependent on the stoichiometric ratio of the Lewis acid regarding croconic acid. Monoprotonated salts were characterized by vibrational spectroscopy and in the case of [H₃O₅C₅][AsF₆] (1) by a single-crystal X-ray structure analysis. [H₃O₅C₅][AsF₆] crystallizes in the monoclinic space group P2₁/c

with four formula units per unit cell. The sesquiprotonated species of croconic acid [(H₃O₅C₅)H(H₃O₅C₅)](SbF₆)₃·2HF (4) was also characterized by single-crystal X-ray structure analysis. It crystallizes in the triclinic space group P $\bar{1}$ with one formula unit per unit cell. The vibrational spectra of the monoprotonated salts were compared to quantum chemical calculations of the [H₃O₅C₅]⁺·3HF cation and experimental data reported for croconic acid.

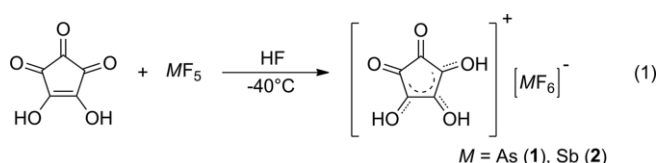
Introduction

In 1963, West and Powell proposed the name “oxocarbons” for a small class of organic compounds.^[1] They defined oxocarbons as compounds in which all or most carbon atoms are linked together in the form of carbonyl groups or hydrated carbonyl groups.^[2] This class of substances includes five known representatives: deltic acid, squaric acid, croconic acid, rhodizonic acid and tetrahydroxy-*p*-benzoquinone.^[2] Croconic acid is the first discovered representative of this substance class and was already synthesized by Gmelin in 1825.^[3] He named the compound after the Greek word for saffron or egg yolk because of its color. However, the cyclical structure was only discovered over 60 years later by Nietzki and Benckiser.^[4] Olah reported in 1993 the existence of mono-, di- and even triprotonation of croconic acid in superacidic solutions, proven by ¹³C-NMR spectroscopy.^[5] In a former study we already confirmed the existence of diprotonated squaric acid, which prompted us to examine the behavior of croconic acid in superacidic media regarding a possible triprotonation which would lead to a first example of 2 π -aromaticity in a five-membered ring.^[6]

Results and Discussion

Synthesis and Properties of [H₃O₅C₅][MF₆] and [(H₃O₅C₅)H(H₃O₅C₅)](MF₆)₂ (M = As, Sb)

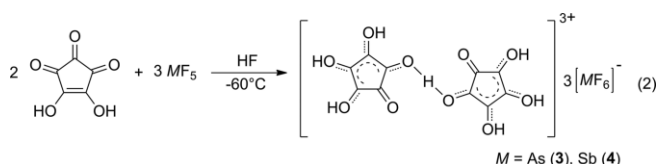
The preparation of the salt containing the mono-cation was carried out according to Equation (1):



Initially, the superacidic systems, HF/AsF₅ and HF/SbF₅, were prepared using an excess of hydrogen fluoride. In order to achieve a complete solvation of the Lewis acid, the mixture was homogenized at –20 °C. Following this, croconic acid was added to the frozen superacidic system under inert gas atmosphere. The reaction mixture was slowly warmed up to –40 °C, resulting in an immediate formation of the protonated species. After the removal of excess *o*HF at –78 °C in vacuo, the air- and temperature-sensitive salts were obtained as yellow solids in quantitative yield.

The monoprotonated salts of croconic acid [H₃O₅C₅][AsF₆] (1) and [H₃O₅C₅][SbF₆] (2), that are stable up to –40 °C, are obtained by using a two-to-five ratio of AsF₅ and a one-to-four ratio of SbF₅ compared to croconic acid.

Reacting croconic acid with at least a threefold excess of Lewis acid in relation to the starting material [Equation (2)], the sesquiprotonated salts [(H₃O₅C₅)H(H₃O₅C₅)](AsF₆)₃·2HF (3) as well as [(H₃O₅C₅)H(H₃O₅C₅)](SbF₆)₃·2HF (4) are obtained, being stable up to –50 °C.



Choosing the superacidic system DF/MF₅ instead of HF/MF₅ (M = As, Sb) leads to the corresponding salts, [D₃O₅C₅][AsF₆] (5) and [D₃O₅C₅][SbF₆] (6) as well as [(D₃O₅C₅)D(D₃O₅C₅)](AsF₆)₃·2DF (7) and [(D₃O₅C₅)D(D₃O₅C₅)](SbF₆)₃·2DF (8). The

[a] Department Chemie, Ludwig-Maximilians-Universität München, Butenandtstr. 5-13, 81377 München, Germany
E-mail: andreas.kornath@cup.uni-muenchen.de
<http://www.org.chemie.uni-muenchen.de/ac/kornath/>

Supporting information and ORCID(s) from the author(s) for this article are available on the WWW under <https://doi.org/10.1002/ejoc.201801035>.

hydroxyl hydrogens are entirely replaced by deuterium, as deuterium fluoride is used in large excess. The degree of deuteration approximates 96 %.

In 1993, Olah reported the existence of di- and triprotonated croconic acid in solution.^[5] In the present work, we were not able to isolate salts of croconic acid with a higher degree of protonation than the sesquiprotonated salt. Even twenty-fold molar excess of Lewis acid in relation to croconic acid did not lead to an isolation of a salt of di- or triprotonated croconic acid.

Vibrational Spectra of $[X_3O_5C_5][MF_6]$ ($M = As, Sb$ and $X = H, D$)

The low-temperature Infrared and Raman spectra of $[H_3O_5C_5][AsF_6]$ (**1**), $[H_3O_5C_5][SbF_6]$ (**2**), $[D_3O_5C_5][AsF_6]$ (**3**), croconic acid ($H_2O_5C_5$) and deuterated croconic acid ($D_2O_5C_5$) are displayed in Figure 1. Table 1 summarizes the observed infrared and Raman frequencies of **1**, **2**, and **3** together with the quantum chemically calculated frequencies of the cations $[H_3O_5C_5]^+ \cdot 3HF$ and $[D_3O_5C_5]^+ \cdot 3DF$.

According to quantum chemical calculations, C_1 -symmetry is predicted for the $[H_3O_5C_5]^+$ and $[D_3O_5C_5]^+$ cations, with 33 fundamental vibrations for the free cation. The assignment of the vibrational frequencies is based on an analysis of the Cartesian displacement vectors of the calculated vibrational modes and on a comparison with the literature values for croconic acid.^[7]

The OH stretching vibrations, with their calculated frequencies of 3322 cm^{-1} , 2836 cm^{-1} and 2800 cm^{-1} , cannot be detected in the Raman spectra due to their low intensities resulting from the poor polarizability of the OH group. In the IR spectrum of **1**, the OH stretching vibrations are overlaid by the $\nu(OH)$ vibrations of water. The existence of condensed water as a broad band around 3250 cm^{-1} for the IR spectra of **1** and **3** is caused by the measuring method. The $\nu(OD)$ vibrations are observed in the Raman and the IR spectrum as weak broad

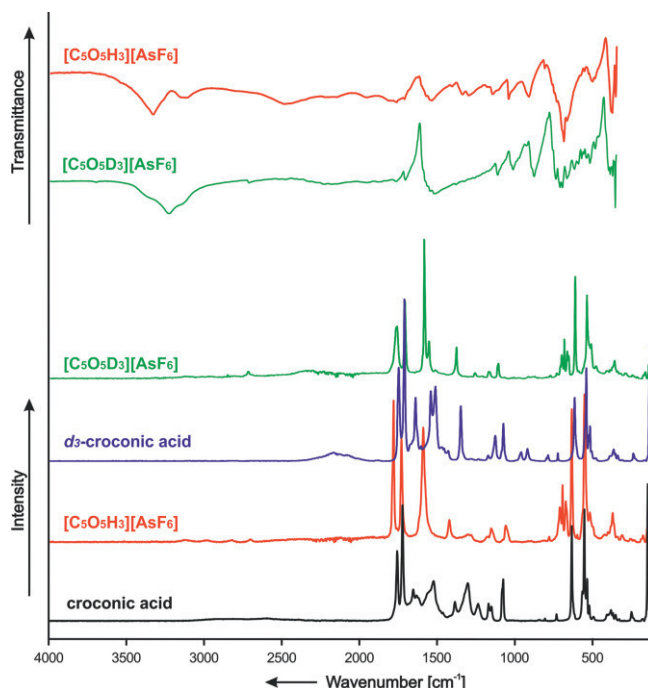


Figure 1. Low temperature Raman spectra of croconic acid, d_3 -croconic acid, $[H_3O_5C_5][AsF_6]$ (**1**), and $[D_3O_5C_5][AsF_6]$ (**3**) as well as the IR spectra of **1** and **3**.

bands, respectively lines in the region from 2350 cm^{-1} to 2150 cm^{-1} .^[8]

All five $\nu(CO)$ vibrations are observed in the region between 1500 cm^{-1} and 1800 cm^{-1} . Especially two of them are affected by O-protonation whilst the other three are in good agreement with the vibrations of the starting material.^[7] The $\nu(CO)$ vibrations (Ra) at 1776 cm^{-1} (**1**), respectively 1780 cm^{-1} (**2**) are blue-shifted by 20 cm^{-1} , respectively 24 cm^{-1} compared to croconic acid.^[7] This blue-shift is likely to be caused by a shortening of the C4–O4 bond length, which will be discussed later. The CO-stretching vibration of monoprotonated croconic acid at

Table 1. Selected experimental low-temperature vibrational frequencies (in cm^{-1}) of $[C_5H_3O_5][AsF_6]$, $[C_5H_3O_5][SbF_6]$, and calculated vibrational frequencies (in cm^{-1}) of $[C_5H_3O_5]^+ \cdot 3HF$ and $[C_5D_3O_5]^+ \cdot 3DF$.

$[C_5H_3O_5][AsF_6]$		$[C_5H_3O_5][SbF_6]$		$[C_5D_3O_5][AsF_6]$		$[C_5H_3O_5]^+ \cdot 3HF$	$[C_5D_3O_5]^+ \cdot 3DF$	Assignment ^[b]
IR	Raman	IR	Raman	IR	Raman	calcd. ^[a] (IR/Raman)	calcd. ^[a] (IR/Raman)	
				2350–2150(w, br)	2350–2150	3322(1467/272)	2423(779/139)	$\nu(OX)$
				2350–2150(w, br)	2350–2150	2836(938/259)	2078(479/104)	$\nu(OX)$
				2350–2150(w, br)	2350–2150	2800(2674/39)	2050(1375/11)	$\nu(OX)$
1776(w, sh)	1780(98)	1776(m)	1778(62)	1769(w)	1770(36)	1796(118/151)	1788(100/188)	$\nu(CO)$
1724(w, sh)	1729(73)	1725(m)	1726(35)	1710(m)	1719(55)	1770(130/139)	1768(124/140)	$\nu(CO)$
1640(vw)		1640(vw)			1594(100)	1660(454/80)	1650(519/70)	$\nu(CO)$
1589(w, sh)	1579(81)	1589(m)	1589(46)	1548(w, sh)	1564(25)	1571(1040/14)	1554(1568/11)	$\nu(CO)$
1548(s, br)		1555(m)		1524(s, br)	1523(4)	1542(209/57)	1530(407/57)	$\nu(CO)$
1350(m)		1354(w)	1340(8)	1383(w)	1387(22)	1376(193/11)	1371(75/46)	$\nu(CC)$
1157(m)	1151(12)	1141(m)	1155(5)	1265(w)	1268(3)	1159(13/9)	1218(16/10)	$\nu(CC)$
				1114(m)	1118(11)	1080(9/11)	1124(36/9)	$\nu(CC)$
1054(s)	1059(13)	1050(s)	1060(7)	1015(m)		1043(24/10)	1020(87/9)	$\nu(CC)$
	634(90)		631(36)	618(m)	624(74)	610(2/39)	606(13/30)	$\nu(CC)$

[a] Calculated at the PBE1PBE/6-311G++(3df, 3pd) level of theory. IR intensity in km/mol and Raman intensity in $\text{\AA}^4/\text{u}$. Abbreviations for IR intensities: v = very, s = strong, m = medium, w = weak, br = broad. Experimental Raman activities are stated to a scale of 1 to 100: Frequencies are scaled with an empirical factor of 0.965. [b] X = H, D.

1630 cm^{-1} is assigned to the C3–O3 bond and is red-shifted by 41 cm^{-1} (Ra) compared to croconic acid for **1** and **2**. This indicates a weaker C–O bond resulting from the protonation, which is in agreement with the geometric parameters of $[\text{H}_3\text{O}_5\text{C}_5][\text{AsF}_6]$ obtained by the single-crystal X-ray structure analysis.

The frequencies of the CC stretching vibrations [1350/1157/1054 cm^{-1} (**1**) and 1340/1141/1054 cm^{-1} (**2**)] in the Infrared spectrum are similar to those of croconic acid, and in accordance with the calculated frequencies, ranging between 1360 cm^{-1} and 1050 cm^{-1} .^[7] The ring-breathing vibration of the five-membered ring occurs for **1** at 634 cm^{-1} and **2** at 631 cm^{-1} in the Raman spectra.^[7]

For the anions $[\text{MF}_6]^-$ ($M = \text{As}, \text{Sb}$) with an ideal octahedral symmetry, two bands in the Infrared spectrum and three lines in the Raman spectrum are expected. In both cases, more than five vibrations are observed. This indicates a lower symmetry, which is in good agreement with the geometric parameters obtained by the single-crystal X-ray structure analysis.

Crystal Structure of $[\text{H}_3\text{O}_5\text{C}_5][\text{AsF}_6]$

The $[\text{AsF}_6]^-$ salt of monoprotonated croconic acid $[\text{H}_3\text{O}_5\text{C}_5][\text{AsF}_6]$ (**1**) crystallizes in the monoclinic space group $P2_1/c$ with four formula units per unit cell. Illustrations of the asymmetric unit and the ionic interactions are shown in Figure 2 and Figure 3. Selected geometric parameters of **1** are listed in Table 2. Table S2 (see Supporting Information) contains the parameters of the single-crystal X-ray structure analysis.

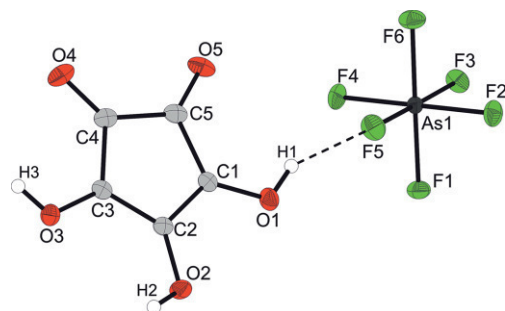


Figure 2. Projection of the formula unit of $[\text{H}_3\text{O}_5\text{C}_5][\text{AsF}_6]$ (50 % probability displacement ellipsoids). Hydrogen bonds are drawn as dashed lines.

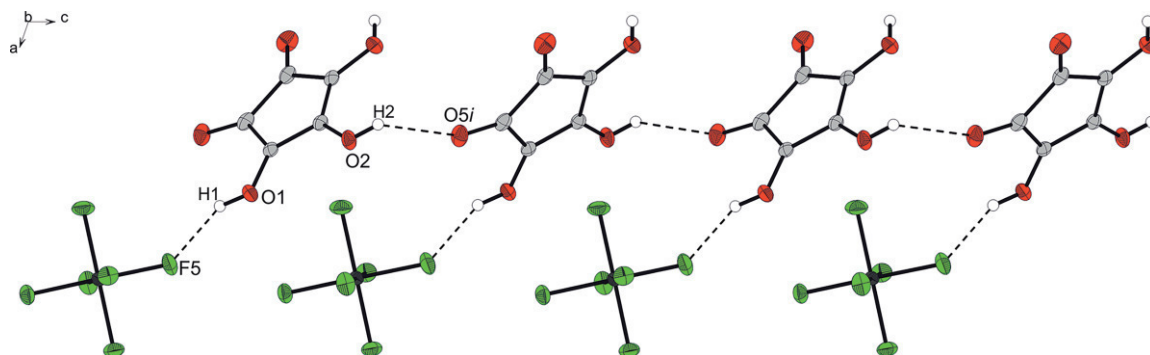


Figure 3. View along the b -axis on the cation chain of **1** (50 % probability displacement ellipsoids). Hydrogen bonds are drawn as dashed lines. Symmetry codes: $i = x, 1.5 - y, 0.5 + z$.

Table 2. Selected bond lengths [in Å] and angles [in deg] of **1** and the literature values for croconic acid^[9] with estimated standard deviations in parentheses. Symmetry codes $i = x, 1.5 - y, 0.5 + z$, $ii = 1 - x, -0.5 + y, 0.5 - z$ and $iii = -1 + x, 1.5 - y, 0.5 + z$.

	$[\text{H}_3\text{O}_5\text{C}_5][\text{AsF}_6]$	$\text{H}_2\text{O}_5\text{C}_5$ ^[9]
Bond length [Å]		
C1–C2	1.401(3)	1.382(5)
C2–C3	1.404(2)	1.442(3)
C3–C4	1.490(3)	1.508(6)
C4–C5	1.521(3)	1.518(6)
C5–C1	1.485(3)	1.466(6)
C1–O1	1.284(2)	1.295(4)
C2–O2	1.310(2)	1.306(4)
C3–O3	1.279(2)	1.233(5)
C4–O4	1.203(2)	1.213(4)
C5–O5	1.205(2)	1.205(2)
Bond angles [°]		
C2–C1–C5	111.75(16)	104.8(2)
C1–C2–C3	107.94(16)	111.2(3)
C2–C3–C4	111.16(16)	111.0(4)
C3–C4–C5	104.74(15)	106.2(4)
C4–C5–C1	104.32(16)	106.8(4)
O1–C1–C2	123.20(17)	128.0(5)
O1–C1–C5	125.04(17)	127.2(5)
O2–C2–C3	130.06(17)	122.1(4)
O2–C2–C1	121.99(16)	126.8(4)
O3–C3–C2	124.22(17)	128.9(4)
O3–C3–C4	124.62(17)	120.0(4)
O4–C4–C3	125.29(18)	128.5(5)
O4–C4–C5	129.97(18)	125.3(4)
O5–C5–C4	130.01(18)	125.4(4)
O5–C5–C1	125.67(17)	127.8(4)
Dihedral angles [°]		
O1–C1–C5–C4	–176.3(2)	
O1–C1–C2–C3	177.4(2)	
C2–C1–C5–C4	3.1(2)	
C1–C2–C3–C4	0.1(2)	
Interatomic distances D...A [Å]		
O1–(H1)...F5 <i>i</i>	2.620(17)	
O2–(H2)...F6 <i>ii</i>	2.741(18)	
O2–(H2)...O5 <i>i</i>	2.925(2)	
O3–(H3)...F3 <i>iii</i>	2.674(17)	

In the cation, the C4–C5 bond length is, with 1.521(3) Å, in accordance with the value for croconic acid [1.518(6) Å].^[9] The C2–C3 bond length [1.404(2) Å] is shortened compared to the

C2–C3 bond length of the starting material [1.442(3) Å], due to mesomeric effects.^[9] The C4–C5 bond length is in good agreement with the data stated in literature for croconic acid.^[9]

In [H₃O₅C₅][AsF₆], all C–O bond lengths [1.203(2) Å to 1.310(2) Å] are between a formal CO single and double bond.^[10]

Compared to the corresponding value for croconic acid [1.233(5) Å], the C3–O3 bond length is significantly elongated [1.279(2) Å], due to the O-protonation, whereas the C1–O1 [1.284(2) Å] and the C4–O4 bond lengths [1.203(2) Å] do not change significantly compared to the starting material [1.295(4) Å and 1.213(4) Å].^[9]

The other C–O bond lengths are in good agreement with the literature values of croconic acid.^[9] All changes in C–O bond lengths are explained by the delocalization of the positive charge in the five-membered ring and the participation of hydrogen bonds.

The five-membered ring differs by 3.1(2)° from a planar structure. Moreover, the carbonyl and hydroxyl groups deviate from the ring plane with a maximum value of 3.7(2)°.

In the [AsF₆][−] anion, the As–F bond lengths are in the range of 1.710(12) Å to 1.744(11) Å. These values are typical for an [AsF₆][−] anion.^[11–13] The As–F bonds, which are involved in hydrogen bonding (As1–F5 and As1–F3), are slightly longer than the other As–F bonds. This leads to a slight distortion of the ideal O_h-symmetry of the anions.

In the crystal structure of **1**, the ions are connected by a network of moderate O–(H)⋯F and O–(H)⋯O hydrogen bonds (Figure 3), with the bond lengths being summarized in Table 2. The cations, connected by hydrogen bonding [O2–(H2)⋯O5*i*], form zigzag-like chains along the *c*-axis. These cation-chains are linked to [AsF₆][−] anions via moderate hydrogen bonds [O1–(H1)⋯F5 and O3–(H3)⋯F3*iii*] and form layers along the *ac*-plane. The layers along the *ac*-plane are connected by weaker hydrogen bonds and are stacked alternately, resulting in a three-dimensional network of the crystal (see Supporting Information).^[14]

Crystal Structure of [(H₃O₅C₅)H(H₃O₅C₅)] [SbF₆]₃·2HF

The [SbF₆][−] salt of sesquiprotonated croconic acid, [(H₃O₅C₅)H(H₃O₅C₅)] [SbF₆]₃·2HF (**4**) crystallizes in the monoclinic space group *P*1̄ with one formula unit per unit cell. The formula unit and interionic interactions of **4** are displayed in Figure 4 and Figure 5. Table 3 contains selected geometric parameters.

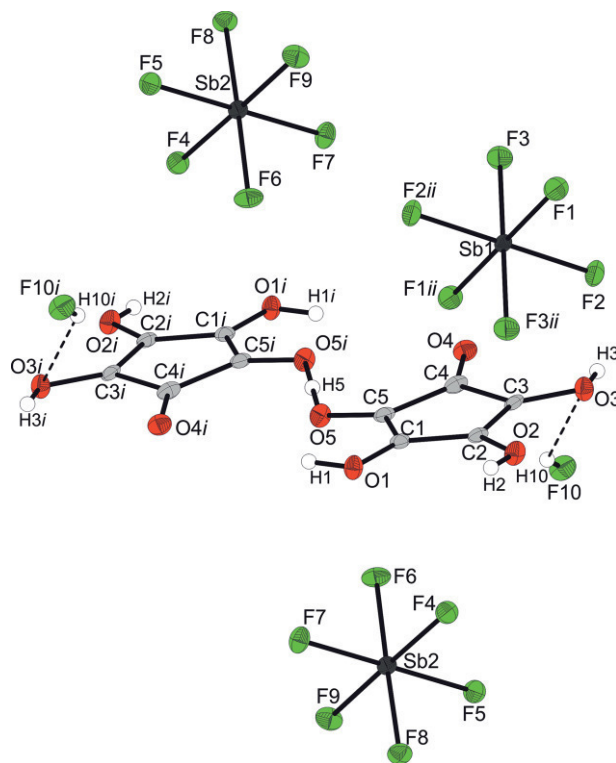


Figure 4. Projection of the formula unit of [(H₃O₅C₅)H(H₃O₅C₅)] [SbF₆]₃·2HF (50 % probability displacement ellipsoids). Hydrogen bonds are drawn as dashed lines. Symmetry code: *i* = −2 − *x*, −1 − *y*, −2 − *z*, *ii* = −1 − *x*, −1 − *y*, −1 − *z*.

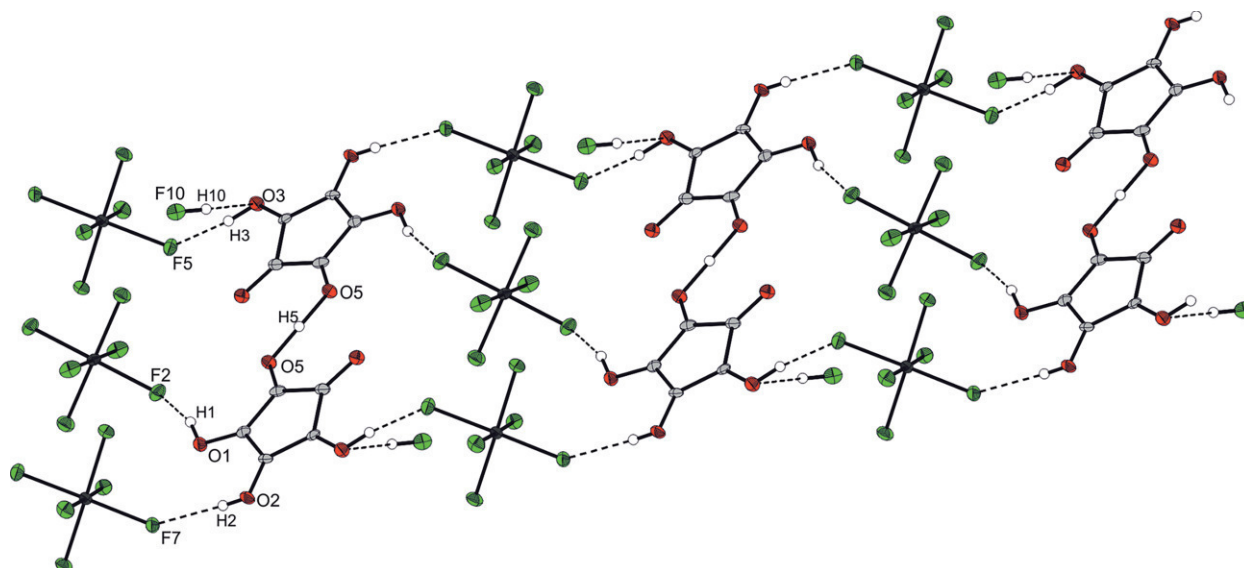


Figure 5. Projection of the interionic contacts between anion and cation of [(H₃O₅C₅)H(H₃O₅C₅)] [SbF₆]₃·2HF (50 % probability displacement ellipsoids). Symmetry codes: *i* = −2 − *x*, −1 − *y*, −2 − *z*; *ii* = −1 + *x*, *y*, *z*; *iii* = −2 − *x*, −2 − *y*, −1 − *z*; *iv* = −1 − *x*, −2 − *y*, −2 − *z*.

Table 3. Selected bond lengths (in Å) and angles (in deg) of **4** with estimated standard deviations in parentheses. Symmetry code: *i* = −2 − *x*, −1 − *y*, −2 − *z*; *ii* = −1 + *x*, *y*, *z*; *iii* = −2 − *x*, −2 − *y*, −1 − *z*; *iv* = −1 − *x*, −2 − *y*, −2 − *z*.

Bond length [Å]			
C1–C2	1.411(6)	C1–O1	1.272(5)
C2–C3	1.418(6)	C2–O2	1.293(5)
C3–C4	1.499(6)	C3–O3	1.269(5)
C4–C5	1.502(6)	C4–O4	1.205(5)
C5–C1	1.434(6)	C5–O5	1.243(5)
Bond angles [°]			
C2–C1–C5	109.4(4)	O2–C2–C1	128.8(4)
C1–C2–C3	109.3(4)	O3–C3–C2	123.8(4)
C2–C3–C4	109.3(3)	O3–C3–C4	126.9(4)
C3–C4–C5	103.5(3)	O4–C4–C3	127.6(4)
C4–C5–C1	108.3(3)	O4–C4–C5	128.9(4)
O1–C1–C2	123.0(4)	O5–C5–C4	128.2(4)
O1–C1–C5	127.6(4)	O5–C5–C1	123.4(4)
O2–C2–C3	121.9(4)		
Dihedral angles [°]			
C1–C2–C3–C4	1.3(5)	C3–C4–C5–C1	4.9(5)
C2–C1–C5–C4	−4.4(5)	O4–C4–C3–C2	173.0(4)
C2–C3–C4–C5	−3.7(5)	O4–C4–C5–C1	171.9(4)
Interatomic distances D...A [Å]			
O2–(H2)...F7 <i>iii</i>	2.609(4)	O5–(H5)...O5 <i>i</i>	2.449(6)
O3–(H3)...F5 <i>iv</i>	2.571(4)	F10–(H10)...O3	3.027(4)
O1–(H1)...F2 <i>ii</i>	2.600(4)		

Each formula unit shown in Figure 4 consists of two mono-protonated croconic acid cations, which are bridged by another proton to form hemi-protonated pairs of single *O*-protonated croconic acid cations. These sesquiprotonated pairs have an inversion center on the shared proton. The structure is completed by two cocrystallizing HF molecules.

In the cation of **4**, the range of the C–C bond lengths [1.411(6) Å to 1.502(6) Å] becomes even smaller than for croconic acid, due to the stronger delocalization of the additional positive charge in the five-membered ring.^[9]

The C–O bonds show a similar tendency as the C–C bonds, concerning the bond lengths. They all are in the range between 1.205(5) Å and 1.293(5) Å, with the unprotonated oxygen O4 forming the shortest C–O bond [C4–O4: 1.205(5) Å]. The remaining *O*-protonated C–O bonds show, due to delocalization of the positive charges, similar bond lengths [1.243(5) Å to 1.293(5) Å] and are all between a formal C–O single (1.43 Å) and double bond (1.19 Å).^[10] The difference in length is dependent on the strength of hydrogen bonding. Moreover, the torsion angles C3–C4–C5–C1 [4.9(5)°] and C3–C4–C5–C1 [171.9(4)°] show, that the sesquiprotonated croconic acid also does not have a completely planar structure.

The Sb–F bond lengths of the [SbF₆][−] anion are in the range of 1.864(2) Å to 1.916(2) Å and in good agreement with the literature values.^[15,16] The predicted octahedral geometry of the [SbF₆][−] anion is slightly distorted, due to the Sb1–F2 [1.895(3) Å], Sb2–F5 [1.916(2) Å] and Sb2–F7 bonds [1.893(2) Å] being involved in hydrogen bonding.^[15,16]

In the crystal structure of [(H₃O₅C₅)H(H₃O₅C₅)] [SbF₆]₃·2HF, the ions are connected by a network of strong and moderate hydrogen bonds.^[14] Two sesquiprotonated cations of croconic

acid are connected by a strong hydrogen bond [O5–(H5)–O5*i*]. The [(H₃O₅C₅)H(H₃O₅C₅)]³⁺ cations and the [SbF₆][−] anions connected via moderate hydrogen bonds [O2–(H2)···F7*iii*, O3–(H3)···F5*iv* and O1–(H1)···F2*ii*] form layers.

Quantum Chemical Calculations

Quantum chemical calculations were performed at the PBE1PBE/6-311G++(3df,3pd) level of theory with the Gaussian program package.^[17] Selected bond lengths and angles of [H₃O₅C₅]⁺·3HF are shown in Figure 6 (the HF molecules were omitted for the sake of clarity). The hydrogen fluoride molecules added to the gas phase structure simulate hydrogen bonding in the solid state.^[18]

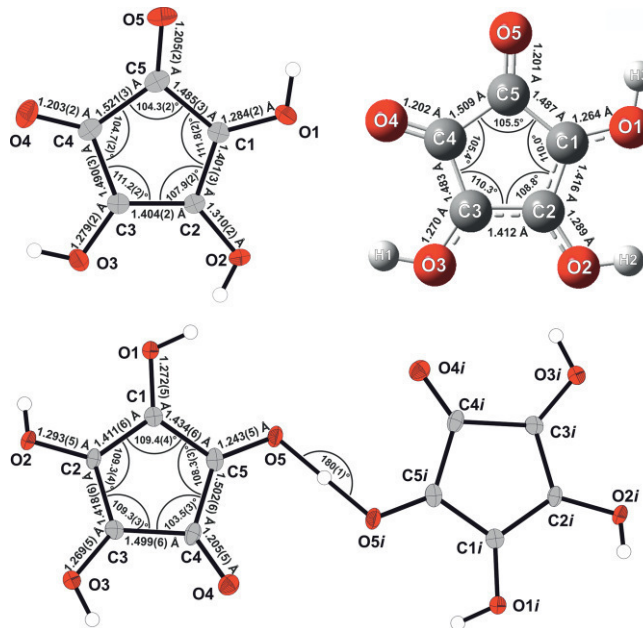


Figure 6. Experimentally obtained and calculated structure of [H₃O₅C₅]⁺ cation and below the experimentally obtained [(H₃O₅C₅)H(H₃O₅C₅)]³⁺ cation of the single-crystal X-ray structure.

Comparing the geometric parameters, obtained by the calculated [H₃O₅C₅]⁺·3HF and the experimental data for the [H₃O₅C₅]⁺ cation, all bond angles and bond lengths are in good accordance with only two exceptions: The experimental C1–O1 and C2–O2 bond lengths are slightly longer than the calculated ones, due to different O–(H)···F distances in the solid state. The calculated frequency of the ν(OH) vibration of the C(2)O(2)–H group is, with 3322 cm^{−1}, overestimated compared to the other hydroxyl groups. This is due to a weaker O–H···F contact in the calculated structure compared to the experimentally observed hydrogen bond in the solid state.

The global minimum of the [(H₃O₅C₅)H(H₃O₅C₅)]³⁺ cation does not reflect the experimental result of the X-ray structure analysis as it is rotated by 106° around the O5···(H)···O10 axis and shows no planarity any more. Despite this the bridging proton is no longer located in the middle between the two oxygen atoms any more resulting in an asymmetric hydrogen bond (Figure S4). Due to better agreement with our experimental results, we used the local minimum structure for the calcula-

tions of the geometric parameters. The structure is illustrated in the Supporting Information (Figure S3).

Conclusions

Monoprotonated croconic acid, $[\text{H}_3\text{O}_5\text{C}_5][\text{AsF}_6]$, was synthesized and isolated in superacidic media. It has been isolated and characterized by vibrational spectroscopy and single-crystal X-ray structure analysis. The experimental data on geometric parameters and vibrational frequencies are supported by quantum chemical calculations.

Sesquiprotonated croconic acid, $[(\text{H}_3\text{O}_5\text{C}_5)\text{H}(\text{H}_3\text{O}_5\text{C}_5)][\text{SbF}_6]_3 \cdot 2\text{HF}$, was isolated for the first time by reacting croconic acid in superacidic media HF/SbF_5 using a large excess of Lewis acid in relation to croconic acid. The existence of $[(\text{H}_3\text{O}_5\text{C}_5)\text{H}(\text{H}_3\text{O}_5\text{C}_5)][\text{SbF}_6]_3 \cdot 2\text{HF}$ was confirmed by single-crystal X-ray structure analysis. Under the reaction conditions described in this paper, neither vibrational spectroscopy nor single-crystal X-ray structure analysis provided evidence of a higher degree of protonation of croconic acid, such as the di- or triprotonation.

Experimental Section

General: Caution! Any contact with the components must be avoided. HF may be released by hydrolysis of the salts, burning skin and causing irreparable damage. Appropriate safety precautions must be implemented when handling these materials.

Apparatus and Materials: All reactions were performed by employing standard Schlenk techniques using a stainless-steel vacuum line. Syntheses were carried out in FEP/PFA reactors, closed with a stainless-steel valve. In advance of usage, all reaction vessels and the stainless-steel line were dried with fluorine. For IR measurements, a cooled cell with a single-crystal CsBr plate coated with a small amount of the sample was used. IR spectra were recorded at a temperature of -196°C with a Bruker Vertex 70 V FTIR spectrometer. Raman measurements were carried out in a cooled glass cell with a Bruker MultiRAM FT-Raman spectrometer with Nd:YAG laser excitation ($\lambda = 1064\text{ nm}$) in vacuo at -196°C . The low-temperature X-ray diffraction of $[\text{H}_3\text{O}_5\text{C}_5][\text{AsF}_6]$ and $[(\text{H}_3\text{O}_5\text{C}_5)\text{H}(\text{H}_3\text{O}_5\text{C}_5)][\text{SbF}_6]_3 \cdot 2\text{HF}$ was performed with an Oxford XCalibur3 diffractometer equipped with a Spellman generator (voltage 50 kV, current 40 mA) and a KappaCCD detector, operating with Mo-K_α radiation ($\lambda = 0.7107\text{ \AA}$). Data collection at 123 K was performed using the CrysAlis CCD software,^[19] the data reductions were carried out using the CrysAlis RED software.^[20] The solution and refinement of the structure was performed with the programs SHELXS^[21] and SHELXL-97^[22] implemented in the WinGX software package^[23] and finally checked with the PLATON software.^[24] The absorption correction was performed with the SCALE3 ABSPACK multi-scan method.^[25] The protons were found in the difference Fourier synthesis and were refined isotopically. Selected data and parameters of the X-ray analysis are given in Table S2 (see Supporting Information). All quantum chemical calculations were performed on the PBE1PBE/6-311G++(3df,3pd) level of theory by Gaussian 09.^[17]

CCDC 1838636 {for $[(\text{H}_3\text{O}_5\text{C}_5)\text{H}(\text{H}_3\text{O}_5\text{C}_5)][\text{SbF}_6]_3 \cdot 2\text{HF}$ }, and 1838637 {for $[\text{H}_3\text{O}_5\text{C}_5][\text{AsF}_6]$ } contain the supplementary crystallographic data for this paper. These data can be obtained free of charge from The Cambridge Crystallographic Data Centre.

Synthesis of $[\text{H}_3\text{O}_5\text{C}_5][\text{AsF}_6]$ (1), $[\text{D}_3\text{O}_5\text{C}_5][\text{AsF}_6]$ (5) and $[(\text{H}_3\text{O}_5\text{C}_5)\text{H}(\text{H}_3\text{O}_5\text{C}_5)][\text{AsF}_6]_3 \cdot 2\text{HF}$ (3), $[(\text{D}_3\text{O}_5\text{C}_5)\text{D}(\text{D}_3\text{O}_5\text{C}_5)][\text{AsF}_6]_3 \cdot 2\text{DF}$ (7): First, arsenic pentafluoride (2.50 mmol or 10.0 mmol, 425 mg or 1700 mg) and anhydrous hydrogen fluoride (150 mmol, 3 mL) were condensed into a 7 mL FEP tube-reactor in order to form the required superacid. The reaction mixture was cooled to -196°C and subsequently warmed up to -40°C for the superacidic system to form. Following this, the temperature of the reaction vessel was again lowered to -196°C and croconic acid (0.50 mmol, 71 mg) was added to the superacid under inert gas atmosphere. For the protonation of croconic acid, the reaction mixture was again warmed up to -30°C for five minutes and then cooled to -78°C . At this temperature, the remaining aHF was removed in a dynamic vacuum, yielding in $[\text{H}_3\text{O}_5\text{C}_5][\text{AsF}_6]$ and $[(\text{H}_3\text{O}_5\text{C}_5)\text{H}(\text{H}_3\text{O}_5\text{C}_5)][\text{AsF}_6]_3 \cdot 2\text{HF}$ as yellow crystalline solids. $[\text{D}_3\text{O}_5\text{C}_5][\text{AsF}_6]$ and $[(\text{D}_3\text{O}_5\text{C}_5)\text{D}(\text{D}_3\text{O}_5\text{C}_5)][\text{AsF}_6]_3 \cdot 2\text{DF}$ were prepared analogously with aDF instead of aHF.

Synthesis of $[\text{H}_3\text{O}_5\text{C}_5][\text{SbF}_6]$ (2), $[\text{D}_3\text{O}_5\text{C}_5][\text{SbF}_6]$ (6) and $[(\text{H}_3\text{O}_5\text{C}_5)\text{H}(\text{H}_3\text{O}_5\text{C}_5)][\text{SbF}_6]_3 \cdot 2\text{HF}$ (4), $[(\text{D}_3\text{O}_5\text{C}_5)\text{D}(\text{D}_3\text{O}_5\text{C}_5)][\text{SbF}_6]_3 \cdot 2\text{DF}$ (8): Anhydrous HF and antimony pentafluoride (2.00 mmol or 10.0 mmol, 434 mg or 2170 mg) were condensed into a 7 mL FEP-tube-reactor at -196°C . The temperature was raised to 0°C for the formation of the superacidic system and subsequently reduced to -196°C again. Croconic acid (0.50 mmol, 71 mg) was added to the superacid under inert gas atmosphere and the reaction mixture was warmed to -40°C to form the protonated species. The reaction vessel was cooled to -78°C after five minutes and the excess of anhydrous hydrogen fluoride was removed in a dynamic vacuum. The according deuterated species were synthesized analogously, using aDF instead of aHF. All products were obtained as a yellow crystalline solid. Traces of antimony pentafluoride are still present, observable in the vibrational spectra.

Acknowledgments

We are grateful to the Department of Chemistry of the Ludwig-Maximilian University, Munich, the Deutsche Forschungsgemeinschaft (DFG), and the F-Select GmbH for the support of this work.

Keywords: Superacidic systems · Structure elucidation · Protonation · Quantum chemical calculations

- [1] R. West, D. L. Powell, *J. Am. Chem. Soc.* **1963**, *85*, 2577–2579.
- [2] A. H. Schmidt, *Chemie Unserer Zeit* **1982**, *16*, 57–67.
- [3] L. Gmelin, *Ann. Phys. Chem.* **1825**, *80*, 31–62.
- [4] R. Nietzki, T. Benckiser, *Ber. Dtsch. Chem. Ges.* **1886**, *19*, 293–309.
- [5] G. Olah, J. Bausch, G. Rasul, H. George, G. Prakash, *J. Am. Chem. Soc.* **1993**, *115*, 8060–8065.
- [6] M. Schickinger, D. Cibu, F. Zischka, K. Stierstorfer, C. Jessen A. Kornath, *Chem. Eur. J.* **2018**, *24*(50), 13355–13361.
- [7] J. G. S. Lopes, L. F. C. de Oliveira, H. G. M. Edwards, P. S. Santos, *J. Raman Spectrosc.* **2004**, *35*, 131–139.
- [8] J. Weidlein, U. Müller, K. Dehnicke in *Schwingungsspektroskopie*, Georg Thieme Verlag, Stuttgart, **1988**, pp. 29–30.
- [9] D. Braga, L. Maini, F. Grepioni, *CrystEngComm* **2001**, *3*, 27.
- [10] A. Holleman, E. Wiberg, *Lehrbuch der anorganischen Chemie* (Ed.: N. Wiberg), 102. ed., de Gruyter, Berlin **2007**, p. 2006.
- [11] K. O. Christe, X. Zhang, R. Bau, J. Hegge, G. A. Olah, G. K. S. Prakash, J. A. Sheehy, *J. Am. Chem. Soc.* **2000**, *122*, 481–487.
- [12] R. Minkwitz, S. Schneider, M. Seifert, H. Hartl, *Z. Anorg. Allg. Chem.* **1996**, *622*, 1404–1410.
- [13] R. Minkwitz, F. Neikes, U. Lohmann, *Eur. J. Inorg. Chem.* **2002**, *2002*, 27–30.

- [14] G. Jeffrey, *An Introduction to Hydrogen Bonding*, Oxford University Press, Oxford **1997**.
- [15] R. Minkwitz, C. Hirsch, T. Berends, *Eur. J. Inorg. Chem.* **1999**, 12, 2249–2254.
- [16] R. Minkwitz, S. Schneider, *Angew. Chem. Int. Ed.* **1999**, 38, 210–212; *Angew. Chem.* **1999**, 111, 229–231.
- [17] Gaussian 09, revision a.02: M. Frisch et al., Gaussian Inc., Pittsburgh (PA, USA), **2003**.
- [18] T. Soltner, N. Goetz, A. Kornath, *Eur. J. Inorg. Chem.* **2011**, 2011, 5429–5435.
- [19] CrysAlisCCD, Version 1.171.35.11 (release 16–05–**2011** CrysAlis 171.NET), Oxford Diffraction Ltd. **2011**.
- [20] CrysAlisRED, Version 1.171.35.11 (release 16–05–**2011** CrysAlis 171.NET), Oxford Diffraction Ltd. **2011**.
- [21] G. Sheldrick, *SHELXS-97, Program for Crystal Structure Solution*, University of Göttingen (Germany), **1997**.
- [22] G. Sheldrick, *SHELXL-97, Program for the Refinement of Crystal Structures*, University of Göttingen, Germany, **1997**.
- [23] L. Farrugia, *J. Appl. Crystallogr.* **1999**, 32, 837–838.
- [24] A. Spek, *PLATON, A Multipurpose Crystallographic Tool*, Utrecht University, Utrecht (The Netherlands), **1999**.
- [25] *SCALE3 ABSPACK – An Oxford Diffraction program*, Oxford Diffraction Ltd. **2005**.

Received: July 4, 2018



Supporting Information

Investigations on Croconic Acid in Superacidic Media

Manuel Schickinger, Christoph Jessen, Yvonne Morgenstern,
Katharina Muggli, Florian Zischka, and Andreas Kornath*

ejoc201801035-sup-0001-SupMat.pdf

Table S1. Experimental vibrational frequencies (in cm^{-1}) of $[\text{C}_5\text{H}_3\text{O}_5][\text{AsF}_6]$, $[\text{C}_5\text{H}_3\text{O}_5][\text{SbF}_6]$, and calculated vibrational frequencies (in cm^{-1}) of $[\text{C}_5\text{H}_3\text{O}_5]^+\cdot 3\text{HF}$ $[\text{C}_5\text{D}_3\text{O}_5]^+\cdot 3\text{DF}$.

$[\text{C}_5\text{H}_3\text{O}_5][\text{AsF}_6]$		$[\text{C}_5\text{H}_3\text{O}_5][\text{SbF}_6]$		$[\text{C}_5\text{D}_3\text{O}_5][\text{AsF}_6]$		$[\text{C}_5\text{H}_3\text{O}_5]^+\cdot 3\text{HF}$	$[\text{C}_5\text{D}_3\text{O}_5]^+\cdot 3\text{DF}$	Assignment
IR	Raman	IR	Raman	IR	Raman	calc. ^[a] (IR/Raman)	calc. ^[a] (IR/Raman)	^[b]
								$\nu(\text{H}_2\text{O})$
								$\nu(\text{H}_2\text{O})$
				2718(w)	2726(4)			$\nu(\text{DF})$
				2350-2150(w, br)	2350-2150	3322(1467/27)	2423(779/139)	$\nu(\text{OX})$
				2350-2150(w, br)	2350-2150	2836(938/259)	2078(479/104)	$\nu(\text{OX})$
				2350-2150(w, br)	2350-2150	2800(2674/39)	2050(1375/11)	$\nu(\text{OX})$
1776(w, sh)	1780(98)	1776(m)	1778(62)	1769(w)	1770(36)	1796(118/151)	1788(100/188)	$\nu(\text{CO})$
1724(w, sh)	1729(73)	1725(m)	1726(35)	1710(m)	1719(55)	1770(130/139)	1768(124/140)	$\nu(\text{CO})$
1640(vw)		1640(vw)			1594(100)	1660(454/80)	1650(519/70)	$\nu(\text{CO})$
1589(w, sh)	1579(81)	1589(m)	1589(46)	1548(w, sh)	1564(25)	1571(1040/14)	1554(1568/11)	$\nu(\text{CO})$
1548(s, br)		1555(m)		1524(s, br)	1523(4)	1542(209/57)	1530(407/57)	$\nu(\text{CO})$
		1451(vw)			1180(5), 1173(4)	1441(813/22)	1130(109/13)	$\delta(\text{COX})$
1419(w)	1412(9)	1412(vw)	1414(11)	925(w)	925(1)	1436(155/2)	964(2/2)	$\delta(\text{COX})$
1350(m)		1354(w)	1340(8)	1383(w)	1387(22)	1376(193/11)	1371(75/46)	$\nu(\text{CC})$
1311(m)	1302(9)	1321(w)	1302(8)	1330(w)				
		1289(w)						
1191(w)		1169(m)		879(s)	884(1)	1230(237/30)	922(132/2)	$\delta(\text{COX})$
1157(m)	1151(12)	1141(m)	1155(5)	1265(w)	1268(3)	1159(13/9)	1218(16/10)	$\nu(\text{CC})$
				1114(m)	1118(11)	1080(9/11)	1124(36/9)	$\nu(\text{CC})$
1054(s)	1059(13)	1050(s)	1060(7)	1015(m)		1043(24/10)	1020(87/9)	$\nu(\text{CC})$
						991(76/0)	720(82/0)	$\gamma(\text{OX})$
925(s)		921(s)				977(147/0)	708(25/0)	$\gamma(\text{OX})$
822(w)		818(m)			780(2)	838(23/1)	789(26/1)	$\delta(\text{CCO})$
				601(vw)		787(56/0)	573(42/0)	$\gamma(\text{OX})$
	778(5)		782(2)			782(45/1)	786(0/1)	$\gamma(\text{CO})$
		746(s)		737(s)	741(3)	724(8/1)	726(3/1)	$\gamma(\text{CO})$
	634(90)		631(36)	618(m)	624(74)	610(2/39)	606(13/30)	$\nu(\text{CC})$
566(s)	552(100)	576(m)	552(47)	558(w)	548(60)	530(4/17)	537(72/14)	$\delta(\text{CCC})$
514(m)	517(21)	507(s)	521(11)			517(3/20)	498(114/13)	$\delta(\text{CCC})$
				518(m)	521(24)	510(0/1)	523(70/1)	$\gamma(\text{CC})$
				484(m)	490(8)	498(2/0)	504(4/1)	$\gamma(\text{CC})$
	400(8)			388(s)		400(20/1)	385(27/2)	$\delta(\text{CCO})$
		369(s)	360(2)			356(2/2)	354(13/1)	$\delta(\text{CCO})$
	342(5)		340(7)	355(s)	349(5)	341(2/2)	342(1/2)	$\delta(\text{CCO})$
	258(3)				256(2)	230(7/1)	228(5/0)	$\gamma(\text{CO})$
						123(0/0)	121(6/0)	$\gamma(\text{CO})$
						91(0/0)	91(0/1)	$\gamma(\text{CO})$
	129(17)		116(11)		126(19)	84(0/2)	83(0/1)	$\gamma(\text{CO})$
		709(vs)	717(66)					SbF_5
		672(s)	673(100)					SbF_5
			498(5)					SbF_5
	710(25)			712(s)	711(17)			$[\text{MF}_6]^-$
698(vs, br)	693(40)	660(m, sh)	661(41)	696(s)	693(28)			$[\text{MF}_6]^-$
680(m, sh)	672(29)		647(41)		675(19)			$[\text{MF}_6]^-$
	598(7)	586(m)		571(m)	572(7)			$[\text{MF}_6]^-$
395(vs)		396(w)		398(s)	398(6)			$[\text{MF}_6]^-$
			274(13)					$[\text{MF}_6]^-$
365(s)	370(21)		244(9)	372(s)	370(13)			$[\text{MF}_6]^-$

[a] Calculated at the PBE1PBE/6-311G++(3df, 3pd) level of theory. IR intensity in km/mol and Raman intensity in $\text{\AA}^4/\text{u}$. Abbreviations for IR intensities: v = very, s = strong, m = medium, w = weak, br = broad. Experimental Raman activities are stated to a scale of 1 to 100. Frequencies are scaled with an empirical factor of 0.965 [b] X = H, D.

Table S2. X-ray data and parameters of **1** and **4**

	[H ₃ O ₅ C ₅][AsF ₆]	[(H ₃ O ₅ C ₅)H(H ₃ O ₅ C ₅)](SbF ₆) ₃ ·2HF
formula	C ₅ H ₃ AsF ₆ O ₅	C ₁₀ H ₉ Sb ₃ F ₂₀ O ₁₀
M _r [g mol ⁻¹]	331.99	1034.42
crystal size, [mm ³]	0.26 x 0.18 x 0.09	0.17 x 0.08 x 0.04
crystal system	monoclinic	triclinic
space group	<i>P</i> 2 ₁ / <i>c</i>	<i>P</i> $\bar{1}$
<i>a</i> [Å]	8.3757(6)	7.820(5)
<i>b</i> [Å]	9.4462(6)	8.166(5)
<i>c</i> [Å]	12.1809(10)	9.808(5)
α [deg]	90.0	81.288(5)
β [deg]	108.762(8)	76.558(5)
γ [deg]	90.0	77.042(5)
<i>V</i> [Å ³]	912.52(12)	590.4(6)
<i>Z</i>	4	1
ρ_{calcd} , [g cm ⁻³]	2.417	2.909
μ [mm ⁻¹]	3.836	3.614
λ (MoK α), [Å]	0.71073	0.71073
<i>F</i> (000)	640	482
<i>T</i> [K]	123	123
hkl range	-10:10; -11:11; -15:15	-9:9; -9:10; -12:12
refl. measured	6843	4438
refl. unique	1857	2405
<i>R</i> _{int}	0.0255	0.0317
parameters	166	213
<i>R</i> (<i>F</i>)/ <i>wR</i> (<i>F</i> ²) [^a] (all reflexions)	0.0233/0.0520	0.0367/0.0687
weighting scheme ^[b]	0.0250/0.1603	0.0283/0.0000
<i>S</i> (GooF) ^[c]	1.058	1.015
residual density [e Å ⁻³]	0.357/-0.343	1.197/-1.166
device type	Oxford XCalibur	Oxford XCalibur
solution	SHELXS-97 ^[21]	SHELXS-97 ^[21]
refinement	SHELXL-97 ^[22]	SHELXL-97 ^[22]
CCDC	1838637	1838636

[a] $R_1 = \sum ||F_o| - |F_c|| / \sum |F_o|$; [b] $wR_2 = [\sum (w(F_o^2 - F_c^2)^2) / \sum (w(F_o^2))]^{1/2}$; $w = [(\sigma_c^2(F_o^2) + (xP)^2 + yP)]^{-1}$; $P = (F_o^2 + 2F_c^2) / 3$; [c] $\text{GooF} = \{\sum [w(F_o^2 - F_c^2)^2] / (n-p)\}^{1/2}$ (*n* = number of reflections; *p* = total number of parameters)

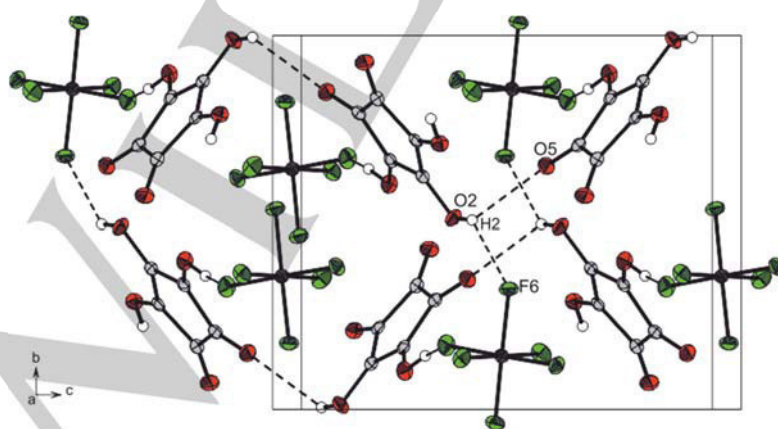


Figure S1. Projection of the interionic contacts between anion and cation of [H₃O₅C₅][AsF₆] (50% probability displacement ellipsoids). Hydrogen bonds are drawn as dashed lines. Symmetry codes: *i* = *x*, 1.5-*y*, 0.5+*z* and *ii* = 1-*x*, -0.5+*y*, 0.5-*z*.

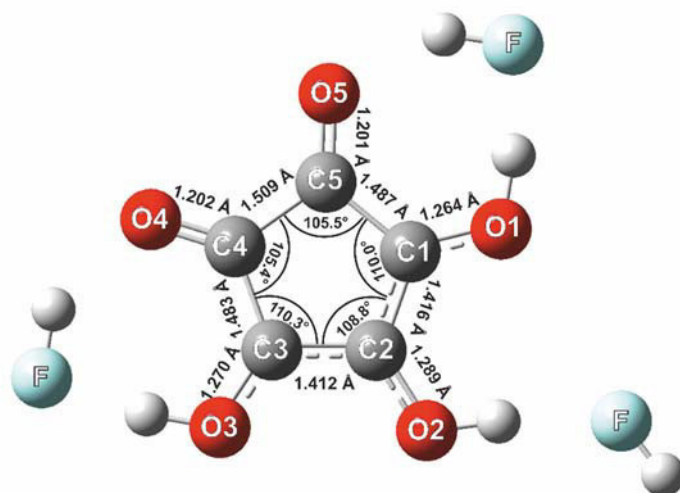


Figure S2. Calculated structure of $[\text{H}_3\text{O}_5\text{C}_5]^+$ cation.

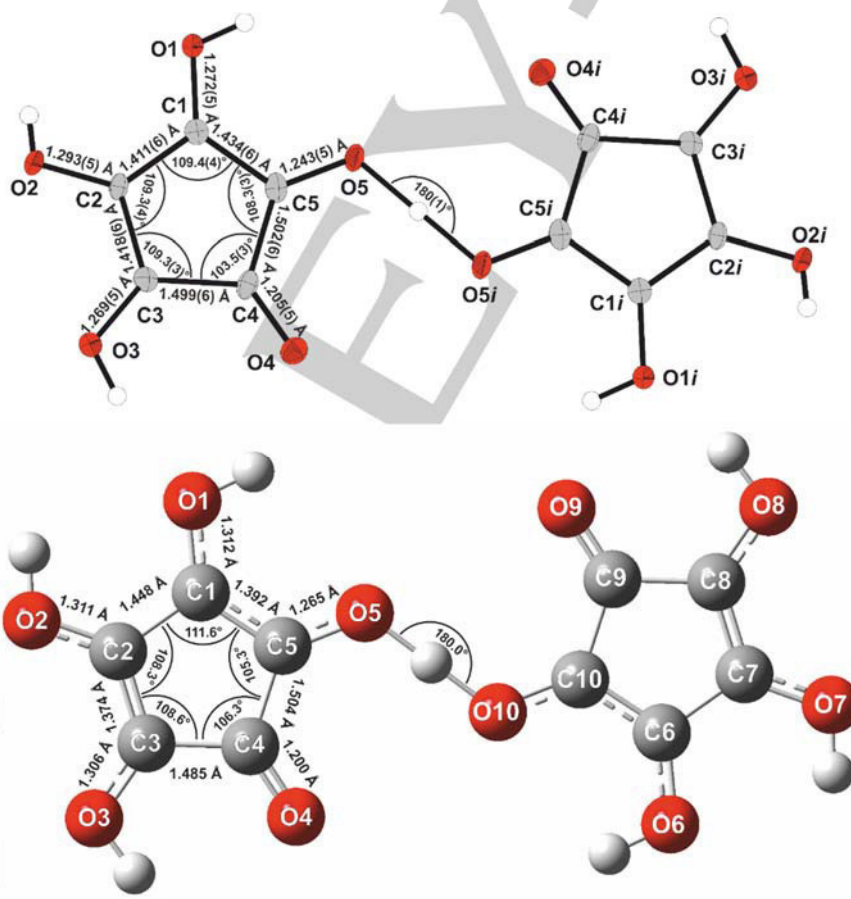


Figure S3. Experimentally obtained and calculated local minimum structure of the $[(\text{H}_3\text{O}_5\text{C}_5)\text{H}(\text{H}_3\text{O}_5\text{C}_5)]^{3+}$ cation.

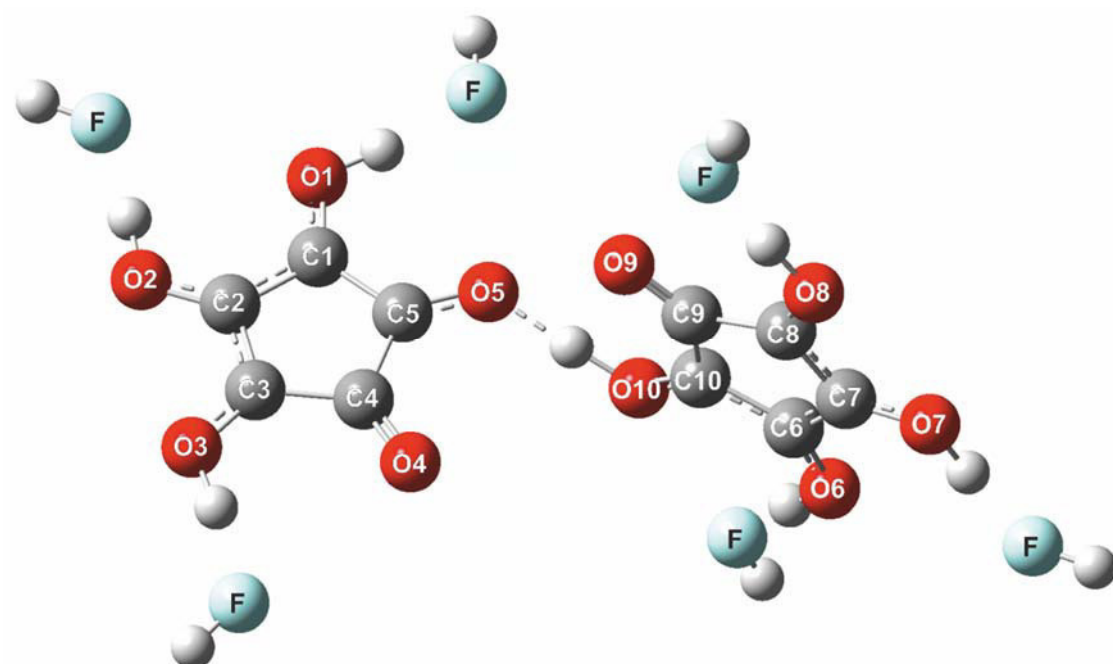


Figure S4. Global minimum structure of the $[(\text{H}_3\text{O}_5\text{C}_5)\text{H}(\text{H}_3\text{O}_5\text{C}_5)]^{3+} \cdot 6\text{HF}$.

Squaric Acid

Investigations on Squaric Acid in Superacidic Media

Manuel Schickinger, Denise Cibu, Florian Zischka, Karin Stierstorfer, Christoph Jessen, and Andreas Kornath*^[a]

Abstract: The syntheses of $[\text{OC}(\text{COX})_3][\text{MF}_6]$ and $[(\text{COX})_4][\text{MF}_6]_2 \cdot 2\text{HF}$ were carried out in superacidic media XF/MF_5 ($\text{M} = \text{As}, \text{Sb}$; $\text{X} = \text{H}, \text{D}$). The degree of protonation is highly dependent on the stoichiometric ratio of the Lewis acid with regard to squaric acid. The salts of diprotonated squaric acid were characterized by Raman spectroscopy and, in the case of $[(\text{COH})_4][\text{MF}_6]_2 \cdot 2\text{HF}$ ($\text{M} = \text{As}, \text{Sb}$), by single-crystal X-ray structure analyses. $[(\text{COH})_4][\text{AsF}_6]$ crystallizes in the monoclinic space group $P2_1/n$ with two formula units per unit cell. Analysis of the vibrational spectra was achieved with the

support of quantum chemical calculations of the cation $[(\text{COH})_4]^{2+} \cdot 4\text{HF}$ on the PBE1PBE/6-311G++(3df,3pd) level of theory. Furthermore, a salt of monoprotonated squaric acid, $[\text{OC}(\text{COH})_3][\text{AsF}_6]$, was characterized by a single-crystal X-ray structure analysis. It crystallizes in the monoclinic space group $P2_1/n$ with four formula units per unit cell. The protonation of squaric acid leads to a change of the carbon skeleton, which is discussed for the entire series, starting with the dianion of squaric acid and ending with the tetrahydroxy dication.

Introduction

3,4-Dihydroxycyclobut-3-ene-1,2-dione, better known as squaric acid, was prepared for the first time by Cohen et al. in 1959.^[1] Due to the high resonance stability of the $[\text{C}_4\text{O}_4]^{2-}$ anion, squaric acid has a remarkable acidity ($\text{p}K_{\text{a}1}$: 1.5 and $\text{p}K_{\text{a}2}$:

3.4), which is the highest among all cyclic oxocarboxylic acids.^[2,3] Already in 1967, Olah predicted the existence of diprotonated squaric acid based on ^{13}C NMR analysis.^[4] Moreover, three different geometries of the $[(\text{COH})_4]^{2+}$ cation were predicted by ab initio calculations, shown in Figure 1.^[5]

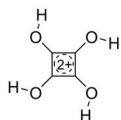
To our knowledge, no further experimental studies on the mono- and diprotonation of squaric acid have been reported. This raised the question concerning the geometry of diprotonated squaric acid and the existence of the monoprotonated species.

Results and Discussion

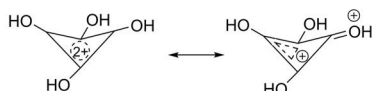
Synthesis and Properties of $[\text{OC}(\text{COH})_3][\text{MF}_6]$ and $[(\text{COH})_4][\text{MF}_6]_2 \cdot 2\text{HF}$ ($\text{M} = \text{As}, \text{Sb}$)

The mono- and diprotonated salts of squaric acid were prepared in two-step syntheses according to Equations (1) and (2): In the first step, the superacid media, HF/AsF_5 and HF/SbF_5 , were prepared and homogenized at -20°C . In the second step, squaric acid was added under inert gas atmosphere at

1) 2π -aromatic structure



2) puckered aromatic and homoaromatic structure



3) carboxonium ion structure

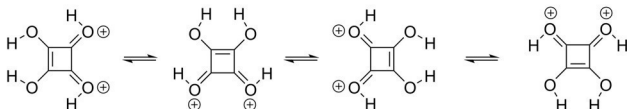
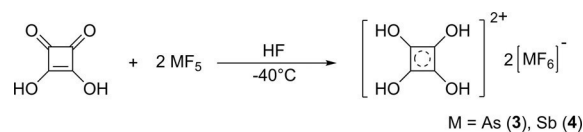
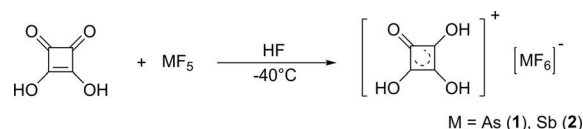


Figure 1. Possible geometries for the $[(\text{COH})_4]^{2+}$ cation.^[5]

[a] M. Schickinger, D. Cibu, F. Zischka, K. Stierstorfer, C. Jessen, Prof. Dr. A. Kornath
Department Chemie, Ludwig-Maximilians-Universität München
Butenandstr. 5-13(D), 81377 München (Germany)
E-mail: andreas.kornath@cup.uni-muenchen.de

Supporting information and the ORCID identification number for the author of this article can be found under:
<https://doi.org/10.1002/chem.201802516>



−196 °C. Allowing the reaction mixture to warm to −40 °C led to the immediate formation of the protonated species. The excess solvent was removed overnight at dry-ice temperature. All products were obtained as colorless salts in quantitative yields.

The monoprotonated salts of squaric acid, $[(\text{OC}(\text{COH})_3)[\text{AsF}_6]$ (1) and $[(\text{OC}(\text{COH})_3)[\text{SbF}_6]$ (2), were prepared using a one-to-one ratio of Lewis acid to squaric acid and are stable up to −50 °C. The diprotonated salts, $[(\text{COH})_4][\text{AsF}_6]_2 \cdot 2\text{HF}$ (3) and $[(\text{COH})_4][\text{SbF}_6]_2 \cdot 2\text{HF}$ (4), however, were prepared using a two-to-one or higher ratio of Lewis acid to starting material and are stable up to −30 °C. All salts are air- and moisture-sensitive.

Changing the solvent to deuterium fluoride leads to the corresponding deuterated species of protonated squaric acid $[(\text{OC}(\text{COD})_3)[\text{AsF}_6]$ (5), $[(\text{OC}(\text{COD})_3)[\text{SbF}_6]$ (6), $[(\text{COD})_4][\text{AsF}_6]_2 \cdot 2\text{HF}$ (7), and $[(\text{COD})_4][\text{SbF}_6]_2 \cdot 2\text{HF}$ (8). The hydroxyl hydrogen atoms are entirely replaced by deuterium because deuterium fluoride was used in large excess. The degree of deuteration approximates 96%.

Neither vibrational spectra of the monoprotonated squaric acid, nor satisfactory IR-measurements of the diprotonated species could be achieved because of the low thermal stability of both salts.

Raman spectra of 3, 4, 7, and squaric acid

The low-temperature Raman spectra of $[(\text{COH})_4][\text{AsF}_6]_2 \cdot 2\text{HF}$ (3), $[(\text{COH})_4][\text{SbF}_6]_2 \cdot 2\text{HF}$ (4), $[(\text{COD})_4][\text{AsF}_6]_2$ (7), and squaric acid are illustrated in Figure 2. The observed frequencies as well as the quantum chemically calculated frequencies are listed in Table 1. According to the quantum chemical calculations, the free cation shows C_{4h} symmetry. Consequently, 30 fundamental vibrations are expected. The Raman lines were assigned by analyzing the Cartesian displacement coordinates of the calculated vibrational modes as well as by comparing the calculated results to reported data of squaric acid.^[6,7]

The poor polarizability of the OH group means that the corresponding Raman lines are usually of low intensity. This is not the case for the OD stretching vibrations. In the Raman spectrum of $[(\text{COD})_4][\text{AsF}_6]_2$, the lines at 2294 cm^{-1} and 2138 cm^{-1}

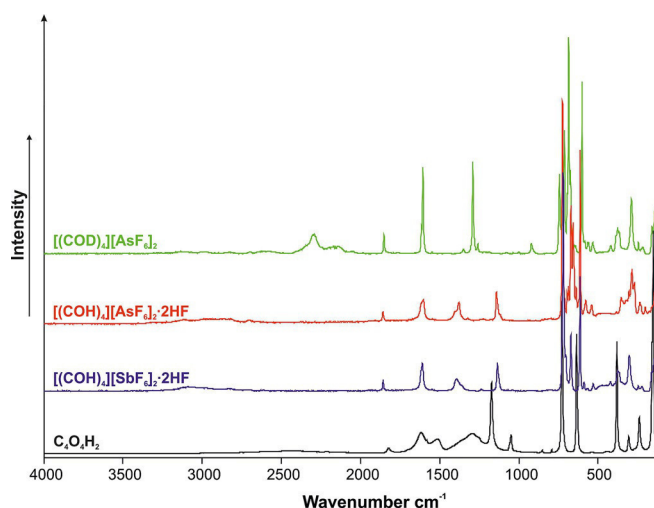


Figure 2. Low-temperature Raman spectra of $\text{C}_4\text{O}_4\text{H}_2$, $[(\text{COH})_4][\text{SbF}_6]_2 \cdot 2\text{HF}$, $[(\text{COH})_4][\text{AsF}_6]_2 \cdot 2\text{HF}$ and $[(\text{COD})_4][\text{AsF}_6]_2$.

represent $\nu(\text{OD})$ stretching vibrations. The $\nu(\text{CO})$ stretching vibrations occur for $[(\text{COH})_4][\text{AsF}_6]_2 \cdot 2\text{HF}$ at 1857 cm^{-1} and 1610 cm^{-1} , for $[(\text{COH})_4][\text{SbF}_6]_2 \cdot 2\text{HF}$ at 1858 cm^{-1} and 1603 cm^{-1} and for $[(\text{COD})_4][\text{AsF}_6]_2$ at 1852 cm^{-1} and 1606 cm^{-1} . These $\nu(\text{CO})$ vibrations are shifted to higher wavenumbers, compared with typical $\nu(\text{CO})$ vibrations (ca. 1750 cm^{-1}), due to coupling effects with ring stretching modes.^[8,9] This especially applies to the $\nu(\text{CO})_{\text{in phase}}$ which is coupled to the ring breathing mode $\nu_3(\text{CC})$.^[10] Comparing all calculated Raman-active $\nu(\text{CC})$ vibrations (1143 cm^{-1} and 716 cm^{-1}) with the experimental data obtained for 3 and 4, they are in good agreement. The same applies to the deuterated species 7. Especially, the ring breathing mode $\nu_3(\text{CC})$ at 719 cm^{-1} does not differ significantly from the reported value of squaric acid (725 cm^{-1}).^[6,7]

For the anions $[\text{MF}_6]^-$ ($\text{M} = \text{As}, \text{Sb}$) with an ideal O_h symmetry, three lines in the Raman spectrum are expected. In all three spectra, more than three vibrations are observed for the anions. This indicates a lower symmetry, which is confirmed by the structural parameters obtained by the crystal structure analysis.

Table 1. Selected experimental vibrational frequencies (in cm^{-1}) of $[(\text{COH})_4][\text{AsF}_6]_2 \cdot 2\text{HF}$ (3), $[(\text{COH})_4][\text{SbF}_6]_2 \cdot 2\text{HF}$ (4), and $[(\text{COD})_4][\text{AsF}_6]_2$ (7), and calculated vibrational frequencies (in cm^{-1}) of $[(\text{COH})_4]^{2+} \cdot 4\text{HF}$ and $[(\text{COD})_4]^{2+} \cdot 4\text{DF}$.					
$[(\text{COH})_4][\text{AsF}_6]_2 \cdot 2\text{HF}$ Raman	$[(\text{COH})_4][\text{SbF}_6]_2 \cdot 2\text{HF}$ Raman	$[(\text{COD})_4][\text{AsF}_6]_2$ Raman	$[(\text{COH})_4]^{2+} \cdot 4\text{HF}$ calc. ^[a] (IR/Raman)	$[(\text{COD})_4]^{2+} \cdot 4\text{DF}$ calc. ^[a] (IR/Raman)	Assignment ^[b]
		2294(9) 2138(3) br	2983 (1/408) 2931 (23/215) 2919 (9912/0)	2191 (0/187) 2144 (0/102) 2136 (5118/0)	$\nu(\text{OX})_{\text{in phase}}$ $\nu(\text{OX})_{\text{out of phase}}$ $\nu(\text{OX})$
1857(5) 1610(13)	1858(5) 1603(10)	1852(9) 1606(40)	1860 (0/5) 1629 (0/28) 1620 (2222/0)	1845 (0/13) 1623 (0/27) 1609 (2638/0)	$\nu(\text{CO})_{\text{in phase}}$ $\nu(\text{CO})_{\text{out of phase}}$ $\nu(\text{CO})$
1394(6) 1135(13)	1402(5) 1142(13)	921(5) 1290(42)	1372 (0/16) 1143 (0/28) 1058 (228/0)	921 (0/6) 1255 (0/37) 1158 (84/0)	$\delta(\text{COX})$ $\nu(\text{CC})$ $\nu(\text{CC})$
719(100)	724(100)	744(28)	716 (0/46)	693 (0/43)	$\nu(\text{CC})$
[a] Calculated at the PBE1PBE/6-311G++(3df,3pd) level of theory. IR intensity in km mol^{-1} and Raman intensity in $\text{\AA}^4/\mu$. Raman activity is stated to a scale of 1 to 100. Frequencies are scaled with an empirical factor of 0.965. [b] X = H, D.					

Crystal structure of $[(\text{COH})_4][\text{AsF}_6]_2 \cdot 2\text{HF}$

The $[\text{AsF}_6]^-$ salt of diprotonated squaric acid $[(\text{COH})_4][\text{AsF}_6]_2 \cdot 2\text{HF}$ (**3**) crystallizes in the monoclinic space group $P2_1/n$ with two formula units per unit cell. The formula unit of **3** is illustrated in Figure 3. Table 2 contains selected geometric parameters. We also obtained single crystals of $[(\text{COH})_4][\text{SbF}_6]_2 \cdot 2\text{HF}$ (**4**), which crystallizes in the monoclinic space group $C2/c$. Given that the bond lengths and angles of **4** are in good agreement with the values of **3**, this crystal structure is not discussed further, but listed in the Supporting Information.

The four carbon atoms of the cation with not significantly different C–C bond distances of 1.439(3) Å and 1.441(4) Å, are between a formal single and double bond.^[11,12] The C–C–C bond angles of 90.2(2)° and 89.8(2)° indicate a squaric geometry.

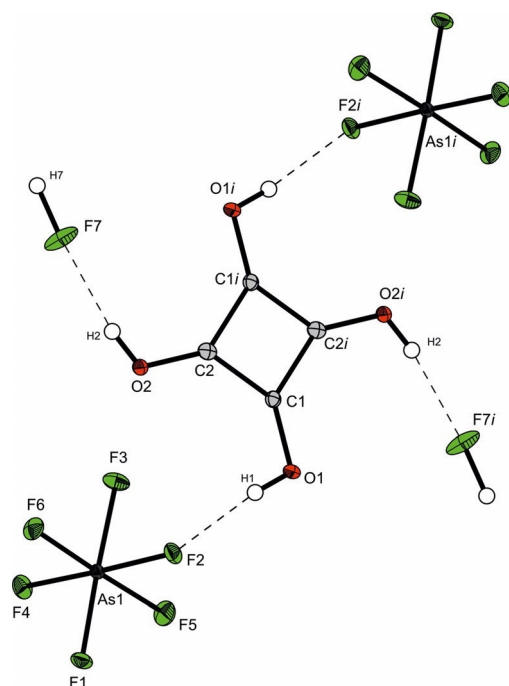


Figure 3. Projection of the interionic contacts between anions and cations of $[(\text{COH})_4][\text{AsF}_6]_2 \cdot 2\text{HF}$ (50% probability displacement ellipsoids). Symmetry code: $i = 2-x, 1-y, 1-z$.

Table 2. Selected bond lengths (in Å) and angles (in deg) of **3** with estimated standard deviations in parentheses.

Symmetry codes: $i = 2-x, 1-y, 1-z$

Bond length [Å]			
C1–C2	1.439(3)	C1–O1	1.268(3)
C1–C2i	1.441(3)	C2–O2	1.266(3)
Bond angles [°]			
C2i–C1–C2	90.2(2)	O1–C1–C2i	131.1(2)
C1–C2–C1i	89.8(2)	O2–C2–C1	133.0(2)
Dihedral angles [°]			
C1–C1i–C2–C2i	0.0(1)	O1–C1–C2–C1i	–179.8(4)
Interatomic distances D–A [Å]			
O1–(H1)⋯F2	2.554(2)	F7–(H7)⋯F6	2.603(2)
O2–(H2)⋯F7	2.614(3)		

try. It should be noted that squaric acid has a trapezoidal structure. This difference will be discussed later. The lengths of all C–O bonds (1.266(3) Å and 1.268(3) Å) do not differ significantly and are between a formal single and double bond.^[11,12]

The planar structure of the $[(\text{COH})_4]^{2+}$ cation is confirmed by the dihedral angles C1–C1i–C2–C2i and O1–C1–C2–C1i.

The expected octahedral geometry of the hexafluoroarsenate is slightly distorted by a hydrogen bond (O1–(H1)⋯F2). All As–F bond lengths are with 1.705(2) Å to 1.775(2) Å in a typical range for an $[\text{AsF}_6]^-$ anion.^[13]

The crystal packing in Figure 4 shows a network of moderate O–(H)⋯F hydrogen bonds along the *b*-axis between anions and cations. Furthermore, moderate hydrogen bonds along the *c*-axis between the co-crystallized HF solvent molecules and the $[(\text{COH})_4]^+$ cations are observed. All O–(H)⋯F contacts are between 2.554(2) Å and 2.614(3) Å and below the sum of the van-der-Waals radii (3.17 Å).^[14,15]

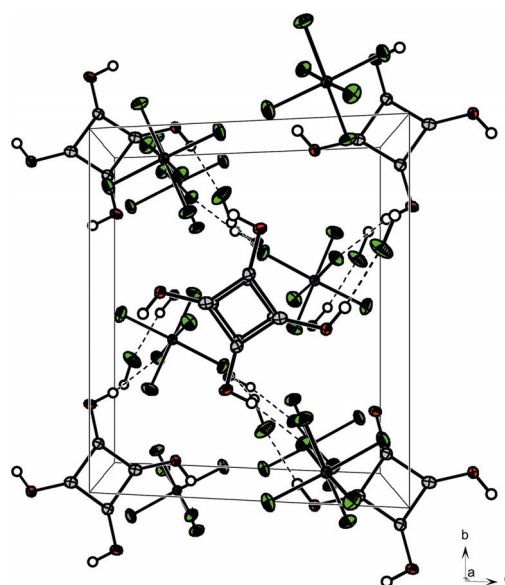


Figure 4. Crystal packing of $[(\text{COH})_4][\text{AsF}_6]_2 \cdot 2\text{HF}$. Hydrogen bonds are drawn as dashed lines (50% probability displacement ellipsoids). Symmetry code: $i = 2-x, 1-y, 1-z$.

Crystal structure of $[\text{OC}(\text{COH})_3][\text{AsF}_6]$

The $[\text{AsF}_6]^-$ salt of monoprotected squaric acid $[\text{OC}(\text{COH})_3][\text{AsF}_6]$ (**1**) crystallizes in the monoclinic space group $P2_1/n$ with four formula units per unit cell. The molecular structure of **1** is shown in Figure 5. Table 3 contains selected geometric parameters.

In the $[\text{OC}(\text{COH})_3]^+$ cation the geometry differs, as expected, from a squaric geometry. Especially the C3–C4–C1-angle of the unprotonated carbonyl group differs with 86.6(2)° from a right angle. Furthermore, the squaric geometry is distorted, because the C4–C1 (1.481(3) Å) and C3–C4 (1.473(3) Å) bond lengths are elongated compared with **3**. In comparison to squaric acid, the C1–O1 bond distance of $[\text{OC}(\text{COH})_3][\text{AsF}_6]$ is shortened, whereas the C3–O3 bond distance is slightly elongated.^[16] The other two C–O bond lengths are comparable to those found

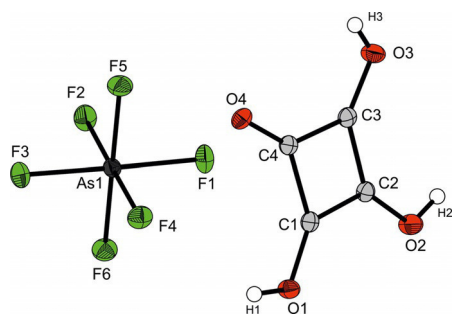


Figure 5. Projection of the interionic contacts between anions and cations of $[\text{OC}(\text{COH})_3][\text{AsF}_6]$ (50% probability displacement ellipsoids).

Table 3. Selected bond lengths (in Å) and angles (in deg) of **1** with estimated standard deviations in parentheses.

Bond length [Å]			
C1–C2	1.421(3)	C1–O1	1.271(2)
C2–C3	1.416(3)	C2–O2	1.292(3)
C3–C4	1.473(3)	C3–O3	1.278(3)
C4–C1	1.481(3)	C4–O4	1.218(3)
Bond angles [°]			
C4–C1–C2	90.9(2)	O1–C1–C2	131.5(2)
C1–C2–C3	91.1(2)	O2–C2–C3	138.1(2)
C2–C3–C4	91.4(2)	O3–C3–C4	136.8(2)
C3–C4–C1	86.6(2)	O4–C4–C1	135.9(2)
Dihedral angles [°]			
C4–C3–C1–C2	179.6(2)	O3–C3–C4–C1	178.7(3)
Interatomic distances D–A [Å]			
O3–(H3)⋯F4	2.671(2)	O2–(H2)⋯F2	2.639(2)

in the starting material.^[16] The dihedral angles, with 179.6(2)° and 178.7(3)°, show an almost planar geometry of the cation.

All As–F bonds are, with bond distances between 1.703(1) Å and 1.750(1) Å, in the typical range for an $[\text{AsF}_6]^-$ anion. The ideal octahedral geometry of the $[\text{AsF}_6]^-$ anion is slightly distorted, due to the As1–F4 (1.750(1) Å) and As1s–F2 (1.735(1) Å) bonds being involved in hydrogen bonding.^[13]

Cations and anions of $[\text{OC}(\text{COH})_3][\text{AsF}_6]$, depicted in Figure 6, are connected by a network of moderate O–(H)⋯F hydrogen bonds.^[14] The bond lengths are listed in Table 3. These donor–acceptor distances are slightly larger than those found in $[(\text{COH})_4][\text{AsF}_6]_2 \cdot 2\text{HF}$, but still below the sum of the van-der-Waals radii (3.17 Å).^[15]

Theoretical calculations

All calculations were performed at the PBE1PBE/6-311G++ (3df,3pd) level of theory with the Gaussian program package.^[17] All data concerning bond lengths and angles of $[\text{OC}(\text{COH})_3]^+ \cdot 2\text{HF} \cdot \text{OCH}_2$ as well as $[(\text{COH})_4]^{2+} \cdot 4\text{HF}$ and their corresponding cations obtained by the crystal-structure analyses are shown in Figures 7 and 8. The hydrogen fluoride molecules added to the gas-phase structure simulate hydrogen bonding in the solid state. Formaldehyde, added to the gas-phase structure of monoprotonated squaric acid, simulates cation–cation interactions in the solid state. This approach is a refinement of our already established method to simulate hydrogen bond-

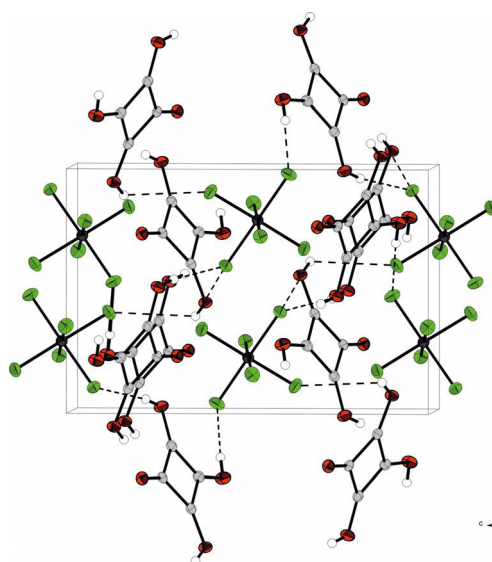


Figure 6. Crystal packing of $[\text{OC}(\text{COH})_3][\text{AsF}_6]$. Hydrogen bonds are drawn as dashed lines (50% probability displacement ellipsoids).

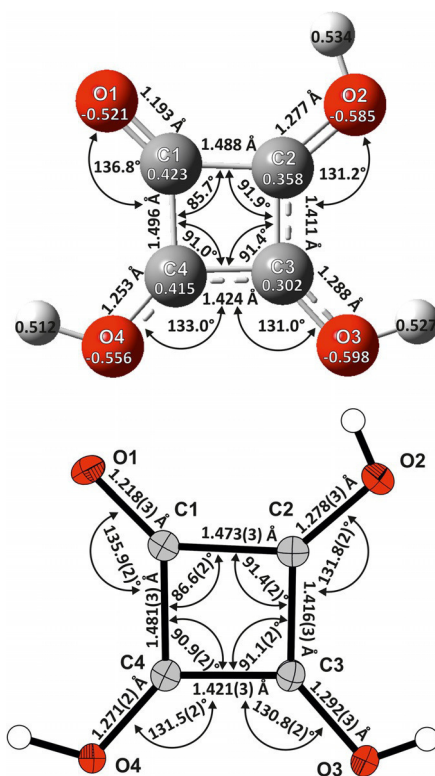


Figure 7. Top: Calculated structure of $[\text{OC}(\text{COH})_3]^+$ cation. Bottom: $[\text{OC}(\text{COH})_3]^+$ cation of the single-crystal X-ray structure.

ing.^[18] For clarity, the additional hydrogen fluoride and formaldehyde molecules have been omitted. The complete set of illustrations is shown in the Supporting Information.

All values, bond lengths and angles for the monoprotonated cation of squaric acid obtained by quantum chemical calculations are in accordance with the experimental data of the crystal structure. Only the C1–C2 and the C1–C4 bond distances

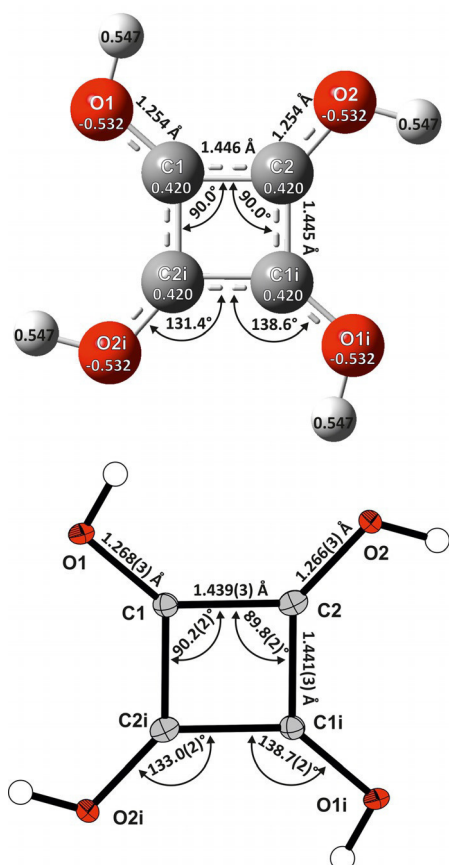


Figure 8. Top: Calculated structure of $[(\text{COH})_4]^{2+}$ cation. Bottom: $[(\text{COH})_4]^{2+}$ cation of the single-crystal X-ray structure.

of the $[\text{OC}(\text{COH})_3]^{+} \cdot 2\text{HF} \cdot \text{OCH}_2$ cation are slightly overestimated compared with the experimental data, since the calculation is only a model and merely the most important cation–cation and cation–anion interactions could be taken into account. In terms of charge distribution, the Natural Population Analysis (NPA) charges were calculated.

All geometric parameters of the diprotonated cation are in good agreement with the data obtained by quantum chemical calculations. The experimentally obtained vibrational frequencies of diprotonated squaric acid are in good agreement with the calculated values, only the $\nu(\text{OH})_{\text{out of phase}}$ vibrations differ slightly, due to too short calculated donor–acceptor distances in the $\text{O}-(\text{H}) \cdots \text{F}$ hydrogen bonds.

Concerning the three possible conformations for the diprotonated squaric acid predicted by Olah, it turned out that, in accordance with the results of Olah, the 2π -aromatic structure most likely represents the $[(\text{COH})_4]^{2+}$ cation.^[4,5] Furthermore, the result of the NPA charge distribution, which shows an even distribution of the positive charge over all ring C-atoms, argues for a 2π -aromatic structure, accompanied by C_{4h} -symmetry for the $[(\text{COH})_4]^{2+}$ cation. Furthermore, negative Nucleus-Independent Chemical Shift (NICS) values, which are obtained for $[(\text{COH})_4]^{2+} \cdot 4\text{HF}$ ($\text{NICS}(\text{O})_{\text{iso}} = -6.47$ and $\text{NICS}(\text{O})_{\text{zz}} = -6.12$) in the middle of the ring, exhibit the presence of induced diatropic ring currents. Moreover, the calculated ^{13}C NMR shift of $\delta = 185.6$ ppm, showing only one signal, is in

accordance with the experimental results of Olah ($\delta = 183.4$ ppm), confirming 2π -aromaticity for the $[(\text{COH})_4]^{2+}$ cation.^[4,5] These results of the structural analysis of the cation of diprotonated squaric acid can be confirmed by our vibrational and single-crystal X-ray structure analysis studies.

In Figure 9, the C–C bond lengths of the four-membered ring of squaric acid with different stages of protonation are listed. The data of squaric acid and its anions is obtained from crystal structures reported in literature.^[16,19–22] Based on this data, it becomes clear that only the diprotonated cation and the completely deprotonated anion of squaric acid have an almost squaric ring structure. This squaric structure is confirmed by the nearby right C–C–C angles of $[\text{C}_4\text{O}_4]^{2-}$ ($90.02(12)^\circ$ and $89.98(12)^\circ$) and $[\text{C}_4\text{O}_4\text{H}_4]^{2+}$ ($90.2(2)^\circ$ and $89.8(2)^\circ$).^[19] Surprisingly, neither the $\text{Na}_2[\text{C}_4\text{O}_4]$ nor the $\text{K}_2[\text{C}_4\text{O}_4]$, but only the $[\text{NH}_4]_2[\text{C}_4\text{O}_4]$ salt show a squaric structure.^[20,21] All other derivatives of squaric acid with different stages of protonation, ranging from minus two to plus one, have a trapezoidal structure of the four-membered ring.

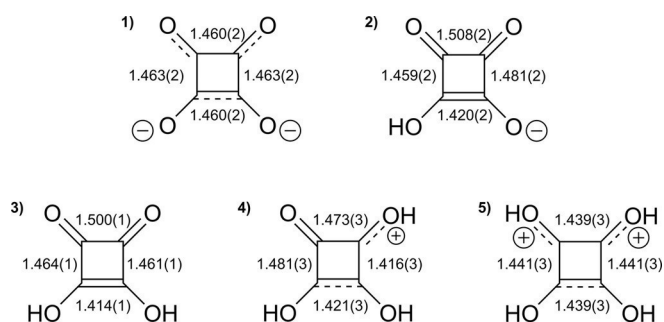


Figure 9. C–C bond distances (in Å) of 1) $[\text{C}_4\text{O}_4]^{2-}$ anion of $[\text{NH}_4]_2[\text{C}_4\text{O}_4]$,^[19] 2) $[\text{C}_4\text{O}_4\text{H}]^{2-}$ anion of $[\text{C}_7\text{H}_{10}\text{N}][\text{C}_4\text{O}_4\text{H}]$,^[22] 3) squaric acid,^[16] 4) $[\text{C}_4\text{O}_4\text{H}_3]^+$ cation of $[\text{OC}(\text{COH})_3][\text{AsF}_6]$ and 5) $[\text{C}_4\text{O}_4\text{H}_4]^{2+}$ cation of $[(\text{COH})_4][\text{AsF}_6]_2 \cdot 2\text{HF}$.

Conclusions

Monoprotonated squaric acid was prepared and isolated for the first time in superacidic media using an equimolar amount of Lewis acid in relation to squaric acid. $[\text{OC}(\text{COH})_3][\text{AsF}_6]$ was characterized by single-crystal X-ray structure analysis. The experimentally obtained geometric parameters are in good agreement with the quantum chemically calculated values.

Diprotonated squaric acid was prepared analogously by raising the ratio of Lewis acid to squaric acid to two-to-one or higher. $[(\text{COH})_4][\text{AsF}_6]_2 \cdot 2\text{HF}$ (**3**) and $[(\text{COH})_4][\text{SbF}_6]_2 \cdot 2\text{HF}$ (**4**) were isolated for the first time and characterized by vibrational spectroscopy and single-crystal X-ray structure analyses. For the $[(\text{COH})_4]^{2+}$ cation C_{4h} -symmetry, accompanied by 2π -aromaticity, is confirmed by this study.

Experimental Section

General

Caution!! Avoid contact with all of these compounds. Hydrolysis of any of these compounds might form hydrogen fluoride. HF burns

skin and causes irreparable damage. Safety precautions should be taken when handling these materials.

Apparatus and materials

All reactions and sample handling were performed by employing standard Schlenk techniques using a stainless-steel vacuum line. The reaction vessels are made of FEP/PFA, closed by a stainless-steel needle valve. In advance of usage, all reaction vessels and the stainless-steel line were dried with fluorine. IR spectra were recorded with a Bruker Vertex 80V FTIR spectrometer. For Raman measurements a Bruker MultiRAM FT-Raman spectrometer with Nd:YAG laser excitation ($\lambda = 1064$ nm) was used. The low-temperature X-ray diffraction of **1**, **3**, and **4** was performed with an Oxford XCalibur3 diffractometer equipped with a Spellman generator (voltage 50 kV, current 40 mA) and a KappaCCD detector, operating with MoK α radiation ($\lambda = 0.7107$ Å). Data collection at 123 K was performed using the CrysAlis CCD software,^[23] the data reductions were carried out using the CrysAlis RED software.^[24] The solution and refinement of the structure was performed with the programs SHELXS^[25] and SHELXL-97^[26] implemented in the WinGX software package^[27] and finally checked with the PLATON software.^[28] The absorption correction was performed with the SCALE3 ABSPACK multi-scan method.^[29] Selected data and parameters of the X-ray analysis are given in Table S2. All quantum chemical calculations were performed on the PBE1PBE/6311G++(3df, 3pd) level of theory by Gaussian 09.^[17] Crystal data and structure refinement of **1**, **3**, and **4** are listed in the Supporting Information (Table S2). CCDC 1588676, 1588677 and 1588678 contain the supplementary crystallographic data for this paper. These data can be obtained free of charge from The Cambridge Crystallographic Data Centre.

Synthesis of [OC(COH)₃][AsF₆] (1**), [OC(COD)₃][AsF₆] (**5**) and [(COH)₄][AsF₆]₂·2HF (**3**), [(COD)₄][AsF₆]₂·2HF (**7**):** For the formation of the required superacid, arsenic pentafluoride (1.00 mmol or 3.00 mmol, 170 mg or 510 mg) and anhydrous hydrogen fluoride (aHF, 150 mmol, 3 mL) were condensed into a 7 mL FEP tube-reactor. The temperature of the reaction mixture was reduced to −196 °C and subsequently raised to −30 °C to form the superacidic system. Hereafter, the temperature of the reaction vessel was again reduced to −196 °C and squaric acid (1 mmol, 114 mg) was added to the superacid under inert gas atmosphere. To enable the protonation of squaric acid, the temperature of the reaction mixture was again raised to −30 °C for 5 min and then reduced to −78 °C. Keeping this temperature, the remaining aHF was removed in a dynamic vacuum at dry-ice temperature, yielding [OC(COH)₃][AsF₆] and [(COH)₄][AsF₆]₂·2HF as colorless crystalline solids in quantitative yield. [OC(COD)₃][AsF₆] and [(COD)₄][AsF₆]₂ were prepared analogously, using deuterium fluoride, DF, instead of aHF.

Synthesis of [OC(COH)₃][SbF₆] (2**), [OC(COD)₃][SbF₆] (**6**), and [(COH)₄][SbF₆]₂·2HF (**4**), [(COD)₄][SbF₆]₂·2HF (**8**):** Anhydrous hydrogen fluoride (aHF, 150 mmol, 3 mL) was added to a 7 mL FEP-tube-reactor in which, prior to this, antimony pentafluoride (SbF₅, 1.00 mmol or 2.00 mmol, 217 mg or 434 mg) had been condensed in at −196 °C. To form the superacidic system, the mixture was warmed to 0 °C. The reaction vessel was again cooled to −196 °C and squaric acid (1 mmol, 114 mg) was added under inert gas atmosphere. The reaction vessel was warmed to −30 °C for 5 min and cooled to −78 °C afterwards. The excess of aHF was removed in a dynamic vacuum at −78 °C. [OC(COH)₃][SbF₆] and [(COH)₄][SbF₆]₂·2HF were obtained as colorless crystalline solids in quantitative yield. [OC(COD)₃][SbF₆] and [(COD)₄][SbF₆]₂ were prepared analogously, using deuterium fluoride, DF, instead of aHF.

Acknowledgements

We are grateful to the Department of Chemistry of the Ludwig-Maximilian University, Munich and the Deutsche Forschungsgemeinschaft (DFG) for the support of this work.

Conflict of interest

The authors declare no conflict of interest.

Keywords: ab initio calculations · protonation · superacidic systems · vibrational spectroscopy · X-ray diffraction

- [1] S. Cohen, J. Lacher, J. Park, *J. Am. Chem. Soc.* **1959**, *81*, 3480.
- [2] R. West, D. Powell, *J. Am. Chem. Soc.* **1963**, *85*, 2577–2579.
- [3] A. F. Holleman, E. Wiberg, *Lehrbuch der Anorganischen Chemie* (Ed.: N. Wiberg), 102nd ed., de Gruyter, Berlin **2007**, p. 905.
- [4] G. Olah, A. White, *J. Am. Chem. Soc.* **1967**, *89*, 4752–4756.
- [5] G. Olah, J. Bausch, G. Rasul, H. George, G. Prakash, *J. Am. Chem. Soc.* **1993**, *115*, 8060–8065.
- [6] Y. Morimoto, S. Koshihara, Y. Tokura, *J. Chem. Phys.* **1990**, *93*, 5429–5435.
- [7] F. Baglin, C. Rose, *Spectrochim. Acta Part A* **1970**, *26*, 2293–2304.
- [8] J. Weidlein, U. Müller, K. Dehnicke, *Schwingungsspektroskopie*, Georg Thieme, Stuttgart, **1988**, pp. 46–47.
- [9] J. Weidlein, U. Müller, K. Dehnicke, *Schwingungsspektroskopie*, Georg Thieme, Stuttgart, **1988**, pp. 146–147.
- [10] M. Ito, R. West, *J. Am. Chem. Soc.* **1963**, *85*, 2580–2584.
- [11] A. F. Holleman, E. Wiberg, *Lehrbuch der Anorganischen Chemie* (Ed.: N. Wiberg), 102nd ed., de Gruyter, Berlin, **2007**, p. 2006.
- [12] F. Allen, O. Kennard, D. Watson, L. Brammer, A. Orpen, R. Taylor, *J. Chem. Soc. Perkin Trans. 2* **1987**, S1–S19.
- [13] R. Minkwitz, F. Neikes, U. Lohmann, *Eur. J. Inorg. Chem.* **2002**, 27–30.
- [14] G. Jeffrey, *An Introduction to Hydrogen Bonding*, Oxford University Press, Oxford, **1997**.
- [15] A. Bondi, *J. Phys. Chem.* **1964**, *68*, 441–451.
- [16] D. Semmingsen, *Tetrahedron Lett.* **1973**, *14*, 807–808.
- [17] M. Frisch, G. Scuseria, M. Robb, J. Cheeseman, J. T. Montgomery, Jr., K. Kudin, J. Burant, J. Millam, S. Iyengar, J. Tomasi, V. Barone, B. Mennucci, M. Cossi, G. Scalmani, N. Rega, G. Petersson, H. Nakatsuji, M. Hada, M. Ehara, K. Toyota, R. Fukuda, J. Hasegawa, M. Ishida, T. Nakajima, Y. Honda, O. Kitao, H. Nakai, M. Klene, X. Li, J. Knox, H. Hratchian, J. B. Cross, C. Adamo, J. Jaramillo, R. Gomperts, R. E. Stratmann, O. Yazyev, A. Austin, R. Cammi, C. Pomelli, J. Ochterski, P. Ayala, K. Morokuma, G. Voth, P. Salvador, J. Dannenberg, V. Zakrzewski, S. Dapprich, A. Daniels, M. Strain, O. Farkas, D. Malick, A. Rabuck, K. Raghavachari, J. Foresman, J. Ortiz, Q. Cui, A. Baboul, S. Clifford, J. Cioslowski, B. Stefanov, G. Liu, A. Liashenko, P. Piskorz, I. Komaromi, R. Martin, D. Fox, T. Keith, M. Al-Laham, C. Peng, A. Nanayakkara, M. Challacombe, P. Gill, B. Johnson, W. Chen, M. Wong, C. Gonzalez, J. Pople, Gaussian, Inc. **2003**, Pittsburgh PA.
- [18] T. Soltner, N. Goetz, A. Kornath, *Eur. J. Inorg. Chem.* **2011**, 3076–3081.
- [19] S. Georgopoulos, R. Diniz, B. Rodrigues, M. Yoshida, L. de Oliveira, *J. Mol. Struct.* **2005**, *753*, 147–153.
- [20] A. Ranganathan, G. Kulkarni, *J. Phys. Chem. A* **2002**, *106*, 7813–7819.
- [21] W. Macintyre, M. Werkema, *J. Chem. Phys.* **1964**, *40*, 3563–3568.
- [22] R. Prohens, A. Portell, M. Font-Bardía, A. Bauzá, A. Frontera, *Cryst. Growth Des.* **2014**, *14*, 2578–2587.
- [23] CrysAlisCCD, Version 1.171.35.11 (release 16-05-2011 CrysAlis 171.NET), Oxford Diffraction Ltd., **2011**.
- [24] CrysAlisRED, Version 1.171.35.11 (release 16-05-2011 CrysAlis 171.NET), Oxford Diffraction Ltd., **2011**.
- [25] G. Sheldrick, SHELXS-97, Program for Crystal Structure Solution, University of Göttingen (Germany), **1997**.
- [26] G. Sheldrick, SHELXL-97, Programm for the Refinement of Crystal Structures, University of Göttingen, Germany, **1997**.

[27] L. Farrugia, *J. Appl. Crystallogr.* **1999**, 32, 837–838.

[28] A. Spek, *PLATON, A Multipurpose Crystallographic Tool*, Utrecht University, Utrecht (The Netherlands), **1999**.

[29] SCALE3 ABSPACK-An Oxford Diffraction program, Oxford Diffraction Ltd., **2005**.

Manuscript received: May 18, 2018

Revised manuscript received: June 13, 2018

Accepted manuscript online: June 14, 2018

Version of record online: August 8, 2018

CHEMISTRY

A **European** Journal

Supporting Information

Investigations on Squaric Acid in Superacidic Media

Manuel Schickinger, Denise Cibu, Florian Zischka, Karin Stierstorfer, Christoph Jessen, and Andreas Kornath^{*[a]}

chem_201802516_sm_miscellaneous_information.pdf

ARTICLE

Additional Author information for the electronic version of the article.

Table S1. Experimental vibrational frequencies (in cm^{-1}) of $[(\text{COH})_4][\text{AsF}_6]_2 \cdot 2\text{HF}$ (**3**), $[(\text{COH})_4][\text{SbF}_6]_2 \cdot \text{HF}$ (**4**), and $[(\text{COD})_4][\text{AsF}_6]_2$ (**7**), and calculated vibrational frequencies (in cm^{-1}) of $[(\text{COH})_4]^{2+} \cdot 4\text{HF}$ and $[(\text{COD})_4]^{2+}$.

$[(\text{COH})_4][\text{AsF}_6]_2 \cdot 2\text{HF}$ Raman	$[(\text{COH})_4][\text{SbF}_6]_2 \cdot 2\text{HF}$ Raman	$[(\text{COD})_4][\text{AsF}_6]_2$ Raman	$[(\text{COH})_4]^{2+} \cdot 4\text{HF}$ calc. ^[a] (IR/Raman)	$[(\text{COD})_4]^{2+}$ calc. ^[a] (IR/Raman)	Assignment
		2294(9)	2983(1/408)	2191(0/187)	$\nu(\text{OX})_{\text{inh}}$
		2138(3) br	2931(23/215)	2144(0/102)	$\nu(\text{OX})_{\text{oop}}$
			2919(9912/0)	2136(5118/0)	$\nu(\text{OX})_{\text{oop}}$
1857(5)	1858(5)	1852(9)	1860(0/5)	1845(0/13)	$\nu(\text{CO})_{\text{ip}}$
1610(13)	1603(10)	1606(40)	1629(0/28)	1623(0/27)	$\nu(\text{CO})_{\text{oop}}$
			1620(2222/0)	1609(2638/0)	$\nu(\text{CO})_{\text{oop}}$
1394(6)	1402(5)	921(5)	1372(0/16)	921(0/6)	$\delta(\text{COX})$
			1345(2/3)	1059(0/0)	$\delta(\text{COX})$
			1343(1096/0)	1013(454/0)	$\delta(\text{COX})$
1135(13)	1142(13)	1290(42)	1143(0/28)	1255(0/37)	$\nu(\text{CC})$
			1058(228/0)	1158(84/0)	$\nu(\text{CC})$
			917(0/0)	665(0/0)	$\gamma(\text{OX})$
			909(392/0)	661(210/0)	$\gamma(\text{OX})$
			896(0/0)	669(0/0)	$\gamma(\text{OX})$
			810(0/0)	754(0/5)	$\delta(\text{CCO})$
			760(0/0)	760(0/0)	$\gamma(\text{CO})$
719(100)	724(100)	744(28)	716(0/46)	693(0/43)	$\nu(\text{CC})$
	637(7)		621(0/1)	601(0/1)	$\gamma(\text{CO})$
613(53)	612(25)	601(78)	597(0/13)	585(0/13)	$\delta(\text{CCC})$
			338(216/0)	297(242/0)	$\delta(\text{CCO})$
302(17)	303(10)	289(25)	314(0/4)	268(0/1)	$\delta(\text{CCO})$
			245(25/0)	241(5/0)	$\gamma(\text{CO})$
			118(0/0)	118(0/0)	$\gamma(\text{CC})$
					$M = \text{As, Sb}$ $X = \text{H, D}$
671(23)	695(6)	728(9)			$[\text{MF}_6]^-$
588(4)	670(48)	713(47)			$[\text{MF}_6]^-$
383(5)	658(24)	685(100)			$[\text{MF}_6]^-$
375(7)	577(7)	564(3)			$[\text{MF}_6]^-$
	539(4)	533(4)			$[\text{MF}_6]^-$
	286(21)	376(11)			$[\text{MF}_6]^-$

[a] Calculated at the PBE1PBE/6-311G++(3df,3pd) level of theory. IR intensity in km/mol and Raman intensity in $\text{\AA}^4/\square$. Raman activity is stated to a scale of 1 to 100. Frequencies are scaled with an empirical factor of 0.965.

Table S2. X-ray data and parameters of **1**, **3** and **4**.

	[OC(COH) ₃][AsF ₆]	[(COH) ₄][AsF ₆] ₂ ·2HF	[(COH) ₄][SbF ₆] ₂ ·2HF
formula	C ₄ H ₃ AsF ₆ O ₄	C ₄ H ₆ As ₂ F ₁₄ O ₄	C ₄ H ₆ Sb ₂ F ₁₄ O ₄
M _r [g mol ⁻¹]	303.98	533.93	627.59
crystal size [mm ³]	0.30 x 0.27 x 0.20	0.30 x 0.25 x 0.18	0.20 x 0.18 x 0.15
crystal system	monoclinic	monoclinic	monoclinic
space group	<i>P</i> 2 ₁ / <i>n</i>	<i>P</i> 2 ₁ / <i>n</i>	<i>C</i> 2/ <i>c</i>
<i>a</i> [Å]	9.7163(6)	7.7712(5)	12.3864(10)
<i>b</i> [Å]	7.4804(4)	10.1172(5)	9.4339(5)
<i>c</i> [Å]	11.3008(7)	9.0980(6)	12.5583(15)
α [deg]	90.0	90.0	90.0
β [deg]	100.187(6)	110.171(7)	112.963(11)
γ [deg]	90.0	90.0	90.0
<i>V</i> [Å ³]	808.41(8)	671.44(7)	1351.2(2)
<i>Z</i>	4	2	4
ρ_{calcd} , [g cm ⁻³]	2.498	2.641	2.987
μ (MoK α), [cm ⁻¹]	0.71073	0.71073	0.71073
μ [mm ⁻¹]	4.308	5.165	4.171
<i>F</i> (000)	584	508	1120
<i>T</i> [K]	173(2)	173(2)	173(2)
hkl range	-10:12; -9:8; -11:14	-9:10; -11:13; -11:9	-14:16; -12:6; -16:16
refl. measured	3607	2610	2879
refl. unique	1847	1527	1543
<i>R</i> _{int}	0.0251	0.0246	0.0256
parameters	148	121	116
<i>R</i> (<i>F</i>)/ <i>wR</i> (<i>F</i> ²) ^[a]	0.0273/0.0488	0.0284/0.0612	0.0269/0.0477
(all reflexions)			
weighting scheme ^[b]	0.0175/0.3709	0.0293/0.0	0.166/0.0
<i>S</i> (GoF) ^[c]	1.047	1.080	1.034
Residual density	0.437/-0.326	0.476/-0.740	0.677/-0.919
[e Å ⁻³]			
device type	Oxford XCalibur	Oxford XCalibur	Oxford XCalibur
solution	SHELXS-97 ^[26]	SHELXS-97 ^[26]	SHELXS-97 ^[26]
refinement	SHELXL-97 ^[27]	SHELXL-97 ^[27]	SHELXL-97 ^[27]
CCDC	1588677	1588678	1588676

[a] $R_1 = \sum ||F_o| - |F_c|| / \sum |F_o|$; [b] $wR_2 = [\sum [w(F_o^2 - F_c^2)^2] / \sum [w(F_o^2)]^{1/2}]$; $w = [\sigma_c^2(F_o^2) + (xP)^2 + yP]^{-1}$; $P = (F_o^2 + 2F_c^2) / 3$ [c] GoF = $\{\sum [w(F_o^2 - F_c^2)^2] / (n - p)\}^{1/2}$ (*n* = number of reflections; *p* = total number of parameters)

Table S3. Selected bond lengths (in Å) and angles (in deg) of **3** and **4** with estimated standard deviations in parentheses.

Symmetry codes: *i* = 2-*x*, 1-*y*, 1-*z* and: *i* = *x*, 1-*y*, -*z*

[(COH) ₄][SbF ₆] ₂ ·2HF (4)		[(COH) ₄][AsF ₆] ₂ ·2HF (3)	
Bond length [Å]			
C1-C2	1.435(4)	C1-C2	1.439(3)
C1-C2 <i>i</i>	1.445(4)	C1-C2 <i>i</i>	1.441(3)
C1-O1	1.265(4)	C1-O1	1.268(3)
C2-O2	1.266(4)	C2-O2	1.266(3)
Bond angles [°]			
C2 <i>i</i> -C1-C2	89.9(3)	C2 <i>i</i> -C1-C2	90.2(2)
C1-C2-C1 <i>i</i>	90.1(3)	C1-C2-C1 <i>i</i>	89.8(2)
O1-C1-C2 <i>i</i>	131.3(3)	O1-C1-C2 <i>i</i>	131.1(2)
O2-C2-C1	132.0(3)	O2-C2-C1	133.0(2)
Dihedral angles [°]			
C1-C1 <i>i</i> -C2-C2 <i>i</i>	0.0(6)	C1-C1 <i>i</i> -C2-C2 <i>i</i>	0.0(1)
O1-C1-C2-C1 <i>i</i>	-179.9(5)	O1-C1-C2-C1 <i>i</i>	-179.8(4)
Interatomic distances D...A [Å]			
O1-(H1)···F1	2.535(3)	O1-(H1)···F2	2.554(2)
O2-(H2)···F3	2.593(3)	O2-(H2)···F7	2.614(3)
F7-(H7)···F5	2.773(4)	F7-(H7)···F6	2.603(2)

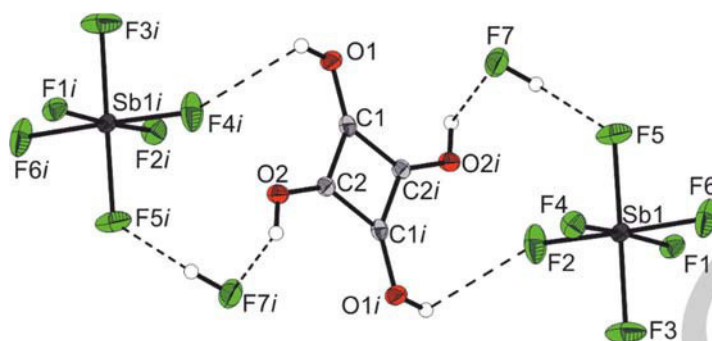


Figure S1. Projection of the interionic contacts between anions and cations of $[(\text{COH})_4][\text{SbF}_6]_2 \cdot 2\text{HF}$ (**4**) (50% probability displacement ellipsoids). Symmetry code: $i = -x, 1-y, -z$.

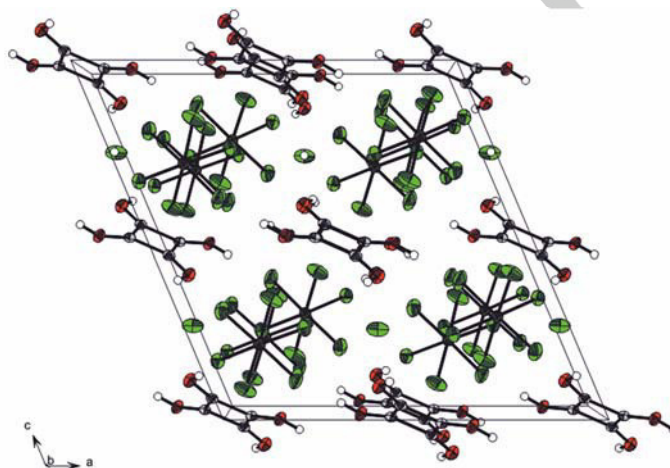


Figure S2. Crystal packing of $[(\text{COH})_4][\text{SbF}_6]_2 \cdot 2\text{HF}$ (**4**). Hydrogen bonds are drawn as dashed lines. (50% probability displacement ellipsoids). Symmetry code: $i = -x, 1-y, -z$.

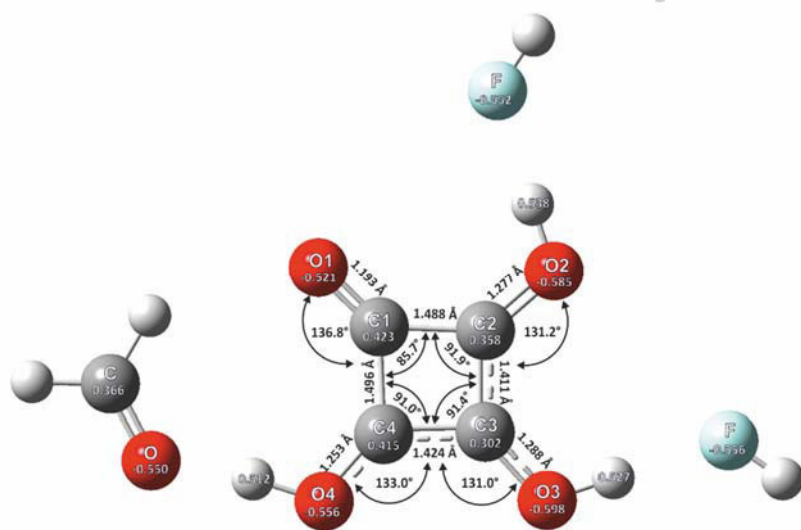


Figure S3. Calculated structure of the $[\text{OC}(\text{COH})_3]^+ \cdot 2\text{HF} \cdot \text{OCH}_2$ -cation

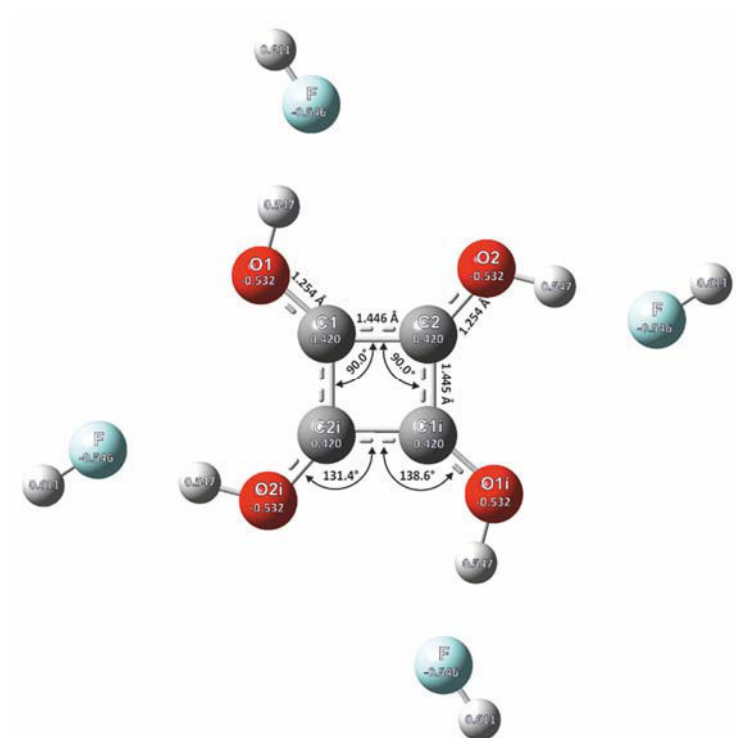


Figure S4. Calculated structure of the $[(\text{COH})_4]^{2+} \cdot 4\text{HF}$ -cation